UNIVERSITY OF CALIFORNIA, SAN DIEGO

The MRE11 complex and ATM activate distinct signaling responses to defend against DNA viruses *versus* DNA breaks

A dissertation submitted in partial satisfaction of the requirements for the degree Doctor of Philosophy

in Biology

by

Govind Anil Shah

Committee in charge:

Professor Clodagh C. O'Shea, Chair
Professor Cornelis Murre, Co-Chair
Professor Daniel J. Donoghue
Professor Tony Hunter
Professor Jean Y.J. Wang
Professer Dong-Er Zhang

2014

The Dissertation of Govind Anil Shah is approved, and it is acceptable in quality and form for publication on microfilm and electronically:

Co-Chair

Chair

University of California, San Diego

2014

Table of Contents

List of Figures

List of Tables

Acknowledgements

The contents of this dissertation, in full, has been submitted for publication of the material as it may appear in Cell, 2015, Shah, G.S. and O'Shea, C.C. The dissertation author was the first author of this paper, and Clodagh C. O'Shea was the senior author, supervising this work. We thank James A.J. Fitzpatrick, Michael Nunn, Nicola Allen and members of the O'Shea laboratory for their support, insights and helpful comments. This work was supported by R01CA137094 and P30CA014195 from the National Cancer Institute. C.C.O. is supported by R01CA137094 from the National Cancer Institute at the National Institutes of Health, The Leona M. and Harry B. Helmsley Charitable Trust grant #2012-PG-MED002, the William Scandling Trust and the Price Family Foundation. G.S. was supported by the T32 GM007240, Cell and Molecular Genetics Training Program and the Chapman Charitable Trust. We thank Jamie Kasuboski and Carolyn O'Connor for technical assistance.

I also thank Conrado T. Soria for training and technical assistance in culturing SAECs, and O'Shea lab members that generated vital resources for this work. The ΔE1/ΔE4-ORF3 and ΔE4-ORF3 viruses were cloned by Horng Der Ou. The ΔE1B-55K virus was cloned by Colin J. Powers. The ΔE1B-55K/ΔE4-ORF3 virus was cloned by Jason DeHart. Viruses used in this work were titered by Colin J. Powers, Conrado T. Soria, Horng Der Ou, Anna Rorick, and Sharmista Acharya. I thank Aaron Yun Chen for performing library preparation and sequencing analysis that led to important conclusions in this work. I also thank members the rest of the O'Shea lab and the

MCBL department for tremendous amounts of advice and assistance during the course of these studies, especially the Lundblad and Karlseder labs for lending resources and technical assistance for Southern blot analysis. I thank my committee members for their attention, guidance, and support through the course of my studies. I thank my friends and family members for their support and encouragement. Finally, I thank Clodagh C. O'Shea for her mentorship, vision, and guidance in this project and for providing the opportunity and resources for us to do this work.

Vita

2007	Bachelor of Science in Molecular Cell and Developmental Biology, University of California, Los Angeles
2008-2011	Teaching Assistant, Division of Biological Sciences, University of California, San Diego
2014	Doctor of Philosophy in Biology, University of California, San Diego

Publications

Shah, G.S., O'Shea, C.C. The MRE11 complex and ATM activate distinct signaling responses to defend against DNA viruses *versus* DNA breaks. (submitted)

Abstract of the Dissertation

The MRE11 complex and ATM activate distinct signaling responses to defend against DNA viruses *versus* DNA breaks

by

Govind Anil Shah

Doctor of Philosophy in Biology

University of California, San Diego, 2014

Professor Clodagh C. O'Shea, Chair

Professor Cornelis Murre, Co-Chair

The MRE11/RAD50/NBS1 (MRN) complex is a sensor for DNA breaks. In response to DNA breaks, MRN activates a global DNA damage response (DDR) through the kinase ATM that prevents cell cycle progression and cell proliferation.

Critical to the amplification of the DDR is the phosphorylation of H2AX (γH2AX), a histone that is broadly distributed throughout cellular chromatin. Here we show that MRN-ATM activates a distinct signaling response to defend the cell against DNA viruses. We reveal a critical localized MRN-ATM response that is inactivated by Adenovirus E1B-55K/E4-ORF3 early viral oncoproteins and a subsequent MRN independent global DDR that does not impact viral replication. Using Adenovirus E1B-55K/E4-ORF3 mutants, we show that MRN binds to replicating Adenovirus genomes, where it activates a localized ATM response that prevents viral but not cellular DNA replication. In contrast to cellular DNA breaks, MRN-ATM activation on the miniscule Adenovirus genome is not amplified by γH2AX across chromatin and does not induce DDR foci and global signaling, hallmarks of cellular DNA damage. Thus, the MRN-ATM response to replicating Adenovirus genomes is uncoupled from the response to cellular DNA breaks. The uncoupling of the cellular and anti-viral MRN-ATM responses permits infected cells to divide and implies that DDR foci and signal amplification have evolved as mechanisms to distinguish ‘self’ and ‘non-self’ pathological DNA and mediate an appropriate response.

Furthermore, cellular DNA breaks can sequester MRN from sensing viral genomes, thus rescuing Adenovirus genome replication. This demonstrates that that cellular DNA damage dampens the host defenses to viral replication which best explains the increased permissiveness for viral genome replication in tumor cell lines. Importantly, this work suggests that elevated genomic instability in cancer cells can be targeted for the development of oncolytic viruses that selectively replicate in cancer cells.

Chapter 1. Introduction

The MRN complex is a sensor for double strand DNA breaks and activates the protein kinase ATM.

Central to life is the faithful replication, inheritance, and maintenance of DNA, which provides the biological blueprint for all organisms. The MRE11/RAD50/NBS1 (MRN) complex and the ATM protein kinase play a critical role in this biological mandate as part of the cellular DNA damage response (DDR) pathway (Ciccia and Elledge, 2010). The role of MRN and ATM in the maintenance of genomic integrity is broadly conserved across eukaryotes (Harper and Elledge, 2007; Yoshiyama et al., 2013). Cellular double strand breaks (DSBs) are sensed by MRN which triggers the activation of the kinase ATM (Costanzo et al., 2004; Falck et al., 2005; Lee and Paull, 2004, 2005; Uziel et al., 2003). ATM interacts with NBS1 through an acidic amino acid patch and an FXF/Y motif at the C-terminus of NBS1 (Falck et al., 2005; You et al., 2005). The C-terminal region of NBS1 that interacts with ATM is required for the recruitment of ATM to DNA breaks and its activation (Falck et al., 2005; You et al., 2005). Consistent with the role of MRN upstream of ATM, MRN is required for the robust phosphorylation of ATM substrates in response to DNA damage *in vivo* (Uziel et al., 2003), and MRN is sufficient to activate ATM in response to double-stranded DNA oligonucleotides *in vitro* (Lee and Paull, 2004, 2005).

However, other DNA damage sensors including the KU70-KU80 complex and PARP-1 are recruited to breaks earlier than MRN complex components (Polo and Jackson, 2011), and may mediate the recruitment of MRN to DNA breaks. PARP-1

binds MRE11, and MRN recruitment to DNA breaks is defective in PARP-1 deficient cells (Haince et al., 2008). Also, KU70 binding is coincident with MRN binding at DNA ends in *Xenopus* egg extracts (You et al., 2007).

Upon activation, ATM can phosphorylate a wide number of cellular proteins that can mediate cellular responses to DNA damage including DNA repair, cell cycle arrest, and apoptosis (Shiloh and Ziv, 2013). The importance of MRN and ATM to genomic integrity is underscored by the fact that *MRE11*, *RAD50*, and *NBS1* are essential genes (Adelman et al., 2009; Luo et al., 1999; Xiao and Weaver, 1997; Zhu et al., 2001); however, *ATM* is not an essential gene, and inherited mutations in *ATM* lead to Ataxia telangiectasia, a condition characterized by developmental defects, radiosensitivity, and cancer predisposition (Savitsky et al., 1995). In addition to ATM, the related atypical protein kinases ATR and DNA-PK can also be activated by single strand and double strand DNA damage, respectively, through distinct DNA damage sensing protein complexes (Falck et al., 2005). Of note, ATM, ATR, and DNA-PK share overlapping protein substrates and preferentially target SQ/TQ peptide motifs (Kim et al., 1999; O'Neill et al., 2000). Together, ATM, ATR, and DNA-PK orchestrate DDR kinase signaling to downstream protein substrates to enact an appropriate response to cellular DNA damage (Ciccia and Elledge, 2010).

The response to DNA breaks is amplified by the assembly of DDR foci.

An important and normal component of the response to cellular DNA breaks is the formation of DDR foci, structures within the nucleus of concentrated DDR proteins and DDR induced post-translational modifications (Haaf et al., 1995; Maser et al., 1997;

Rogakou et al., 1998; Schultz et al., 2000). The formation of DDR foci at sites of DNA breaks has been an important tool for studying the sequential recruitment of DDR proteins to DNA breaks (Nelms et al., 1998; Paull et al., 2000). An important mediator of the formation of DDR foci is a histone H2A variant, H2AX (Fernandez-Capetillo et al., 2004). Upon DNA damage, H2AX is phosphorylated by ATM at Ser139, close to its C-terminus, and is called γH2AX once phosphorylated (Burma et al., 2001; Paull et al., 2000; Rogakou et al., 1998). The MDC1 scaffolding protein binds to γH2AX through BRCT repeats in MDC1 and mediates the recruitment of additional MRN and ATM at DNA breaks (Goldberg et al., 2003; Lukas et al., 2004; Stewart et al., 2003; Stucki et al., 2005; Xu and Stern, 2003). This is achieved through interaction between the FHA and BRCT domains in MDC1 (Goldberg et al., 2003) and the FHA domain in NBS1 (Lukas et al., 2004). Thus, the local activation of ATM at DSBs is amplified by the critical mediator γH2AX, which allows for the formation of DDR foci and can span megabases of flanking chromatin from sites of DNA breaks (Bassing et al., 2002; Celeste et al., 2002; Iacovoni et al., 2010; Rogakou et al., 1999; Rogakou et al., 1998).

The assembly of DDR foci is conserved from yeast to humans (Lisby et al., 2004) and is one of the most sensitive hallmarks of cellular DNA damage (Mah et al., 2010). However, in contrast to MRN components (Adelman et al., 2009; Luo et al., 1999; Xiao and Weaver, 1997; Zhu et al., 2001), H2AX- and MDC1-null mice, which are defective for the formation of DDR foci, are viable and are only partially defective in DSB repair (Bassing et al., 2002; Celeste et al., 2002; Lou et al., 2006). Thus, the functional requirement and logic of modifying megabases of flanking chromatin to protect the genome against DNA breaks remains one of the most cryptic aspects of the

DDR (Cleaver, 2011; Fernandez-Capetillo et al., 2003). Of note, the assembly of DDR foci through H2AX and MDC1 plays an important role in nucleating and amplifying the global phosphorylation of DDR substrates that elicit cell cycle arrest, repair, senescence or apoptosis (Bassing et al., 2002; Celeste et al., 2002; Goldberg et al., 2003; Lou et al., 2006; Soutoglou and Misteli, 2008; Stewart et al., 2003). For example, H2AX-deficient cells are defective for triggering cell cycle arrest upon low doses of DNA damage, but not high doses of DNA damage (Fernandez-Capetillo et al., 2002). Importantly, a single DSB can be sufficient to elicit cell cycle arrest (Bennett et al., 1993; Huang et al., 1996; Moore and Haber, 1996). Thus, while MRN is sufficient to activate ATM *in vitro* (Lee and Paull, 2004, 2005), the formation of DDR foci by γH2AX and MDC1 plays an important role in amplifying ATM signaling and triggering cell cycle arrest *in vivo*.

Adenovirus is a nuclear DNA virus and ubiquitous human pathogen.

The anti-viral functions of the DDR pathway remain unclear. DNA viruses are a persistent threat across all domains of life. Adenoviruses are ubiquitous human pathogens (Yu et al., 2012). Adenovirus has a linear double strand DNA genome, similar to the host chromosomes; however, at roughly 36 kbp, the Adenovirus genome is at least 1000 times shorter than the shortest human chromosome (Knipe and Howley, 2013). The Adenovirus capsid delivers the viral genome directly to the nuclear interior (Greber et al., 1993). Adenovirus serotype 5 normally infects quiescent airway epithelial cells in which early viral proteins activate E2F transcription of cellular and viral genes to drive concomitant cellular and viral DNA replication within the nucleus (Ben-Israel and Kleinberger, 2002). Adenovirus genome replication can be

reconstituted *in vitro* with precursor Terminal Protein (pTP), the E2B viral DNA polymerase and the E2A single strand DNA binding protein (Challberg and Kelly, 1979). The first rounds of Adenovirus genome replication are semi-conservative (initiated from double stranded DNA genomic substrates), similar to eukaryotic genome replication, but subsequent rounds can be initiated from displaced single strand DNA that accumulate at high concentrations in specialized nuclear domains with E2A (de Jong et al., 2003).

The requirement of MRN inactivation by E1B-55K/E4-ORF3 for Adenovirus replication is unclear.

The discovery of Adenovirus serotype 5 (Ad5) early proteins that target MRN excited great interest, suggesting that the cellular DDR also has a critical anti-viral role (Stracker et al., 2002). However, despite numerous studies, the role of MRN and global cellular DDR signaling in viral replication has been difficult to decipher. Thus, an outstanding question is whether MRN activates distinct signaling responses to protect the cell against viral DNA genomes and cellular DNA breaks. A unifying feature of viruses is that they have smaller genomes compared to their hosts. In principle, miniscule viral DNA genomes would not support the spreading of DDR proteins across megabases of DNA to induce global DDR signaling and cell cycle arrest. Furthermore, given the frequency of viral infection, the induction of cell cycle arrest or apoptosis in response to viral DNA may be detrimental to tissue homeostasis.

Ad5 expresses early viral proteins that target MRN through two independent mechanisms (Figure 2.1A) (Stracker et al., 2002). The Ad5 E1B-55K binds to MRE11

and forms a complex with another Ad5 early protein, E4-ORF6, which, as part of a CUL5-ELOB/C Cullin-RING E3 ubiquitin ligase complex, targets cellular proteins for ubiquitylation and degradation in the proteasome, including MRE11 (Querido et al., 2001; Stracker et al., 2002). Independently of E1B-55K/E4-ORF6 mediated MRE11 degradation, a third Ad5 early protein, E4-ORF3, assembles a multivalent homopolymer network in the nucleus that mislocalizes and sequesters MRN components (Ou et al., 2012; Stracker et al., 2002). Studies using E4 deleted viruses that lack both E4-ORF6 and E4-ORF3 and additional E4 genes have led to the prevailing model that the inactivation of MRN is necessary to prevent global cellular ATM and ATR DDR signaling (Carson et al., 2009; Carson et al., 2003) inducing the 'repair' of viral genomes into end-to-end concatemers that limit replication (Boyer et al., 1999; Stracker et al., 2002; Weiden and Ginsberg, 1994). However, viral genomes assemble at high concentrations in late E2A replication domains in cells infected with E4 deleted viruses (Carson et al., 2003; Stracker et al., 2002), indicating that global DDR signaling has a limited impact on viral genome replication. Furthermore, multiple studies have shown that the concatemer phenomenon is irrelevant for viral genome replication and is not dependent on ATM and ATR (Evans and Hearing, 2003; Gautam and Bridge, 2013; Shepard and Ornelles, 2004). More perplexing still, wild type Ad5 has been reported to activate global DNA damage signaling (Blackford et al., 2008; Forrester et al., 2011; Nichols et al., 2009), which is difficult to reconcile with the inactivation of MRN by E1B-55K/E4-ORF3. Therefore, despite intense study over the past fifteen years, an anti-viral role of MRN and DDR signaling in the Adenovirus lifecycle remains contentious and confounding.

The assumption that the anti-viral role of MRN is similar to the response induced by cellular DNA breaks has confounded our understanding of the host anti-viral DDR. Our studies reveal that the cell activates two temporally and mechanistically distinct MRN and ATM DDRs at different stages of Adenovirus replication: a localized, early MRN dependent ATM response that, through an unknown mechanism, specifically prevents viral genome replication and a global, late MRN independent DDR that does not impact viral genome replication. Using virus mutants that lack E1B-55K and E4-ORF3, we show that MRN recruits ATM to early replicating viral genomes and activates a localized signaling response that prevents replication. In contrast to chromosomal breaks, ATM activation at small viral genomes is not amplified by H2AX phosphorylation, which normally occurs across megabases of nucleosome bound cellular DNA and does not trigger the assembly of DDR foci and ATM dependent global signaling. As such, cells that have activated the critical MRN anti-viral DDR appear 'undamaged'. The localized MRN-ATM anti-viral DDR selectively prevents viral and not cellular replication. This provides an elegant mechanism to neutralize viral replication without jeopardizing cell viability. However, the requirement of MRN to sense both cellular DSBs and viral genomes has profound consequences. Cellular DNA damage sequesters MRN and prevents the cell sensing and restricting viral genome replication.

Summary of methods and results in Chapters 2-4

In Chapter 2, we investigate the functional requirement for MRN inactivation by E1B-55K and E4-ORF3 for viral replication. Using a new series of deleted

Adenoviruses and infection of primary human lung epithelial cells, we demonstrate that E1B-55K and E4-ORF3 are required for viral genome replication *in vivo* and identify human A549 non-small cell lung carcinoma cells as a useful tool for investigating further questions. Using RNAi knockdown of MRN complex components in A549 cells, we demonstrate that MRN restricts viral genome replication early during infection through a distinct mechanism from its role in cellular DNA breaks, in that it neither requires nor triggers the global amplification of DDR kinase signaling as measured by immunoblot. Using selective inhibitors of viral cellular DNA replication, we demonstrate that wild type (WT) Adenovirus DNA replication and assembly of E2A viral replication domains in the nucleus triggers global ATM and DDR kinase signaling through a novel MRN independent mechanism.

In Chapter 3, we investigate the mechanism by which MRN restricts viral genome replication. Using ChIP analysis, we demonstrate that MRN-ATM signaling components localizes to replicating viral genomes, where phosphorylated SQ/TQ peptide motifs are found. Using inhibitors to ATM kinase and immunofluorescence imaging, we demonstrate that localized MRN-ATM activation at sites of viral genomes restricts viral genome replication, yet does not trigger global DDR kinase phosphorylation or the formation of DDR foci. Using ChIP, we demonstrate that viral genomes lack the histone occupancy typical of cellular chromatin and are not associated with γH2AX/MDC1 that normally serves to amplify DDR kinase signaling and focus formation. Using cell cycle analysis, we demonstrate that the localized MRN-ATM anti-viral DDR specifically blocks viral genome replication and not cellular genome replication or division.

In Chapter 4, we investigate whether MRN sensing of viral genomes is saturable by competitive DNA damage substrates. Using treatment with genotoxic drugs or superinfection with Adenovirus, we demonstrate that cellular DNA damage or high numbers of incoming genomes can sequester MRE11 away from viral genomes and rescues viral genome replication, bypassing the requirement for E1B-55K/E4-ORF3 to inactivate MRN. Using infection in various human cancer cell lines, we demonstrate that tumor cell lines exhibit differential permissiveness for viral genome replication, possibly due to genomic instability inherent to cancer cells, analogous to the rescue of viral genome replication by genotoxic drugs. Using an inhibitor of MRE11 nuclease activity, we demonstrate that while MRE11 localization is required to restrict viral genome replication, its nuclease activity plays a minor role. The results in Chapter 4 may resolve results in the literature that conflict with our results from Chapters 2 and 3.

Together, this work reveals a distinct signaling response by MRN-ATM to viral genomes and cellular DNA damage.

Chapter acknowledgements

The contents of this chapter, in full, has been submitted for publication of the material as it may appear in Cell, 2015, Shah, G.S. and O'Shea, C.C. The dissertation author was the first author of this paper, and Clodagh C. O'Shea was the senior author, supervising this work.

Chapter 2. MRN blocks Adenovirus genome replication irrespective of global DDR kinase signaling.

E1B-55K and E4-ORF3 target MRN and are critical for viral genome replication *in vivo* but do not prevent global DDR kinase signaling in wild type Adenovirus infection

To date, nearly all of the studies of the cellular DDR to Adenovirus infection have been performed in tumor cell lines or SV40 immortalized fibroblast lines (Blackford et al., 2008; Carson et al., 2009; Carson et al., 2003; Forrester et al., 2011; Gautam and Bridge, 2013; Lakdawala et al., 2008; Mathew and Bridge, 2007, 2008; Nichols et al., 2009; Prakash et al., 2012). However, viral oncoproteins and tumor mutations can impair DNA damage checkpoints (Kastan and Bartek, 2004; Wu et al., 2004). Therefore, for these studies we used human primary small airway epithelial cells (SAECs) maintained at near-physiological oxygen to minimize genotoxic stress. In addition, we also used A549 lung adenocarcinoma cells that have been used before in several studies. Previous studies have used hybrid Ad2/5 viruses (Shepard and Ornelles, 2004) or viruses that are deleted for multiple E4 genes (E4-ORF1, E4-ORF2, E4-ORF3, E4-ORF3/4, E4-ORF4, E4-ORF6, E4-ORF6/7) (Carson et al., 2009; Carson et al., 2003; Gautam and Bridge, 2013; Lakdawala et al., 2008; Mathew and Bridge, 2007, 2008), which obfuscates the specific requirements of E1B-55K and E4-ORF3 in viral replication. E1B-55K binds to MRE11 in the absence of E4-ORF6 (Carson et al., 2003; Schwartz et al., 2008), which could subvert MRN complex functions. Therefore, in addition to using previously reported viruses, we used a new series of Ad5 viruses that

have specific single or compound deletions of E1B-55K and E4-ORF3 gene sequences generated by the O'Shea lab (Figure 2.1B). All viruses were grown and titered on complementing cell-lines and infections performed at minimal experimentally determined multiplicities of infection (MOIs) to exclude possible artifacts arising from superinfection. Thus, using infection in primary SAECs with this new series of mutant viruses, we investigated the functional relevance of MRN inactivation in facilitating Adenovirus replication (Figure 2.1A).

The degradation and mislocalization of MRN components by E1B-55K/E4-ORF6 and E4-ORF3 was confirmed by immunoblotting and immunofluorescence analysis of SAECs infected with ΔE1, WT, ΔE1B-55K, ΔE4-ORF3 or ΔE1B-55K/ΔE4-ORF3 viruses (Figures 2.1B-D). ΔE1 is a virus that lacks the E1 region and is also deleted for E4-ORF3 that serves as a control for virus infection and incoming genomes since it does not replicate or express viral proteins. In place of E1 sequences there is a CMV-GFP expression cassette to identify infected cells based on GFP expression (Figure 2.1B). In WT and ΔE4-ORF3 infected SAECs, E1B-55K binds to MRE11 and recruits E4-ORF6 and cellular proteins involved in ubiquitylation that target MRE11 and, as a consequence, RAD50 for degradation in the proteasome (Figure 2.1B). In ΔE1B-55K infected cells, MRE11 is not degraded but is sequestered by E4-ORF3 that assembles a multivalent polymer in the nucleus (Figure 2.1C). Likewise, NBS1 is also sequestered in E4-ORF3 polymers in ΔE1B-55K infected cells in which MRE11 is not degraded (Figure 2.1D). ΔE1B-55K/ΔE4-ORF3 viruses neither degrade nor mislocalize MRE11 (Figures 2.1B-D) and thus enable the anti-viral role of MRN to be determined (Figures 2.1A).

Figure 2.1. New E1B-55K/E4-ORF3 deletion viruses allow the investigation of the MRN anti-viral function.

(A) MRN is targeted for degradation by Adenovirus 5 (Ad5) early proteins through two independent mechanisms. E1B-55K targets MRE11 for proteasome degradation and E4-ORF3 sequesters and mislocalizes MRN by forming a nuclear polymer. The functional requirement for inactivating MRN and global DDR signaling during viral infection is unclear.
(B) Quiescent primary small airway epithelial cells (SAECs) were infected with mock (ΔE1), wild type Ad5 (WT), ΔE4-ORF3, ΔE1B-55K or ΔE1B-55K/ΔE4-ORF3 viruses and analyzed by immunoblot. Protein lysates were collected at 24 h.p.i., normalized by cell number and immunoblotted for E1A, E1B-55K, E4-ORF3, GFP, MRE11, RAD50, and NBS1. β-ACTIN is a loading control. "t = 0" indicates uninfected cells collected immediately prior to infection. Arrows and asterisks indicate specific and non-specific bands, respectively.
(C and D) SAECs were infected with either mock (ΔE1), Ad5 (WT), ΔE4-ORF3, ΔE1B-55K, or ΔE1B-55K/ΔE4-ORF3 viruses and analyzed by immunofluorescence. SAECs were fixed at 24 h.p.i. and immunostained for E4-ORF3 (green) and either MRE11 (red) (C) or NBS1 (red) (D). Nuclei were counterstained with Hoechst-33342 and are outlined in white. The merged panel is an overlay of the red and green channels. A representative image is shown. Scale bar: 10 μm.

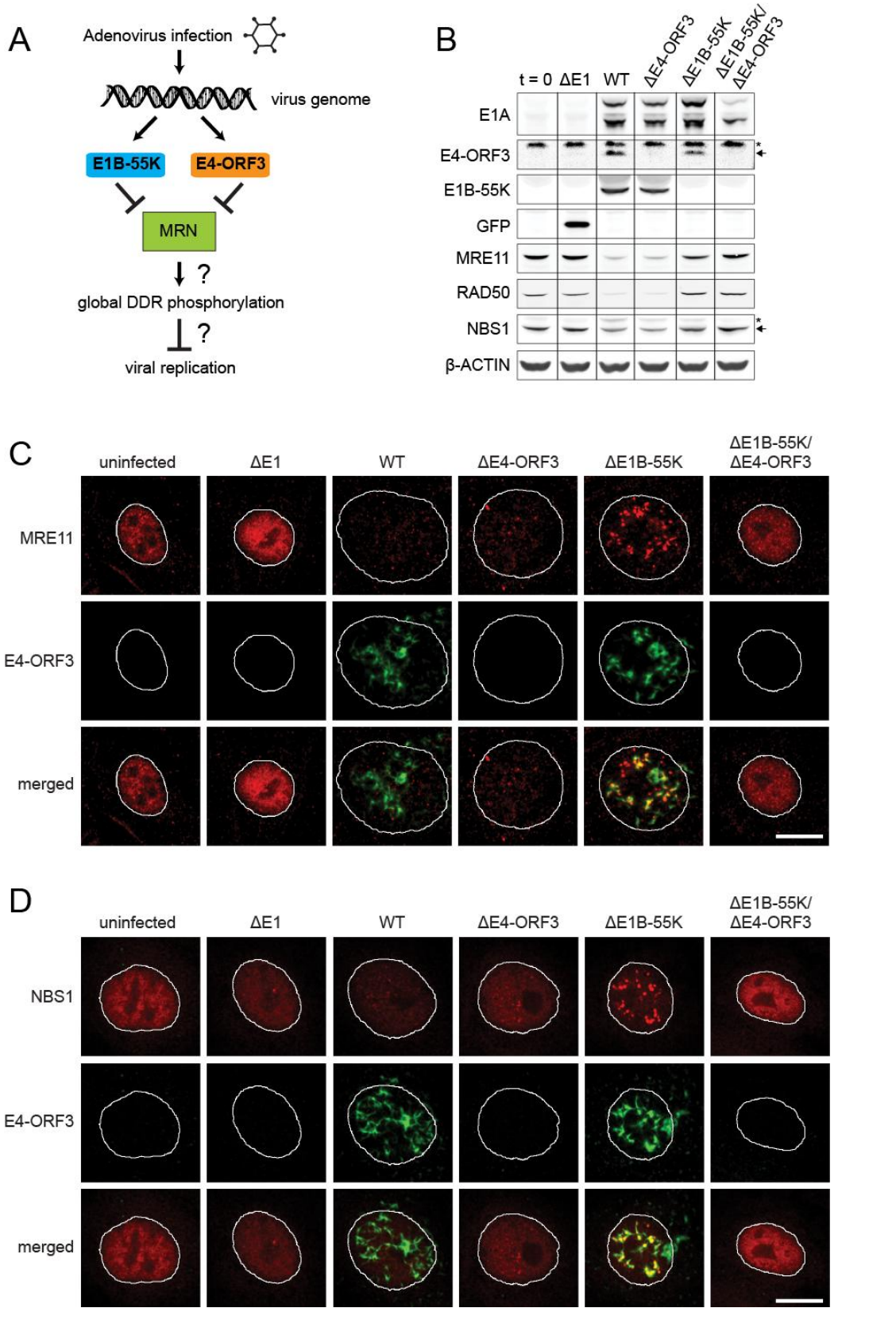
A
Adenovirus infection
virus genome
E1B-55K
E4-ORF3
MRN
?
global DDR phosphorylation
?
viral replication
B
t = 0
ΔE1
WT
ΔE4-ORF3
ΔE1B-55K
ΔE1B-55K/ ΔE4-ORF3
E1A
E4-ORF3
E1B-55K
GFP
MRE11
RAD50
NBS1
β-ACTIN
C
uninfected
ΔE1
WT
ΔE4-ORF3
ΔE1B-55K
ΔE1B-55K/ ΔE4-ORF3
MRE11
E4-ORF3
merged
D
uninfected
ΔE1
WT
ΔE4-ORF3
ΔE1B-55K
ΔE1B-55K/ ΔE4-ORF3
NBS1
E4-ORF3
merged

The requirement for MRN inactivation by E1B-55K and E4-ORF3 in the Adenovirus lifecycle remains unclear. Previous studies with HeLa cells infected with *dl*3112, an E1B-55K/E4-ORF3 double deletion virus, reported no defect in viral genome replication (Shepard and Ornelles, 2004). Other studies using E4 or E4-ORF6 mutant viruses that still express E1B-55K have reported a mild, 10-fold or less, defect in viral genome replication (Evans and Hearing, 2003, 2005; Gautam and Bridge, 2013; Lakdawala et al., 2008; Mathew and Bridge, 2007, 2008). Thus, the specific requirement for E1B-55K and E4-ORF3 in facilitating viral genome replication, an early step within the virus lifecycle (Knipe and Howley, 2013), is unclear. Therefore, to determine if E1B-55K or E4-ORF3 are required for viral genome replication in quiescent primary epithelial cells, we infected SAECs with ΔE1, WT, ΔE4-ORF3, ΔE1B-55K or ΔE1B-55K/ΔE4-ORF3 viruses and harvested total viral and cellular DNA at 24 and 48 hours post infection (h.p.i.). Viral genomes were quantified using Q-PCR and normalized relative to cellular 18S rDNA. WT, ΔE4-ORF3 and ΔE1B-55K viruses undergo logarithmic replication to similar levels (Figure 2.2A). In contrast, ΔE1B-55K/ΔE4-ORF3 viruses are highly defective for viral genome replication (Figure 2.2A). The levels of WT virus genomes are 10^4 times higher than ΔE1B-55K/ΔE4-ORF3 virus genomes at the 48 h.p.i. (Figure 2.2A). We conclude that either E1B-55K or E4-ORF3 is required for viral genome replication, and the double deletion of E1B-55K and E4-ORF3 renders Adenovirus genome replication defective.

Adenovirus DNA replication can be reconstituted *in vitro* and does not require E1B-55K or E4-ORF3 (Challberg and Kelly, 1979). This suggests that *in vivo*, E1B-55K/E4-ORF3 is required to inactivate a cellular checkpoint that otherwise prevents

Adenovirus genome replication. MRN is a sensor for cellular DSBs, and the phosphorylation of DDR proteins by DDR kinases is critical for its role in inducing various responses to DNA breaks such as cell cycle arrest and DNA repair (Shiloh and Ziv, 2013). To determine if Adenovirus mutants that fail to degrade or mislocalize MRN activate global DDR kinase signaling, we analyzed total protein lysates from infected SAECs for the induction of canonical cellular DDR kinase phosphorylated substrates. Doxorubicin treatment was used as a positive control to induce cellular DNA breaks, which triggers the global phosphorylation of DDR kinase substrates, including ATM-Ser1981, NBS1-Ser343, TRIM28-Ser824, H2AX-Ser139 and RPA32-Ser4/Ser8 (Figures 2.2B).

In WT virus infected cells the sequestration and degradation of MRN by E4-ORF3 and E1B-55K, respectively, was expected to prevent DDR signaling. However, contrary to expectations, global DDR signaling is activated in WT virus infected cells as evidenced by the phosphorylation of DDR kinase substrates: ATM-Ser1981, H2AX-Ser139, TRIM28-Ser824, RPA32-Ser4/Ser8 and DNA-PKcs-Ser2056 (Figure 2.2B). DDR phosphorylated substrates are also induced in ΔE1B-55K and ΔE4-ORF3 infected cells, but to a slightly lower level than WT virus infected cells (Figure 2.2B). In ΔE1B-55K/ΔE4-ORF3 infected cells, MRN was expected to activate a global DDR signaling response to viral genomes. However, contrary to expectations, DDR phosphorylated substrates are not globally induced in ΔE1B-55K/ΔE4-ORF3 infected cells and are at similar levels to control and ΔE1 infected cells (Figure 2.2B). This is made more obvious by quantification of Phospho- to Total-protein ratios (Figure 2.2C). We conclude that ΔE1B-55K/ΔE4-ORF3 infection in primary SAECs does not include the

global activation of DDR phosphorylation.

An alternative explanation for these results is that the absence of global DDR phosphorylation and defect of ΔE1B-55K/ΔE4-ORF3 virus genome replication is anomalous and exclusive to the new deletion viruses generated by the O'Shea lab. Therefore, we infected SAECs with previously described Ad2/5 viruses that have E1B-55K and E4-ORF3 gene deletions: *dl*312, WtD, ONYX-015/*dl*1520 and *dl*3112 (Figure 2.3A) (Barker and Berk, 1987; Bischoff et al., 1996; Jones and Shenk, 1979; Shepard and Ornelles, 2003). This series of viruses demonstrates a similar phenotype (Figure 2.3). Infection with WtD (WT) triggers global DDR phosphorylation (Figure 2.3C). The *dl*3112 virus (ΔE1B-55K/ΔE4-ORF3) is defective for virus genome replication and does not trigger global DDR phosphorylation (Figures 2.3B and 2.3C).

Figure 2.2. E1B-55K and E4-ORF3 and are required for Adenovirus genome replication but do not prevent global DDR signaling in WT virus infected SAECs.

SAECs were infected with either mock (ΔE1), Ad5 (WT), ΔE4-ORF3, ΔE1B-55K, or ΔE1B-55K/ΔE4-ORF3 viruses and analyzed by immunofluorescence, Q-PCR and immunoblotting.
(A) Total DNA samples were collected at 24 and 48 h.p.i. Viral genomes were quantified by Q-PCR using a Taqman probe that detects all viruses. Viral genomes were normalized relative to cellular 18S rDNA. Q-PCR was performed in triplicate, and error bars indicate standard deviation (nd: not done).
(B) Protein lysates were collected at 24 or 48 h.p.i., normalized by cell number and immunoblotted for E1A, E1B-55K, E4-ORF3, MRE11, RAD50, NBS1, Phospho-NBS1-Ser343, ATM, Phospho-ATM-Ser1981, H2AX, γH2AX, RPA32, Phospho-RPA32-Ser4/Ser8, DNA-PKcs and Phospho-DNA-PKcs-Ser2056. β-ACTIN is a loading control. "t = 0" indicates uninfected cells collected immediately prior to infection. Doxorubicin treatment was used as a positive control to induce cellular DNA damage. Arrows and asterisks indicate specific and non-specific bands, respectively.
(C) Quantification of total and phosphorylated protein bands for immunoblots in (B) was performed using a LI-COR Scanner and Odyssey software. The ratio of the total to phosphorylated bands was calculated for each sample. For comparison purposes, the ratios are plotted on the same graph relative to "t = 0".

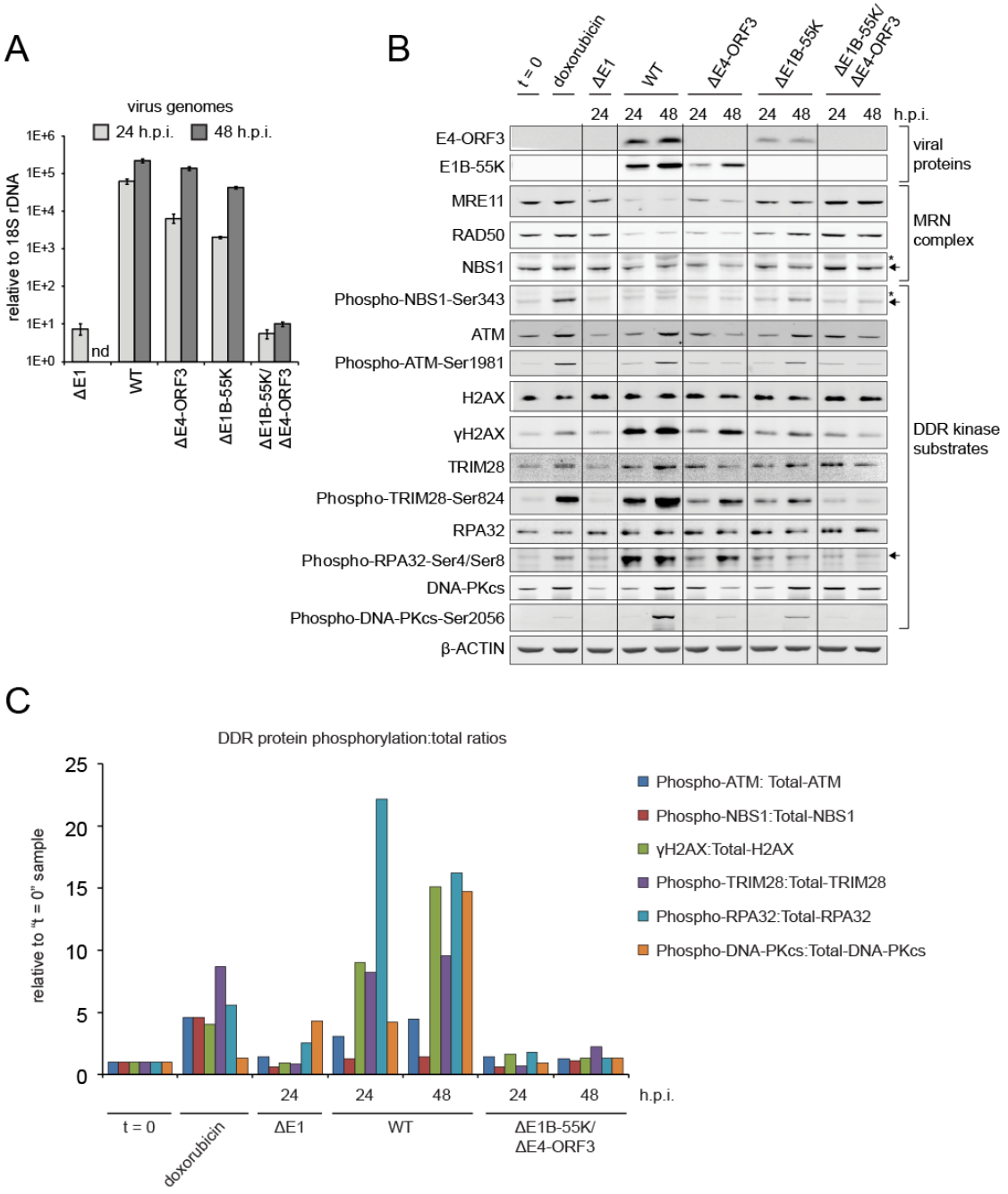
A
virus genomes
24 h.p.i.
48 h.p.i.
relative to 18S rDNA
1E+6
1E+5
1E+4
1E+3
1E+2
1E+1
1E+0
nd
ΔE1
WT
ΔE4-ORF3
ΔE1B-55K
ΔE1B-55K/ ΔE4-ORF3
B
t = 0
doxorubicin
ΔE1
WT
ΔE4-ORF3
ΔE1B-55K
ΔE1B-55K/ ΔE4-ORF3
24 24 48 24 48 24 48 24 48 h.p.i.
E4-ORF3
E1B-55K
MRE11
RAD50
NBS1
Phospho-NBS1-Ser343
ATM
Phospho-ATM-Ser1981
H2AX
γH2AX
TRIM28
Phospho-TRIM28-Ser824
RPA32
Phospho-RPA32-Ser4/Ser8
DNA-PKcs
Phospho-DNA-PKcs-Ser2056
β-ACTIN
viral proteins
MRN complex
DDR kinase substrates
C
DDR protein phosphorylation:total ratios
relative to "t = 0" sample
25
20
15
10
5
0
Phospho-ATM: Total-ATM
Phospho-NBS1:Total-NBS1
γH2AX:Total-H2AX
Phospho-TRIM28:Total-TRIM28
Phospho-RPA32:Total-RPA32
Phospho-DNA-PKcs:Total-DNA-PKcs
24 24 48 24 48 h.p.i.
t = 0
doxorubicin
ΔE1
WT
ΔE1B-55K/ ΔE4-ORF3

A

virus	genotype
*dl*312	ΔE1
WtD	wild type
ONYX-015/*dl*1520	ΔE1B-55K
*dl*3112	ΔE1B-55K/ΔE4-ORF3

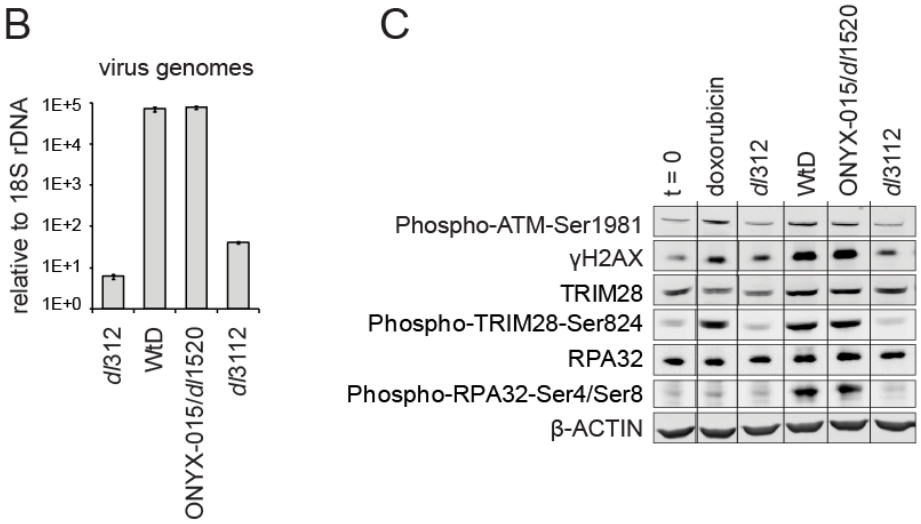

Figure 2.3. Previously described E1B-55K/E4-ORF3 deletion viruses demonstrate identical phenotypes to new deletion viruses.

SAECs were infected with previously reported Ad2/5 hybrid viruses, ΔE1 (*dl*312), WT (WtD), ΔE1B-55K (ONYX-015/*dl*1520), or ΔE1B-55K/ΔE4-ORF3 (*dl*3112), and harvested at 48 h.p.i.

(A) Table of virus nomenclature and corresponding genotype.

(B) Viral genomes were quantified by Q-PCR and normalized relative to cellular 18S rDNA. Q-PCR was performed in triplicate, and error bars indicate the standard deviation.

(C) Protein lysates were collected at 48 h.p.i., normalized by cell number, and immunoblotted for Phospho-ATM-Ser1981, γH2AX, TRIM28, Phospho-TRIM28-Ser824, RPA32, and Phospho-RPA32-Ser4/Ser8. β-ACTIN is a loading control. "t = 0" indicates uninfected cells collected immediately prior to infection. Doxorubicin was used as a positive control for cellular DNA damage.

We also analyzed virus genome replication and DDR signaling in a panel of tumor cell lines. ΔE1B-55K/ΔE4-ORF3 viral DNA replication is partially rescued in many tumor cell lines, including U2OS, HeLa and H1299, which will be shown in Chapter 4. However, we found that A549 cells exhibit a similar restriction and signaling response to SAECs upon ΔE1B-55K/ΔE4-ORF3 infection. Therefore, we used A549 cells for experiments that required siRNA transfection or large numbers of cells. Adenovirus replication is generally higher and faster in tumor cells and WT virus replication is accelerated by about 12 hours in A549 cells (Figure 2.4A). Similar to SAECs, the levels of WT virus genomes are 10^4 times higher than ΔE1B-55K/ΔE4-ORF3 virus genomes at 36 h.p.i (Figure 2.4A). Furthermore, WT, ΔE4-ORF3, and ΔE1B-55K virus infection induces global DDR kinase phosphorylated substrates: ATM-Ser1981, H2AX-Ser139, TRIM28-Ser824, RPA32-Ser4/Ser8 and DNA-PKcs-Ser2056 (Figure 2.4B). However, DDR phosphorylated substrates are not globally induced in ΔE1B-55K/ΔE4-ORF3 infected A549 cells and are at similar levels to control and ΔE1 infected cells (Figure 2.4B). This is also reflected by quantification of Phospho- to Total-protein ratios (Figure 2.4C).

We additionally analyzed the phosphorylation of CHK1 and CHK2, proteins previously shown to be phosphorylated in response to infection with E4 mutant viruses in HeLa and U2OS cells (Carson et al., 2009; Carson et al., 2003). CHK1-Ser345 and CHK2-Thr68 phosphorylation is induced in response to doxorubicin and is higher in WT versus ΔE1B-55K/ΔE4-ORF3 infected cells (Figure 2.4B). CHK1 phosphorylation appears to be induced in all virus infections and peaks at 24 h.p.i. (Figure 2.4B), suggesting the effects are related to the cell cycle and of no relevance to the defect in

ΔE1B-55K/ΔE4-ORF3 genome replication. This pattern of CHK1 phosphorylation at the midpoint of infection is also observed in SAECs and does not correlate with defective viral genome replication (data not shown). These results demonstrate that ΔE1B-55K/ΔE4-ORF3 infection does not trigger the activation of global DDR phosphorylation and identify A549 cells as a useful cell line for interrogating the anti-viral functions of MRN in experiments that required siRNA transfection and large cell numbers.

Figure 2.4. E1B-55K and E4-ORF3 are also required for Adenovirus genome replication in A549 cells, but do not prevent global DDR signaling in WT infection.

A549 cells were infected with either ΔE1, WT, ΔE4-ORF3, ΔE1B-55K, or ΔE1B-55K/ΔE4-ORF3 viruses and harvested at 12, 24, and 36 h.p.i.
(A) Viral genomes were quantified by Q-PCR and normalized relative to cellular 18S rDNA. Q-PCR was performed in quadruplicate, and error bars indicate standard deviation.
(B) Protein lysates were immunoblotted for MRE11, RAD50, NBS1, Phospho-NBS1-Ser343, H2AX, γH2AX, RPA32, Phospho-RPA32-Ser4/Ser8, and Phospho-DNA-PKcs-Ser2056, CHK1, Phospho-CHK1-Ser345, CHK2, and Phopsho-CHK2-Thr68. β-ACTIN is a loading control. Doxorubicin was used as a positive control to induce cellular DNA damage. Arrows and asterisks indicate specific and non-specific bands respectively.
(C) Quantification of total and phosphorylated protein bands for immunoblots in (B) was determined using a LI-COR Scanner and Odyssey software. The ratio of the total to phosphorylated bands was calculated for each sample. For comparison purposes, the ratios are plotted on the same graph relative to "t = 0".

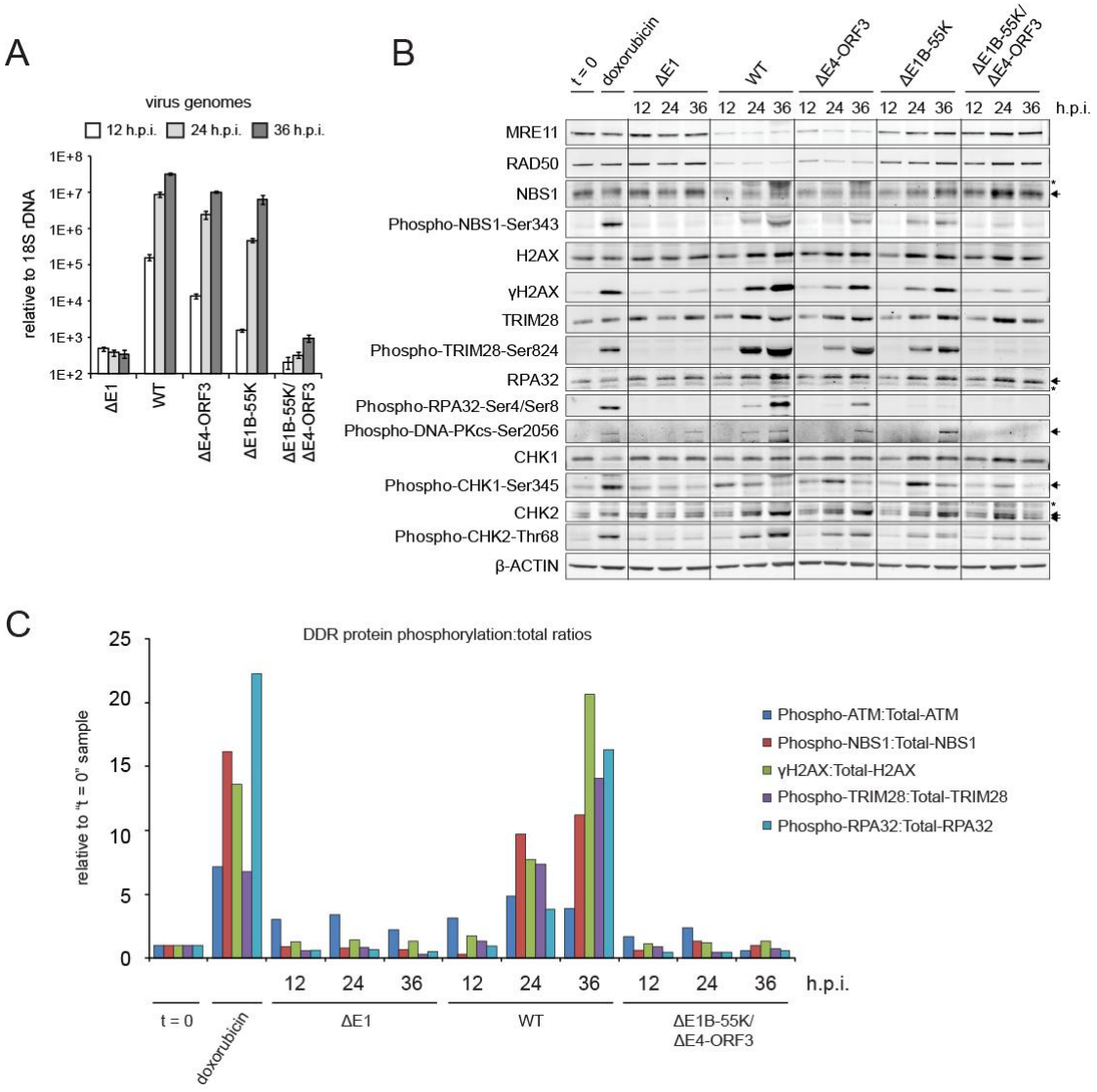
A
virus genomes
12 h.p.i.
24 h.p.i.
36 h.p.i.
relative to 18S rDNA
1E+8
1E+7
1E+6
1E+5
1E+4
1E+3
1E+2
ΔE1
WT
ΔE4-ORF3
ΔE1B-55K
ΔE1B-55K/ ΔE4-ORF3
B
t = 0
doxorubicin
ΔE1
WT
ΔE4-ORF3
ΔE1B-55K
ΔE1B-55K/ ΔE4-ORF3
12 24 36 12 24 36 12 24 36 12 24 36 12 24 36 h.p.i.
MRE11
RAD50
NBS1
Phospho-NBS1-Ser343
H2AX
γH2AX
TRIM28
Phospho-TRIM28-Ser824
RPA32
Phospho-RPA32-Ser4/Ser8
Phospho-DNA-PKcs-Ser2056
CHK1
Phospho-CHK1-Ser345
CHK2
Phospho-CHK2-Thr68
β-ACTIN
C
DDR protein phosphorylation:total ratios
relative to "t = 0" sample
25
20
15
10
5
0
Phospho-ATM:Total-ATM
Phospho-NBS1:Total-NBS1
γH2AX:Total-H2AX
Phospho-TRIM28:Total-TRIM28
Phospho-RPA32:Total-RPA32
12 24 36 12 24 36 12 24 36 12 24 36 h.p.i.
t = 0
doxorubicin
ΔE1
WT
ΔE1B-55K/ ΔE4-ORF3

We conclude that the expression of E1B-55K/E4-ORF3 is critical to facilitate viral genome replication *in vivo*. However, despite normal MRN protein expression levels and distribution within the nucleus, ΔE1B-55K/ΔE4-ORF3 infected cells do not trigger a global cellular DNA damage signaling response. One interpretation is that MRN and the DDR pathway are irrelevant for restricting viral genome replication. However, this is not consistent with the evolution of two independent sets of proteins that target MRN within the diminutive Ad5 genome. Furthermore, previous studies have shown that MRN mutations or knockdown increased viral genome replication in cells infected with E4 mutant viruses (Evans and Hearing, 2005; Lakdawala et al., 2008; Mathew and Bridge, 2007, 2008). Therefore, an alternative interpretation is that the MRN DDR to viral genomes is distinct to that at cellular DNA breaks, and the MRN DDR restricts virus genome replication without triggering the global DDR kinase signaling that is famously associated with its functional activation (Costanzo et al., 2004; Falck et al., 2005; Lee and Paull, 2004, 2005; Uziel et al., 2003). This still leaves unexplained the other confounding observation that WT virus infection triggers global DDR phosphorylation with no apparent effect on virus genome replication (Figures 2.3B and 2.4B), a phenotype also observed previously (Blackford et al., 2008 41; Forrester et al., 2011; Nichols et al., 2009). We reasoned that both paradoxes could be reconciled if global DDR signaling is triggered as a downstream consequence of viral genome replication and after E1B-55K/E4-ORF3 mediated inactivation of a novel MRN DDR, one that would otherwise prevent viral genome replication (Figure 2.8B). The experimental prediction is that knockdown of MRN by RNAi should rescue ΔE1B-

55K/ΔE4-ORF3 virus genome replication, and as a consequence, activate global DDR kinase signaling, analogous to that observed in WT virus infected cells.

Inactivation of MRN by early viral proteins or RNAi is required for logarithmic Adenovirus genome replication, which triggers downstream global DDR signaling

The stable knockdown of MRN is lethal due to its role in normal cellular DNA replication (Adelman et al., 2009; Luo et al., 1999; Xiao and Weaver, 1997; Zhu et al., 2001). Primary SAECs are refractory to transient siRNA transfections, but A549 cells are more amenable and exhibit a similar response to WT and mutant virus infections (Figure 2.4). Therefore, we used A549 cells to determine if RNAi mediated knockdown of MRN components phenocopies the functions of E1B-55K/E4-ORF3 in viral genome replication. A549s were transfected with control non-silencing, *MRE11, RAD50,* or *MRE11* and *RAD50* siRNAs and infected after 48 hours. The simultaneous knockdown of *MRE11* and *RAD50* reduced MRE11 and RAD50 levels by 90% in ΔE1B-55K/ΔE4-ORF3 infected cells compared to control siRNA (Figures 2.5A and 2.5B).

Figure 2.5. MRN blocks ΔE1B-55K/ΔE4-ORF3 viral genome replication irrespective of global DDR signaling.

A549 cells were transfected with 20 nM *control*, *MRE11* or *RAD50* siRNAs. Cells were infected 48 hours post transfection with ΔE1, WT or ΔE1B-55K/ΔE4-ORF3 viruses and harvested at 24 h.p.i.
(A) Protein lysates were immunoblotted for MRE11 and RAD50. β-ACTIN is a loading control. The "t = 0" sample was harvested at the time of virus infection.
(B) Quantification of MRE11 and RAD50 protein bands for immunoblots in (A) was performed using a LI-COR Scanner and Odyssey software. The ratio of MRE11 to β-ACTIN levels and RAD50 to β-ACTIN levels was calculated for ΔE1B-55K/ΔE4-ORF3 immunoblots. For comparison, the ratios are plotted relative to "*control* siRNA" treated cells.
(C) Viral genomes were quantified by Q-PCR and normalized relative to cellular 18S rDNA. Q-PCR was performed in triplicate, and error bars indicate the standard deviation.
(D) Protein lysates were immunoblotted for ATM, Phospho-ATM-Ser1981, H2AX, γH2AX, TRIM28, Phospho-TRIM-Ser824, RPA32, and Phospho-RPA32-Ser4/Ser8.

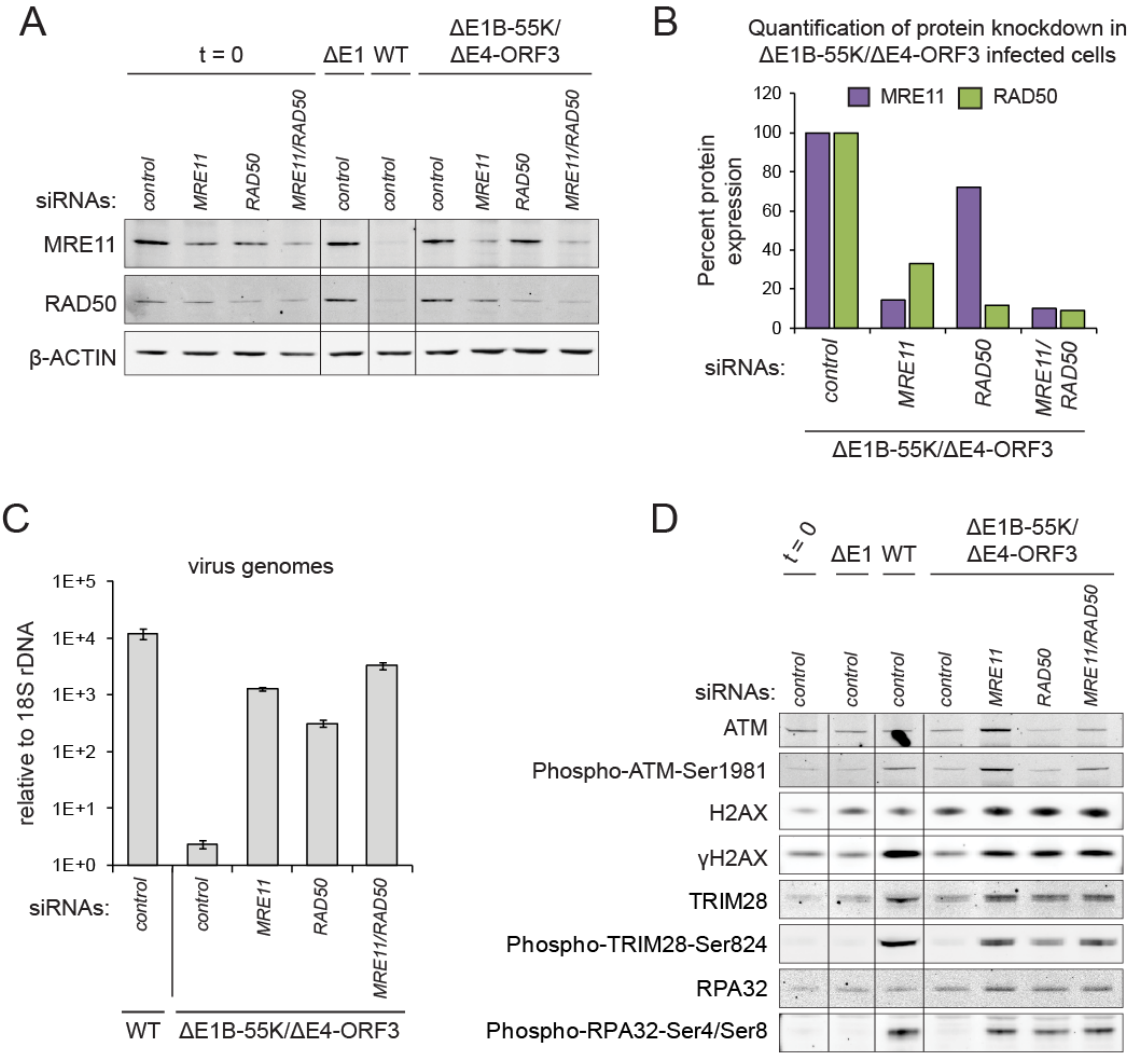
A
t = 0
ΔE1
WT
ΔE1B-55K/
ΔE4-ORF3
siRNAs:
control
MRE11
RAD50
MRE11/RAD50
MRE11
RAD50
β-ACTIN
B
Quantification of protein knockdown in
ΔE1B-55K/ΔE4-ORF3 infected cells
MRE11
RAD50
Percent protein expression
120
100
80
60
40
20
0
siRNAs:
control
MRE11
RAD50
MRE11/
RAD50
ΔE1B-55K/ΔE4-ORF3
C
virus genomes
relative to 18S rDNA
1E+5
1E+4
1E+3
1E+2
1E+1
1E+0
siRNAs:
control
control
MRE11
RAD50
MRE11/RAD50
WT
ΔE1B-55K/ΔE4-ORF3
D
t = 0
ΔE1
WT
ΔE1B-55K/
ΔE4-ORF3
siRNAs:
control
control
control
control
MRE11
RAD50
MRE11/RAD50
ATM
Phospho-ATM-Ser1981
H2AX
γH2AX
TRIM28
Phospho-TRIM28-Ser824
RPA32
Phospho-RPA32-Ser4/Ser8

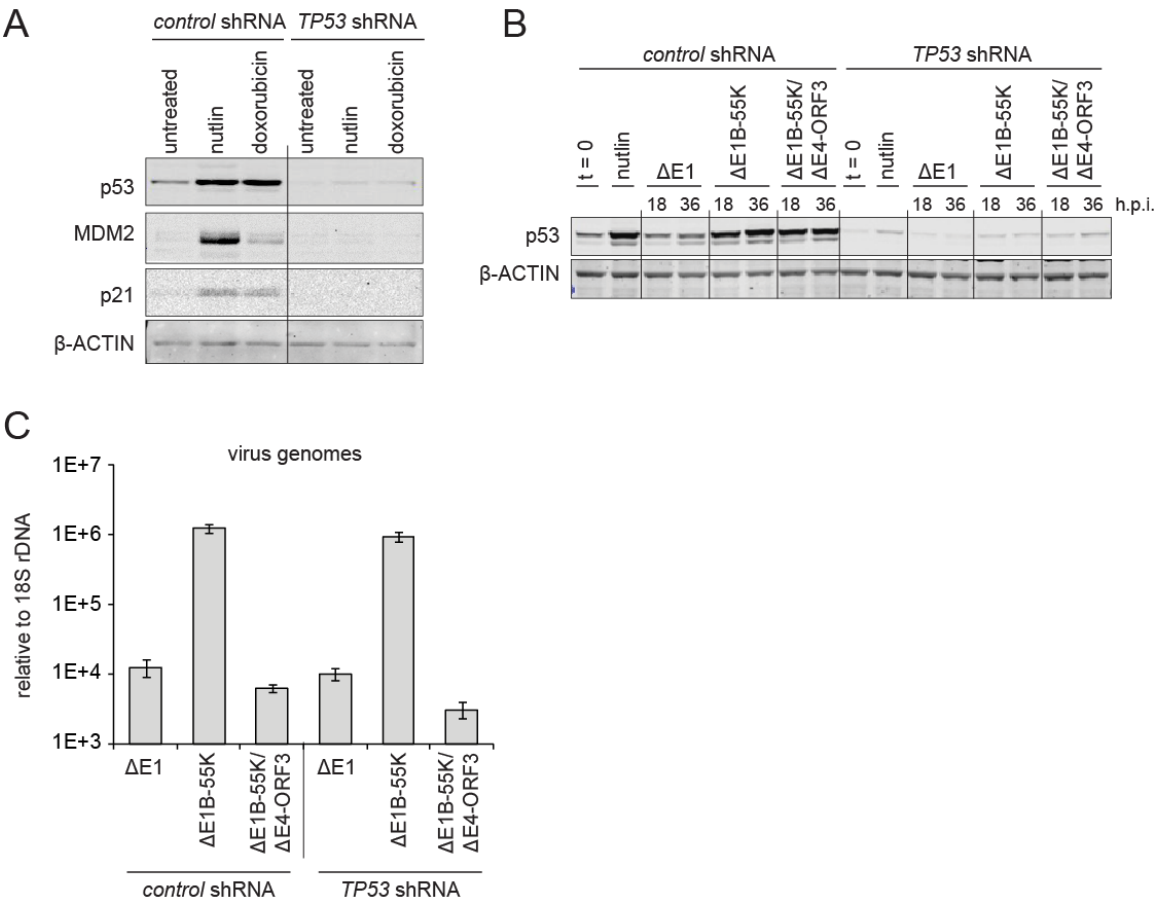

Figure 2.6. *TP53* knockdown is not sufficient to rescue ΔE1B-55K/ΔE4-ORF3 genome replication.

(A) A549 cells stably expressing control shRNA or an shRNA against *TP53* were untreated, or treated with either 10 μM nutlin or 0.5 μg/ml doxorubicin to activate p53. Total protein lysates were immunoblotted for p53, MDM2, and p21. β-ACTIN is a loading control.
(B and C) A549 *control* and *TP53* shRNA stable cell lines were infected with either ΔE1, ΔE1B-55K or ΔE1B-55K/ΔE4-ORF3 viruses. (B) Protein lysates were collected at 18 and 36 h.p.i. and immunoblotted for p53. β-ACTIN is a loading control. (C) Total DNA samples were collected at 36 h.p.i. Viral genomes were quantified by Q-PCR and normalized relative to cellular 18S rDNA. Q-PCR was performed in triplicate, and error bars indicate the standard deviation.

MRE11 and *RAD50* siRNAs rescue ΔE1B-55K/ΔE4-ORF3 viral genome replication by 558- and 135-fold, respectively (Figure 2.5C). The combined knockdown of *MRE11* and *RAD50* (*MR* knockdown) results in the greatest rescue of viral genome replication, 1405-fold relative to control siRNA (Figure 2.5C). This demonstrates that MRN restricts ΔE1B-55K/ΔE4-ORF3 viral genome replication. In addition to inactivating MRN, E1B-55K and E4-ORF3 also have overlapping functions in inactivating the p53 transcription factor (Soria et al., 2010), which can phosphorylated downstream of MRN in response to DNA damage (Uziel et al., 2003). Therefore, we explored the possibility that in addition to MRN, p53 plays a role in restricting ΔE1B-55K/ΔE4-ORF3 viral genome replication. We generated A549 cells stably expressing an shRNA targeting *TP53*, which encodes for the p53 protein. A549 cells expressing the *TP53* shRNA show significantly reduced p53 protein expression and induction of p53 targets, MDM2 and p21, upon treatment with nutlin or doxorubicin, activators of p53 (Figure 2.6A). However, in contrast to *MR* knockdown, knockdown of *TP53*, does not rescue ΔE1B-55K/ΔE4-ORF3 viral genome replication (Figures 2.6B and 2.6C). These results were reproduced in SAECs, in which p53 activation is not compromised by mutations in cancer cells (data not shown). We conclude that MRN inactivation is the critical target of E1B-55K/E4-ORF3 that is required for viral genome replication, irrespective of its role in modulating p53.

To determine if the rescue of viral genome replication by *MR* knockdown activates global DDR signaling in ΔE1B-55K/ΔE4-ORF3, we analyzed H2AX, TRIM28, and RPA32, which are phosphorylated in WT virus infected cells (Figures 2.2B and 2.4B). Strikingly, *MR* knockdown induces H2AX, TRIM28, and RPA32

phosphorylation in ΔE1B-55K/ΔE4-ORF3 infected cells (Figure 2.5D), analogous to WT virus infected cells, in which MRN is inactivated by E1B-55K and E4-ORF3. In an independent experiment, we compared the effects of *MR* knockdown in cells infected with ΔE1, WT or ΔE1B-55K/ΔE4-ORF3 viruses. WT virus infection in *control* siRNA transfected cells leads to high levels of virus genomes and global DDR phosphorylation (Figure 2.7). *MR* knockdown does not logarithmically increase WT virus genome replication (Figure 2.7A) or prevent the induction of global DDR phosphorylated substrates (Figure 2.7B). We conclude that global DDR signaling is triggered through an MRN independent mechanism and is unlikely to be triggered by residual MRN expression in WT virus infected cells. Furthermore, *MR* knockdown induces global DDR phosphorylated substrates upon ΔE1B-55K/ΔE4-ORF3 but not control ΔE1 virus infection (Figure 2.7B). These data strongly suggest that global DDR kinase signaling is activated as a consequence of *MR* knockdown rescuing ΔE1B-55K/ΔE4-ORF3 viral genome replication and the accumulation of high levels of viral genomes. If this is the case, then inhibiting viral genome replication during WT infection should prevent global DDR kinase signaling (Figure 2.8B).

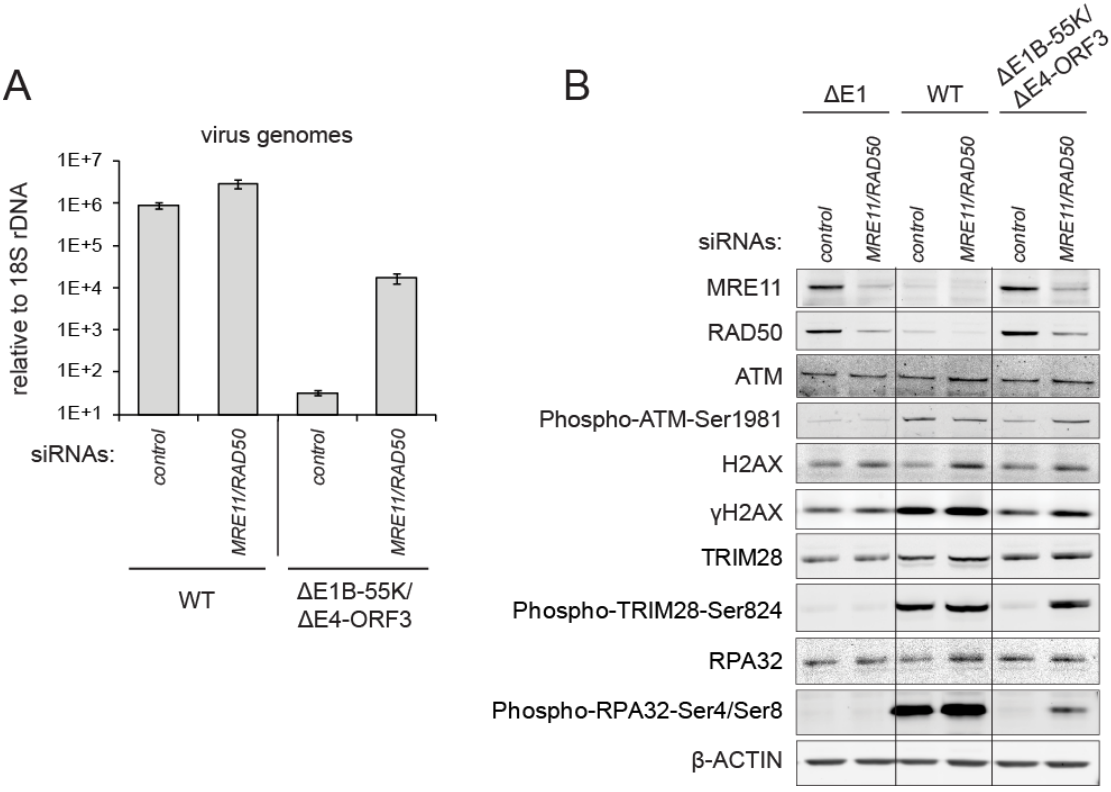

Figure 2.7. Inactivation of MRN by E1B-55K/E4-ORF3 or RNAi is necessary for Adenovirus genome replication that activates downstream global DDR signaling.

A549 cells were transfected with *control* siRNAs or siRNAs against both *MRE11* and *RAD50* at a total concentration of 20 nM. Cells were infected 48 hours post transfection with ΔE1, WT, or ΔE1B-55K/ΔE4-ORF3 viruses and harvested at 24 h.p.i.
(A) Viral genomes were quantified by Q-PCR and normalized relative to cellular 18S rDNA. Q-PCR was performed in triplicate, and error bars indicate the standard deviation.
(B) Protein lysates were immunoblotted for MRE11, RAD50, ATM, Phospho-ATM-Ser1981, H2AX, γH2AX, TRIM28, Phospho-TRIM-Ser824, RPA32, and Phospho-RPA32-Ser4/Ser8. β-ACTIN is a loading control.

The global activation of DDR phosphorylated substrates is a downstream consequence of Adenovirus genome replication and MRN inactivation

Adenovirus E1A activates E2F transcription of cellular and viral genes that drive cellular S phase entry and the concomitant replication of Adenovirus genomes (Ben-Israel and Kleinberger, 2002; O'Shea et al., 2004). The early rounds of DNA replication on incoming double stranded Adenovirus genomes are semi-conservative, but later rounds are initiated from displaced single strand DNA that assemble at high concentrations in specialized replication domains in the nucleus with the viral single strand DNA binding protein E2A (Knipe and Howley, 2013). WT, ΔE1B-55K, ΔE4-ORF3 virus infection in SAECs triggers the assembly of E2A viral replication domains over the course of infection, coincident with the replication of viral genomes (Figure 2.8A). In contrast, in ΔE1B-55K/ΔE4-ORF3 infected cells, E2A is diffuse in the nucleus (Figure 2.8A), consistent with MRN preventing viral genome replication at the earliest stages that precede the formation of E2A viral replication domains (Figure 2.8B).

Furthermore, the assembly of E2A viral genome replication centers is coincident with the activation of DDR phosphorylated substrates (Figures 2.2B and 2.4B). We hypothesized that high concentrations of viral genomes trigger the MRN independent activation of DDR kinases (Figure 2.8B). To dissociate the effects of cellular and viral genome replication, we treated WT virus infected cells with hydroxyurea (HU) or aphidicolin. The effects of HU and aphidicolin on cellular and viral DNA replication were assessed by measuring total DNA content or by quantifying viral genomes by Q-PCR, respectively. HU inhibits the synthesis of deoxynucleotide precursors and

prevents both cellular and viral DNA replication (Figures 2.9A-C). At low concentrations (1 μM), aphidicolin inhibits cellular DNA replication by eukaryotic DNA polymerases α and γ, but not viral DNA replication by Adenovirus E2B polymerase (Figures 2.9A-C) (Foster et al., 1982; Kwant and van der Vliet, 1980). HU but not aphidicolin, inhibits viral genome replication and the phosphorylation of H2AX, DNA-PKcs, TRIM28, and RPA32 in WT virus infected cells (Figure 2.9D). Thus, blocking viral DNA replication, but not cellular DNA replication, prevents global DDR kinase phosphorylation during WT virus replication. We conclude that global DDR kinase phosphorylation is activated through an MRN independent mechanism as a downstream consequence of viral genome replication during WT adenovirus infection.

Given that ATM and its related kinases phosphorylate overlapping targets, we investigated the contribution of ATM in DDR phosphorylation during WT virus infection and whether ATM is activated independently of MRN. We treated WT virus infected cells with an ATM kinase inhibitor KU-55933 (Hickson et al., 2004). KU-55933 reduces the induction of ATM, H2AX, RPA32, TRIM28 and DNA-PKcs phosphorylation in response to WT virus replication and doxorubicin treatment (Figure 2.10A). However, KU-55933 reduces the levels of DDR phosphorylated substrates less than HU (Figure 2.10A). This demonstrates that ATM is indeed activated during WT virus infection, upon which MRN is degraded, and is responsible for the phosphorylation of several DDR proteins during WT Adenovirus infection. However, other DDR kinases are also independently activated by WT infection and contribute to the global DDR phosphorylation phenotype. We also investigated whether ATM activation during WT virus infection is required for viral replication. Treatment with

KU-55933 has no impact on virus genome replication in WT virus infected cells (Figure 2.10B). We conclude that the global activation of ATM and DDR kinases occurs after the critical MRN DDR checkpoint through an MRN independent mechanism and does not impact viral genome replication.

Taken together, these data demonstrate that MRN functions as a critical early cellular checkpoint to viral genome replication. Inactivation of MRN by E1B-55K/E4-ORF3 or RNAi is required for the logarithmic replication of viral genomes. In WT virus infected cells, high concentrations of viral genomes assemble late E2A replication domains and trigger global DDR kinase signaling through an MRN independent mechanism. In ΔE1B-55K/ΔE4-ORF3 infected cells, MRN prevents viral genome replication, but does not activate canonical global cellular DDR signaling. Thus, using the widely used metric by which MRN functional activation is determined, the phosphorylation of downstream signaling components, is not sufficient to detect its activation in such an anti-viral context. This may explain why the critical MRN anti-viral DDR has been difficult to deconvolute.

Chapter acknowledgements

The contents of this chapter, in full, has been submitted for publication of the material as it may appear in Cell, 2015, Shah, G.S. and O'Shea, C.C. The dissertation author was the first author of this paper, and Clodagh C. O'Shea was the senior author, supervising this work.

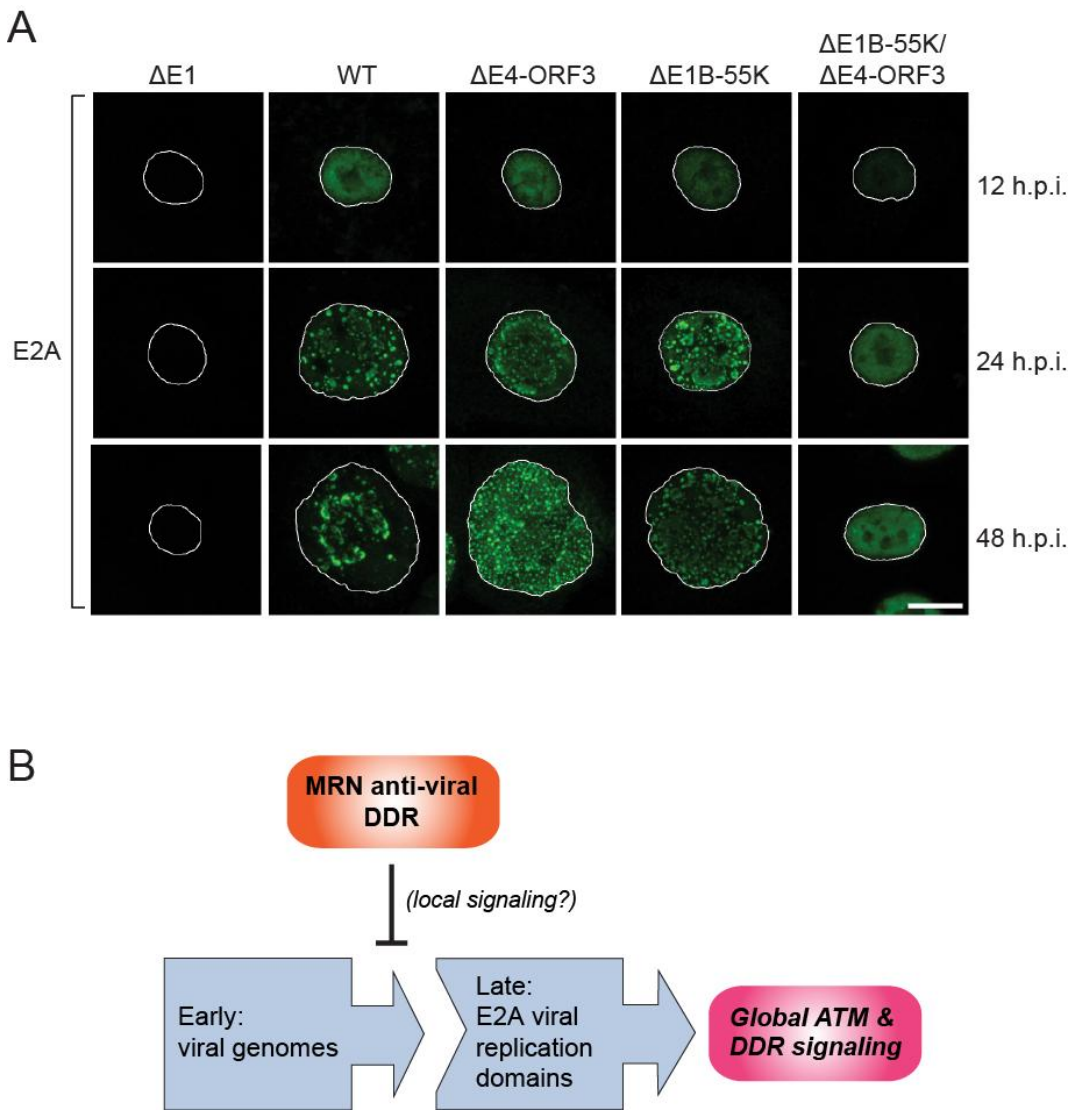

Figure 2.8. Adenovirus genome replication and the formation of E2A viral replication domains is coincident with global ATM and DDR kinase signaling.

(A) The MRN DDR checkpoint prevents the replication of viral genomes at the earliest stages. MRN inactivation enables logarithmic viral genome replication. High concentrations of viral genome assemble with the E2A single strand DNA binding protein in late replication domains that trigger global ATM and DDR signaling.
(B) SAECs were infected with ΔE1, WT, ΔE4-ORF3, ΔE1B-55K, or ΔE1B-55K/ΔE4-ORF3 viruses, fixed at 12, 24, and 48 h.p.i. Late virus genome replication domains were visualized by staining for Adenovirus E2A (green). Nuclei were counterstained with Hoechst-33342 and outlined in white. Representative images are shown. Scale bar: 10 μm.

Figure 2.9. Global DDR kinase phosphorylation is activated through an MRN independent mechanism as a downstream consequence of Adenovirus genome replication.

Quiescent SAECs were infected with ΔE1 and WT viruses. WT infected cells were untreated or treated with either 2 mM hydroxyurea (HU) or 1 μM aphidicolin at 2 h.p.i. and analyzed at 12, 24, 36, and 48 h.p.i.
(A) Diagram of the differential effects of hydroxyurea (HU) and aphidicolin on viral versus cellular DNA replication.
(B) Virus genomes were quantified by Q-PCR and normalized relative to cellular 18S rDNA. Q-PCR was performed in triplicate, and error bars indicate the standard deviation.
(C) Cells were fixed at 48 h.p.i., stained with Hoechst, and imaged for DNA fluorescence. The percentage of cells with DNA content of 2N or >2N are indicated.
(D) Protein lysates were immunoblotted for ATM, Phospho-ATM-Ser1981, H2AX, γH2AX, TRIM-28, Phospho-TRIM28-Ser824, RPA32, Phospho-RPA32-Ser4/Ser8, DNA-PKcs, and Phospho-DNA-PKcs-Ser2056. β-ACTIN is a loading control. Doxorubicin was used as a positive control to induce cellular DNA damage. Arrow indicates specific band.

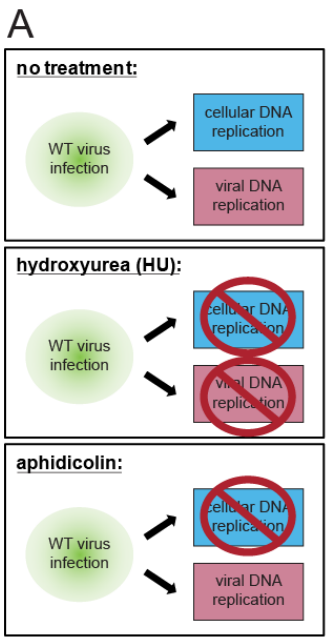
A
no treatment:
WT virus infection
cellular DNA replication
viral DNA replication
hydroxyurea (HU):
WT virus infection
cellular DNA replication
viral DNA replication
aphidicolin:
WT virus infection
cellular DNA replication
viral DNA replication

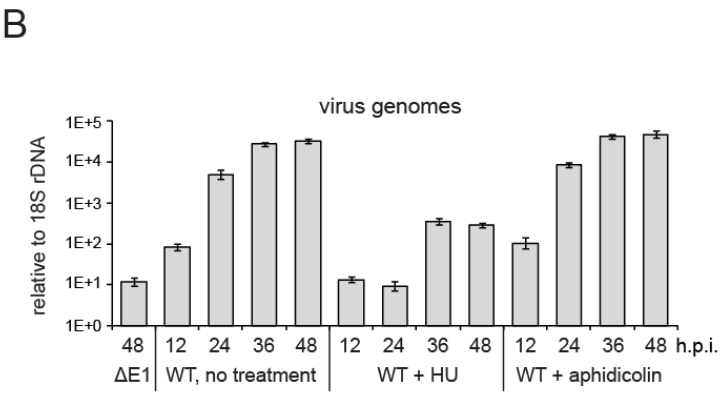
B
virus genomes
relative to 18S rDNA
1E+5
1E+4
1E+3
1E+2
1E+1
1E+0
48 12 24 36 48 12 24 36 48 12 24 36 48 h.p.i.
ΔE1
WT, no treatment
WT + HU
WT + aphidicolin

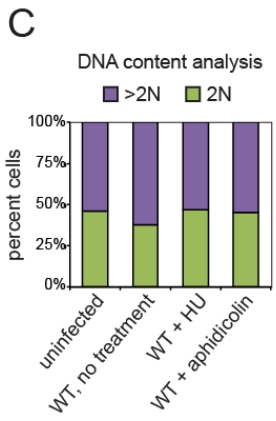
C
DNA content analysis
>2N
2N
percent cells
100%
75%
50%
25%
0%
uninfected
WT, no treatment
WT + HU
WT + aphidicolin

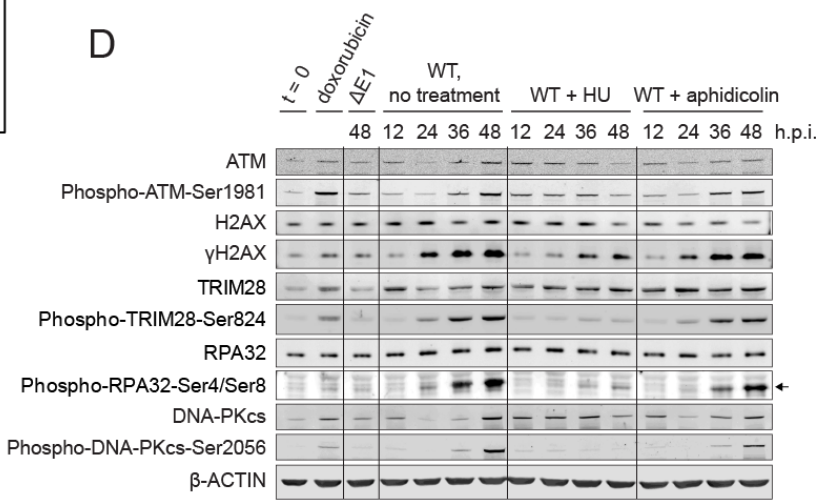
D
t = 0
doxorubicin
ΔE1
WT, no treatment
WT + HU
WT + aphidicolin
48 12 24 36 48 12 24 36 48 12 24 36 48 h.p.i.
ATM
Phospho-ATM-Ser1981
H2AX
γH2AX
TRIM28
Phospho-TRIM28-Ser824
RPA32
Phospho-RPA32-Ser4/Ser8
DNA-PKcs
Phospho-DNA-PKcs-Ser2056
β-ACTIN

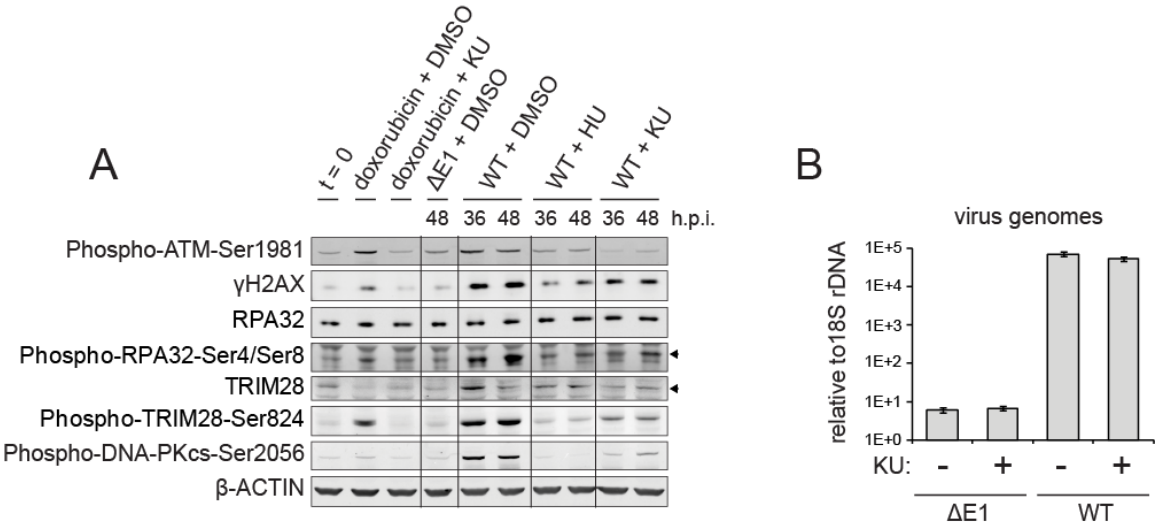

Figure 2.10. ATM is activated through an MRN independent mechanism during WT infection and contributes to DDR kinase signaling.

(A) SAECs were infected with ΔE1 or WT viruses. WT virus infected cells were treated with solvent (DMSO), 2 mM HU or 10 μM ATM inhibitor KU-55933 (KU) at 2 h.p.i. Doxorubicin was used as a positive control for cellular DNA damage. As a control for KU treatment, doxorubicin was added to cells either with DMSO or KU. Protein lysates were harvested at 36 or 48 h.p.i., normalized by cell number, and immunoblotted for Phospho-ATM-Ser1981, γH2AX, RPA32, Phospho-RPA32-Ser4/Ser8, TRIM-28, Phospho-TRIM28-Ser824 and Phospho-DNA-PKcs-Ser2056. β-ACTIN is a loading control. Arrows indicate specific bands.
(B) SAECs were infected with ΔE1 and WT viruses and treated with solvent, DMSO (-) or 10 μM KU (+) at 2 h.p.i. Total DNA samples were collected at 48 h.p.i. Virus genomes were quantified by Q-PCR and normalized relative to cellular 18S rDNA. Q-PCR was performed in triplicate, and error bars indicate the standard deviation.

Chapter 3. MRN-ATM activation localized at virus genomes restricts viral but not cellular genome replication

MRN senses replicating virus genomes and recruits ATM that activates a local DDR to prevent viral genome replication.

In response to DSBs, MRN senses and binds to DSBs where it recruits and activates ATM (Figure 3.1) (Costanzo et al., 2004; Falck et al., 2005; Lee and Paull, 2004, 2005; Uziel et al., 2003). As shown in Chapter 2, MRN restricts ΔE1B-55K/ΔE4-ORF3 virus genome replication; however, it does so without triggering global DDR signaling. We investigated whether MRN then restricts virus genome replication irrespective of sensing and binding to viral DNA, through an altogether novel mechanism. To determine if MRN senses and binds to Adenovirus genomes, we performed MRE11 chromatin immunoprecipitation (ChIP) on A549 cells that had been infected with ΔE1, WT, ΔE4-ORF3, ΔE1B-55K, or ΔE1B-55K/ΔE4-ORF3 viruses. The association of MRE11 with viral genomes was quantified by Q-PCR using two sets of primers that amplify sequences at the left (Ad5 PS1) and right (Ad5 PS2) ends of the genome in WT and mutant viruses.

MRE11 binds to viral genomes in ΔE1B-55K/ΔE4-ORF3 infected cells but not WT, ΔE4-ORF3 or ΔE1B-55K infected cells (Figure 3.2A). These data demonstrate that either MRN degradation by E1B-55K or mislocalization by E4-ORF3 is sufficient to prevent MRN binding to viral genomes (Figure 3.2A). Furthermore, this result in consistent with MRN restricting ΔE1B-55K/ΔE4-ORF3 genome replication through sensing and binding viral DNA, analogous to its role in response to cellular DNA

breaks.

Interestingly, MRE11 does not bind to ΔE1 virus genomes (Figure 3.2A). ΔE1 is a replication incompetent vector and control for infection with virus genomes (Figures 2.1B and 2.4A). In contrast to ΔE1 virus vectors, ΔE1B-55K/ΔE4-ORF3 viruses initiate limited replication as evidenced by a two- to three-fold increase in viral genome copies over the timecourse of infection (Figures 2.2A and 2.4A). This was verified by performing absolute quantification of viral genome copies from nuclei purified from infected A549 cells (Figure 3.2B). ΔE1B-55K/ΔE4-ORF3 infection results in roughly 10 average genome copies per nucleus at 2 h.p.i. and roughly 35 average genomes copies per nucleus at 48 h.p.i. (Figure 3.2B). These data are consistent with ΔE1B-55K/ΔE4-ORF3 viruses initiating viral genome replication, despite a tremendous defect in genome replication in comparison to WT.

We hypothesized that MRN specifically senses replicating Adenovirus genomes at early stages of infection. To test this, we treated ΔE1B-55K/ΔE4-ORF3 infected A549 cells with inhibitors of viral DNA replication. Hydroxyurea and 5-fluorouracil block deoxynucleotide synthesis. Camptothecin blocks topoisomerase class I activity, which is required for robust Adenovirus DNA replication (Nagata et al., 1983). Roscovitine inhibits Cdk activity and E1A transcriptional activation, which are required for multiple steps of Adenovirus replication (Fax et al., 2000). Treatment with either class of viral genome replication inhibitors prevents MRE11 recruitment to ΔE1B-55K/ΔE4-ORF3 viral genomes (Figure 3.3B). We conclude that MRN senses and restricts replicating viral genomes at the earliest stages of viral genome replication such that it prevents further viral genome replication. Furthermore, MRN inactivation by

E1B-55K/E4-ORF3 is required to prevent MRN sensing and binding viral genomes.

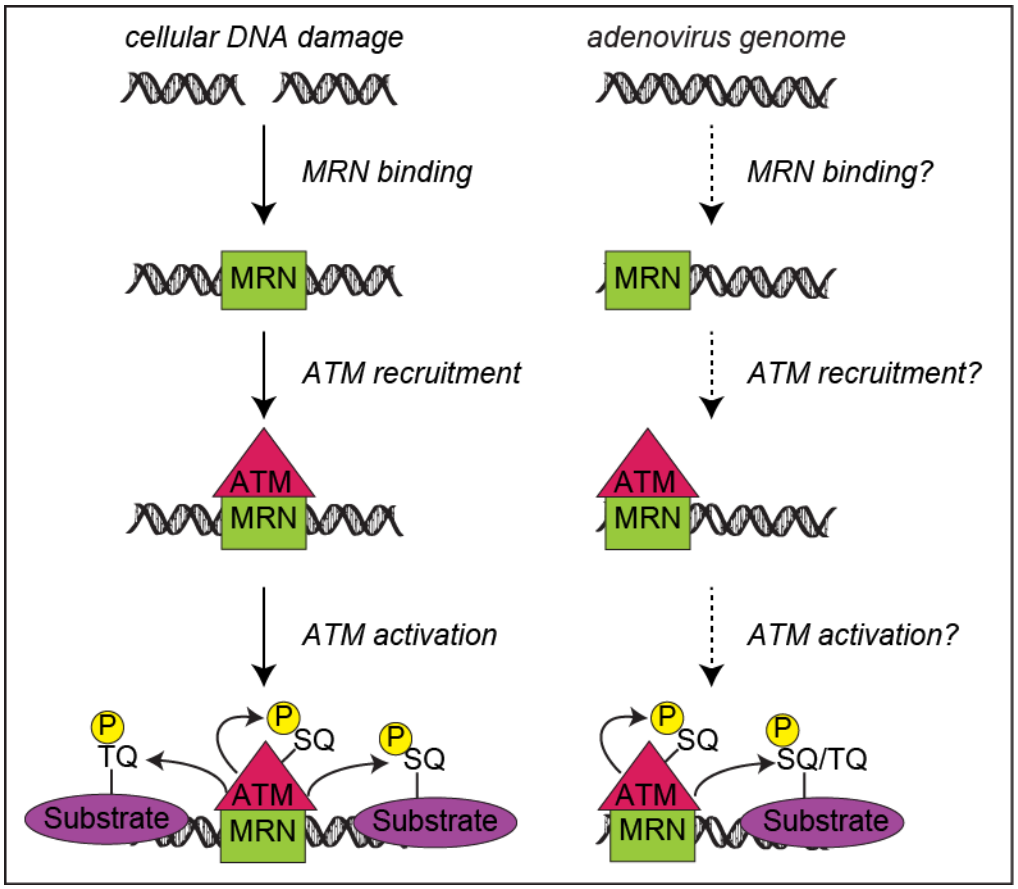

Figure 3.1. MRN activation at cellular DNA breaks recruits and activates ATM.

Cellular DNA breaks are first sensed by MRN, which recruits ATM and activates ATM induced phosphorylation of SQ/TQ peptide motifs on DDR protein substrates. A major question is if MRN binds to viral genomes and activates a localized ATM DDR to prevent viral genome replication.

To determine if MRN recruits ATM at viral genomes, similar to its role at cellular DNA breaks, we performed ChIP for MRE11 and ATM. Additionally, we performed ChIP with antibodies that target epitopes with the preferred phosphorylated SQ/TQ substrate motifs for ATM and related kinases (Kim et al., 1999; O'Neill et al., 2000). To facilitate side-by-side comparisons on the same graph, the different antibody ChIPs are plotted as fold enrichment relative to ΔE1 samples (Figure 3.2D). Total ATM protein levels are similar in WT and ΔE1B-55K/ΔE4-ORF3 infected cells (Figures 2.5D and 2.7B). However, ATM and SQ/TQ phosphorylated epitopes are enriched at viral genomes in ΔE1B-55K/ΔE4-ORF3 infected cells but not WT or ΔE1 infected cells (Figure 3.2D). This mirrors the binding of MRE11 to ΔE1B-55K/ΔE4-ORF3 genomes (Figure 3.2D). This result demonstrates that MRE11 and ATM localize to ΔE1B-55K/ΔE4-ORF3 viral genomes, consistent with the model that MRN restriction of viral genome replication is dependent on MRN binding and localization to viral genomes.

We conclude that MRN and ATM sense and bind replicating ΔE1B-55K/ΔE4-ORF3 genomes. These results are most consistent with the model that, similar to its response to cellular DSBs, MRN senses and binds viral genomes, where it recruits ATM and triggers the localized activation of DDR phosphorylation through ATM. In contrast to its function in response to cellular DSBs, MRN-ATM localization to ΔE1B-55K/ΔE4-ORF3 viral genomes during infection is not sufficient to trigger global DDR phosphorylation as demonstrated in Chapter 2.

An important feature of MRN-ATM activation at cellular DSBs is the spreading of MRN-ATM activation up to megabase long regions across chromosomes, which is a critical mechanism by which the DDR enacts cell cycle arrest (Polo and Jackson, 2011).

We therefore analyzed the spread of MRN-ATM across viral genomes by using additional Q-PCR primers that detect the middle of the Adenovirus genome within our ChIP assay. For the purpose of comparing enrichment across primer sets, data was expressed as percent input. MRE11, ATM, and phosphorylated SQ/TQ substrates are enriched to much higher levels at the ends of ΔE1B-55K/ΔE4-ORF3 viral genomes than to the middle (Figure 3.3). This demonstrates that MRN-ATM activation localizes primarily to the ends of ΔE1B-55K/ΔE4-ORF3 genomes, with only limited spreading across the viral genome. These data demonstrate a key difference between cellular and anti-viral DDR and are consistent with the initial sensing of the viral genome ends, where enrichment of MRE11, ATM, and phosphorylated SQ/TQ motifs are highest. Paradoxically, the ends of ΔE1 Adenovirus genomes are not sufficient to trigger MRN-ATM sensing and binding, despite the absence of E1B-55K/E4-ORF3 expression (Figures 2.1B and 3.2A). Thus, while binding occurs at the ends of viral genomes, the ends themselves are not sufficient to trigger MRN-ATM binding. Of note, Adenovirus genome replication occurs at either end of the genome where the replication origins are located within inverted terminal repeat sequences (Knipe and Howley, 2013). Therefore, taken together, the best explanation for these results is that, in the absence of E1B-55K/E4-ORF3 expression, MRN senses a product or intermediate of viral genome replication at or near the ends of viral genomes, where replication origins are located, and this stops further genome replication.

Figure 3.2. MRN recruits and locally activates ATM at ΔE1B-55K/ΔE4-ORF3 viral genomes.

(A) A549 cells were infected with either ΔE1, WT, ΔE4-ORF3, ΔE1B-55K or ΔE1B-55K/ΔE4-ORF3 viruses and harvested for ChIP analysis at 12 h.p.i. ChIP was performed using MRE11 antibodies or an IgG control. Virus genomes were quantified by Q-PCR using two independent primer sets that amplify the left and right ends of the Ad5 genome, Primer Set 1 (Ad5 PS1) and Primer Set 2 (Ad5 PS2). Data is expressed as percent input. Q-PCR was performed in quadruplicate and error bars indicate the standard deviation.
(B) A549 cells were infected with ΔE1 or ΔE1B-55K/ΔE4-ORF3 viruses. Total nuclear DNA was collected at 2, 24, and 48 h.p.i. Absolute copies of virus genomes were determined by Q-PCR using a standard curve. Q-PCR was performed in triplicate, and error bars indicate the standard deviation. Top, data is graphed as virus genome copies relative to 2 h.p.i. Bottom, data is expressed as average genome copies per nucleus.
(C) A549 cells were infected with ΔE1 or ΔE1B-55K/ΔE4-ORF3 viruses. ΔE1B-55K/ΔE4-ORF3 infected cells were untreated or treated with 2 mM hydroxyurea and 50 µg/ml 5-flurouracil (H/F), 10 mM camptothecin (campt), 20 µM roscovitine (rosco) at 2 h.p.i. An equal volume of DMSO was added to all samples. Cells were harvested for ChIP analysis at 12 h.p.i. ChIP was performed using MRE11 antibodies. An IgG control (not shown) yielded less than 0.05% input in all samples. Virus genomes were quantified using Ad5 PS1 and Ad5 PS2 as in (A). Data is expressed as fold enrichment relative to the ΔE1 ChIP sample.
(D) A549 cells were infected with ΔE1, WT or ΔE1B-55K/ΔE4-ORF3 viruses and harvested for ChIP analysis at 12 h.p.i. ChIP was performed using MRE11, ATM and Phospho-SQ/TQ substrate motif antibodies. An IgG control (not shown) yielded less than 0.05% input in all samples. Virus genomes were quantified using Ad5 PS1 and Ad5 PS2 as in (A). For comparison, MRE11, ATM and Phospho-SQ/TQ ChIPs are plotted on the same graph as fold enrichment relative to ΔE1 ChIP samples.

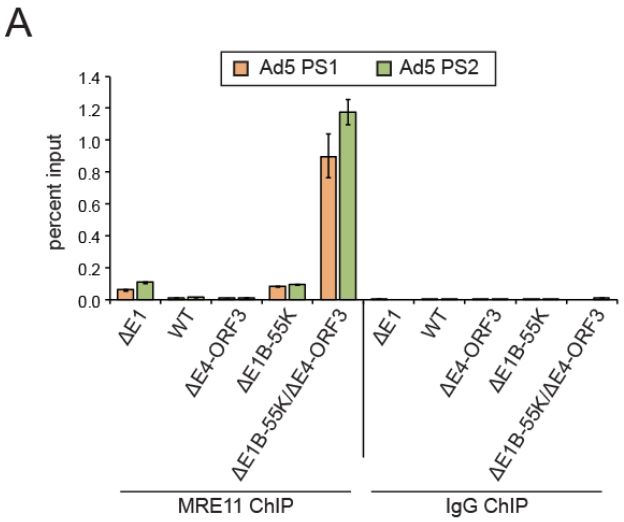

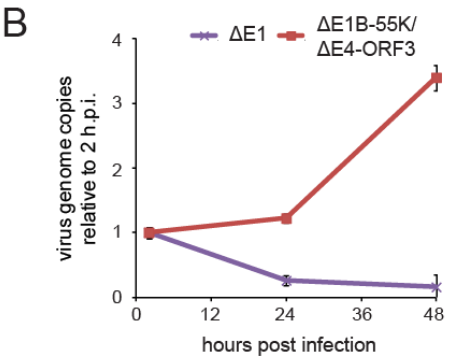

average genome copies per nucleus			
h.p.i.	2	24	48
ΔE1	61.0 ± 5.6	15.7 ± 0.7	9.6 ± 0.4
ΔE1B-55K/ ΔE4-ORF3	10.4 ± 0.9	12.7 ± 0.7	35.4 ± 2.0

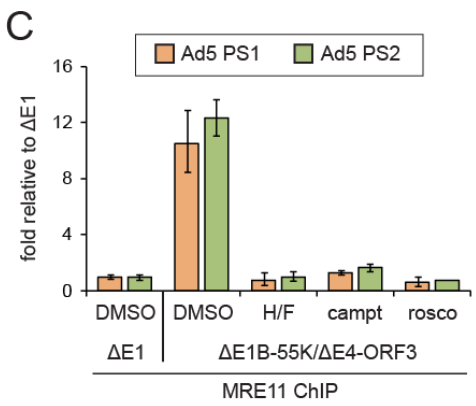

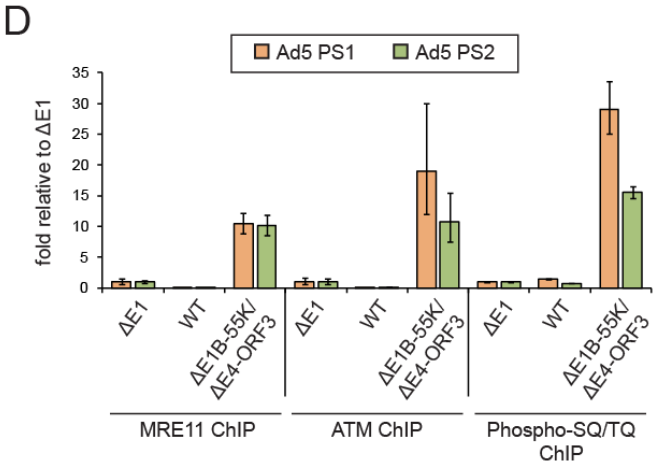

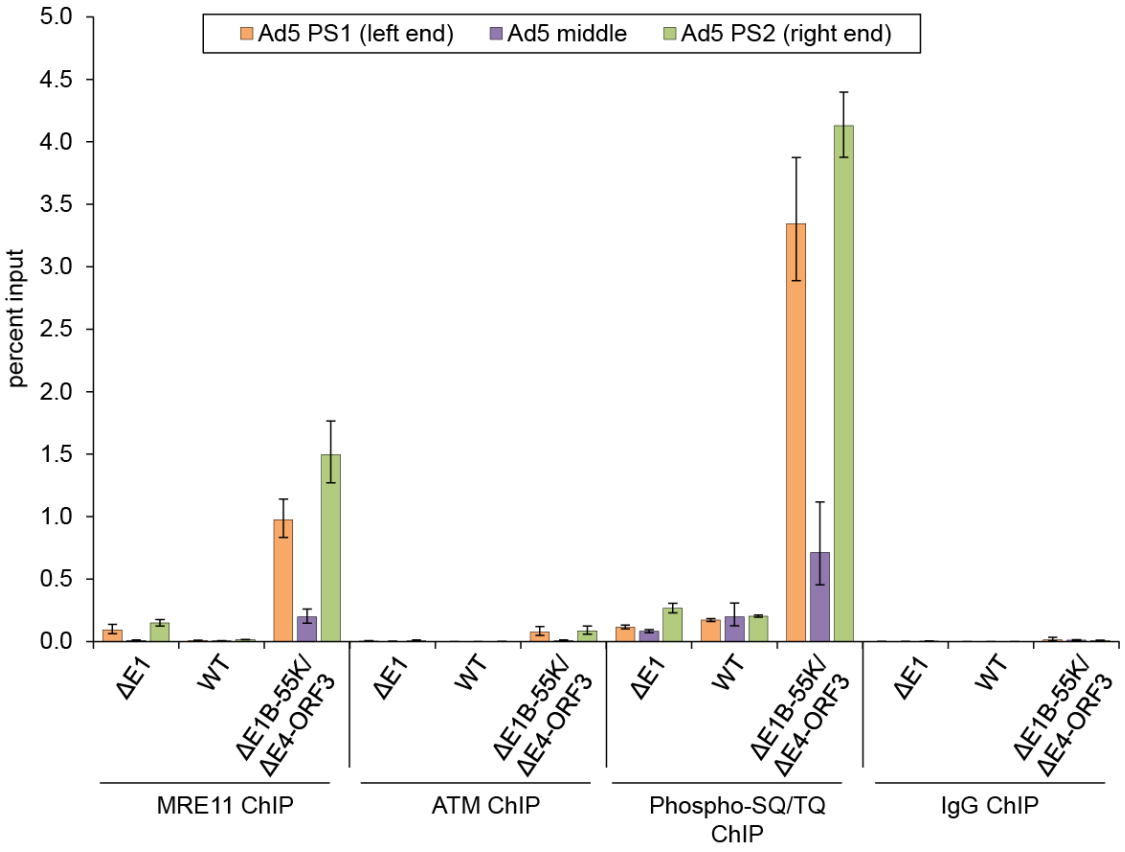

Figure 3.3. MRN-ATM localizes to the ends of ΔE1B-55K/ΔE4-ORF3 virus genomes.

A549 cells were infected with ΔE1, WT or ΔE1B-55K/ΔE4-ORF3 viruses and harvested for ChIP at 12 h.p.i. as in Figure 3.2D. Virus genomes were quantified by Q-PCR using three independent primer sets that amplify the left end, middle, and right end regions of the Ad5 genome: Ad5 PS1, Ad5 middle, and Ad5 PS2, respectively. For comparison of individual primer sets within each sample, data is expressed as percent input. Q-PCR was performed in quadruplicate and error bars indicate the standard deviation.

To determine if ATM kinase activation at viral genome prevents viral genome replication through a localized signaling response, we treated ΔE1B-55K/ΔE4-ORF3 infected cells with an ATM kinase inhibitor, KU-55933 (Hickson et al., 2004). If localized ATM activation contributes to the restriction of viral genome replication, treatment with KU-55933 would rescue ΔE1B-55K/ΔE4-ORF3 genome replication. Consistent with previous experiments (Figures 2.2 and 2.4), ΔE1B-55K/ΔE4-ORF3 infection does not trigger global levels of ATM phosphorylated substrates in total lysates from ΔE1B-55K/ΔE4-ORF3 infected A549 cells and SAECs (Figures 3.4A and 3.4D). However, despite this, treatment with KU-55933 rescues viral genome replication in both ΔE1B-55K/ΔE4-ORF3 infected A549 cells and SAECs by roughly 10-fold (Figures 3.4B and 3.4D). This result demonstrates that ATM kinase activity contributes to restricting ΔE1B-55K/ΔE4-ORF3 genome replication, and, in parallel to its role in response to cellular DSBs, this result is consistent with ATM activation functioning downstream of MRN sensing viral genomes. However, the degree of rescue of ΔE1B-55K/ΔE4-ORF3 viral genome replication by ATM inhibition is less than that by *MR* knockdown (Figures 2.5C and 2.7B). This is consistent with ATM playing an auxiliary role in the MRN anti-viral DDR. Taken together, with the enrichment of MRN-ATM at ΔE1B-55K/ΔE4-ORF3 viral genomes (Figure 2.4), we conclude that MRN, in concert with ATM, restricts viral genome replication through a localized anti-viral DDR that includes ATM kinase activation, but neither triggers nor requires global activation of DDR phosphorylation.

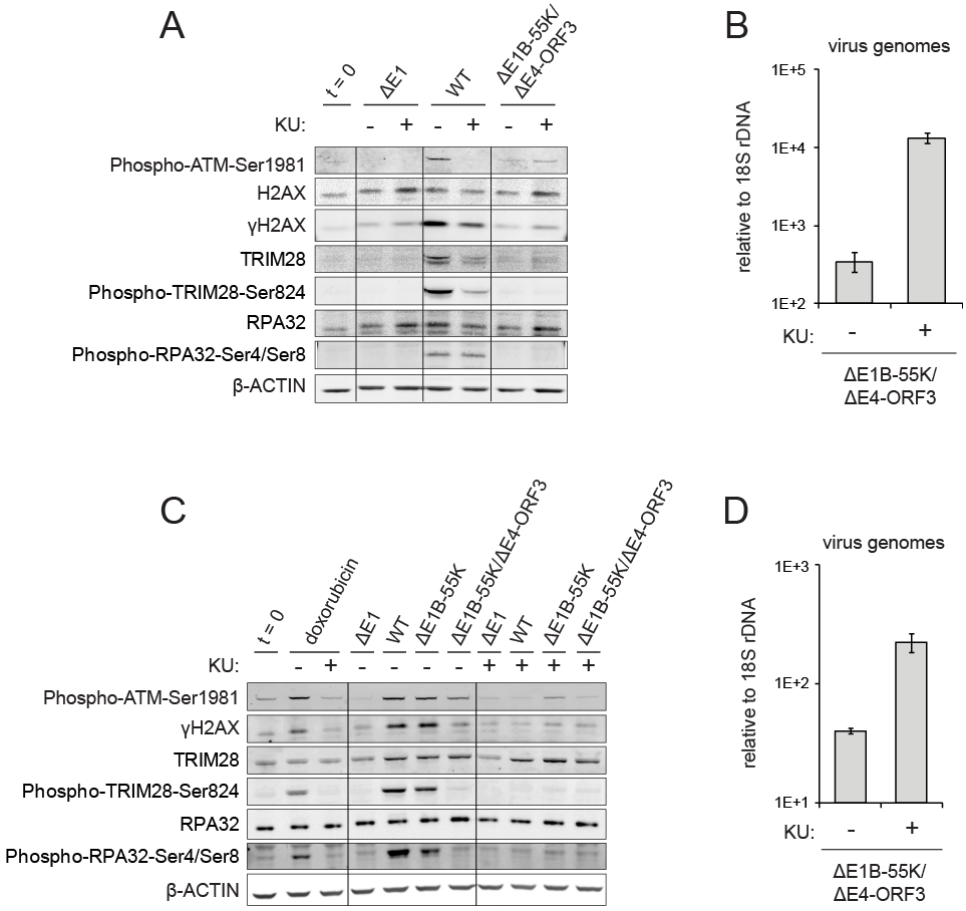

Figure 3.4. ATM kinase activity contributes to MRN restriction of ΔE1B-55K/ΔE4-ORF3 viral genome replication.

(A and B) A549 cells were infected with ΔE1, WT, or ΔE1B-55K/ΔE4-ORF3 viruses and treated with DMSO (-) or KU-55933 (KU) (+) at 2 h.p.i. and harvested at 24 h.p.i. (A) Protein lysates were immunoblotted for Phospho-ATM-Ser1981, H2AX, γH2AX, TRIM28, Phospho-TRIM-Ser824, RPA32, and Phospho-RPA32-Ser4/Ser8. β-ACTIN is a loading control. (B) Virus genomes were quantified by Q-PCR and normalized relative to cellular 18S rDNA. Q-PCR was performed in quadruplicate, and error bars indicate the standard deviation.
(C and D) SAECs were infected with ΔE1, WT, ΔE1B-55K, or ΔE1B-55K/ΔE4-ORF3 viruses and treated with DMSO (-) or KU (+) at 4 h.p.i and analyzed at 48 h.p.i. Doxorubicin was used as a positive control for cellular DNA damage. As a positive control for ATM inhibition by KU, doxorubicin was added to cells with either DMSO or KU. (C) Protein lysates were immunoblotted for Phospho-ATM-Ser1981, γH2AX, TRIM28, Phospho-TRIM-Ser824, RPA32, and Phospho-RPA32-Ser4/Ser8. β-ACTIN is a loading control. (D) Virus genomes were quantified by Q-PCR as in (B).

MRN-ATM activation at viral genomes is not amplified by γH2AX to trigger the assembly of DDR foci and global DDR signaling

Our data suggest that the MRN-ATM anti-viral DDR is restricted to viral genomes and not amplified to induce global cellular DDR signaling (Figure 3.5). At cellular DSBs, ATM signaling is amplified by the phosphorylation of H2AX across megabases of chromatin flanking the break (Bassing et al., 2002; Celeste et al., 2002; Iacovoni et al., 2010; Rogakou et al., 1999; Rogakou et al., 1998). MDC1 binds to γH2AX and recruits additional MRN, DDR kinases and effectors that assemble at high concentrations in nuclear foci, which amplifies DDR kinase activation and facilitates the global phosphorylation of DDR effectors (Goldberg et al., 2003; Lukas et al., 2004; Stewart et al., 2003; Stucki et al., 2005; Xu and Stern, 2003).

Given the absence of global DDR signaling in ΔE1B-55K/ΔE4-ORF3 infected cells, we hypothesized that viral genomes do not trigger the assembly of DDR foci and consequent amplification of global ATM phosphorylation. We assessed the formation of DDR foci in ΔE1B-55K/ΔE4-ORF3 by immunofluorescence. As a positive control, we used etoposide to induce cellular DNA damage, which triggers the assembly of NBS1, γH2AX, MDC1, and 53BP1 DDR foci, as expected (Figure 3.6A-D). However, MRN-ATM recruitment and activation at ΔE1B-55K/ΔE4-ORF3 viral genomes does not trigger the assembly of NBS1, γH2AX, MDC1, and 53BP1 DDR foci (Figure 3.6A-D). Similar conclusions are obtained in ΔE1B-55K/ΔE4-ORF3 infected SAECs upon staining for γH2AX and 53BP1 (Figure 3.6E-F). Thus, the MRN-ATM anti-viral DDR neither triggers nor requires the assembly of DDR foci and amplification of global cellular DDR signaling to prevent viral genome replication.

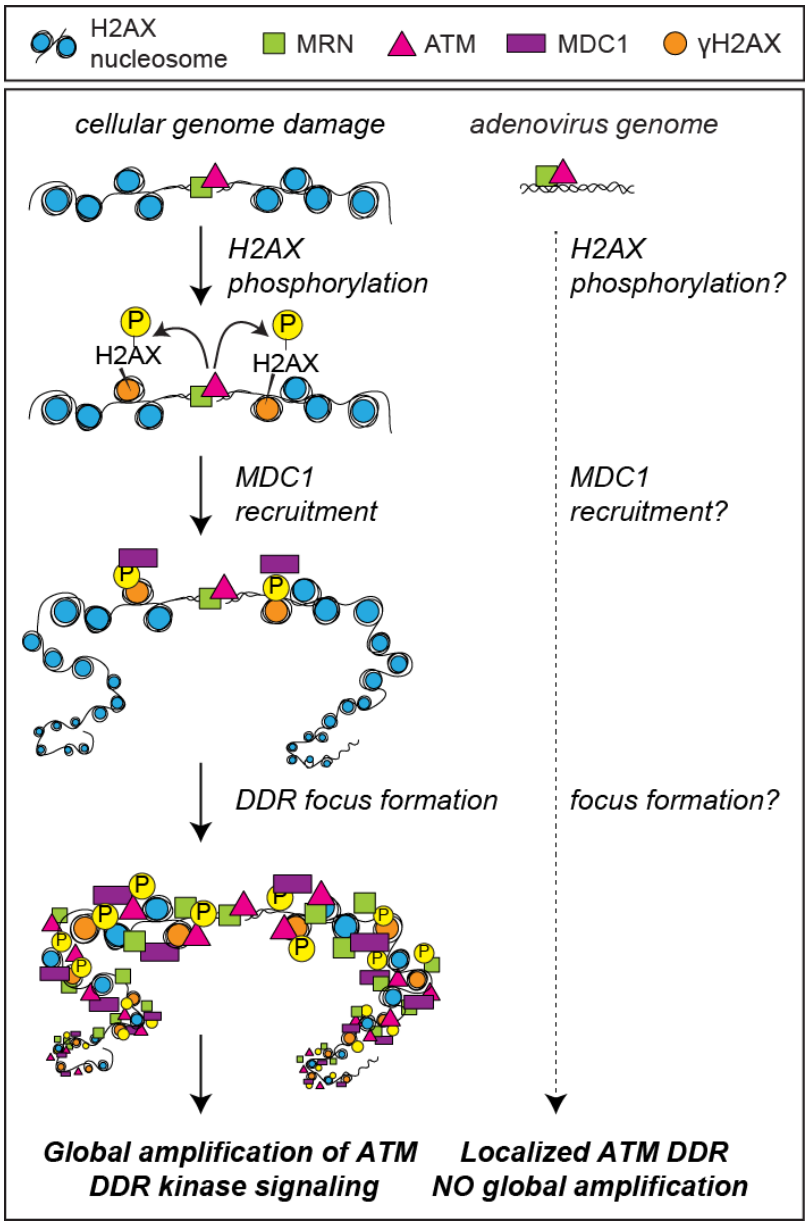

Figure 3.5. MRN-ATM activation at cellular DNA breaks triggers the assembly of DDR foci and global signaling.

MRN-ATM activation at cellular DSBs is amplified across megabases by H2AX phosphorylation that recruits MDC1 and additional DDR proteins to assemble nuclear foci. A key question is if small viral genomes preclude the amplification of global DDR signaling through the assembly of γH2AX foci.

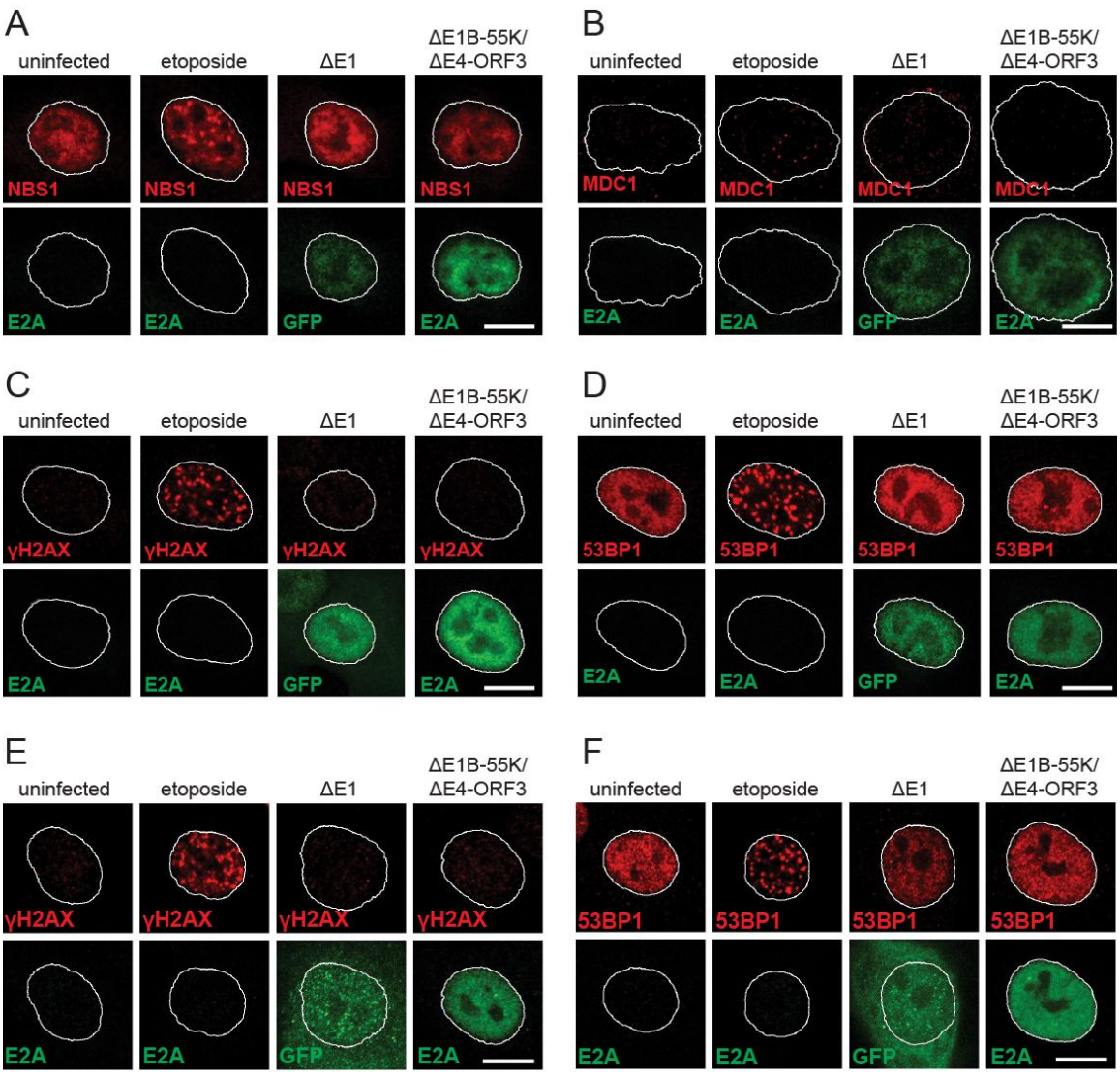

Figure 3.6. MRN-ATM activation at small viral genomes does not induce the assembly of DDR foci.

(A-D) A549 cells were treated with DMSO or 30 μg/ml etoposide and infected with either ΔE1 or ΔE1B-55K/ΔE4-ORF3 viruses. Cells were fixed at 12 h.p.i. and stained for E2A (green) and NBS1 (red) (A), γH2AX (red) (B), MDC1 (red) (C), or 53BP1 (red) (D). Nuclei were counterstained with Hoechst-33342 and are outlined in white. Representative images are shown. Scale bar: 10 μm.
(E and F) SAECs were treated with DMSO or 30 μg/ml etoposide and infected with ΔE1 or ΔE1B-55K/ΔE4-ORF3 viruses. Cells were fixed at 12 h.p.i. and stained for E2A (green) and either γH2AX (red) (E) or 53BP1 (red) (F). The ΔE1 virus expresses GFP (green). Nuclei were counterstained with Hoechst-33342 and outlined in white. Representative images are shown. Scale bar: 10 μm.

In contrast to human chromosomes, the Adenovirus genome is only 36 kb, which by definition precludes the recruitment of DDR proteins across megabase long regions. Furthermore, Adenovirus DNA is compacted by the late viral protein VII in capsids, rather than histones. Upon unpacking and early gene transcription, Adenovirus genomes may dissociate from VII and bind to cellular histones (Chatterjee et al., 1986; Everitt et al., 1973; Knipe and Howley, 2013). Thus, the association to cellular histones may confer upon viral genomes a unique chromatin context that determines the anti-viral response by MRN-ATM. To compare the association of nucleosomes at multi-copy cellular genome Alu sequences and Adenovirus genome sequences, we performed ChIP for histone H3. There is less H3 associated with WT versus ΔE1 and ΔE1B-55K/ΔE4-ORF3 virus genomes (Figure 3.7A). However, H3 levels are still almost five times higher at cellular Alu genome sequences than Adenovirus genomes in ΔE1 and ΔE1B-55K/ΔE4-ORF3 infected cells (Figure 3.7A). This result is highly suggestive that viral genomes lack the chromatin context required by MRN-ATM to amplify DDR signaling, most importantly, the histone H2AX (Fernandez-Capetillo et al., 2004).

H2AX, the amplifier of DDR signaling, comprises approximately 10% of the cellular H2A pool and is broadly distributed throughout chromatin based on ChIP and immunofluorescence studies (Bewersdorf et al., 2006; Fernandez-Capetillo et al., 2004; Seo et al., 2012; Yukawa et al., 2014). We reasoned that the smaller size of Adenovirus genomes and their lower nucleosome occupancy is below the threshold for the global amplification of ATM activation through H2AX phosphorylation and MDC1 recruitment. To test this, we performed MRE11, γH2AX and MDC1 ChIPs. γH2AX is below the limits of detection at ΔE1B-55K/ΔE4-ORF3 viral genomes and at

background IgG levels (0.053% input) (Figure 3.7B). MDC1 binding is enriched above background IgG levels (0.24% input); however, normalizing relative to ΔE1 ChIP samples, there is four times more MRE11 than MDC1 at ΔE1B-55K/ΔE4-ORF3 viral genomes (Figure 3.7B). We conclude that MRN-ATM activates a localized DDR to restrict viral genome replication that is not amplified through the assembly of γH2AX foci to induce global cellular DDR signaling.

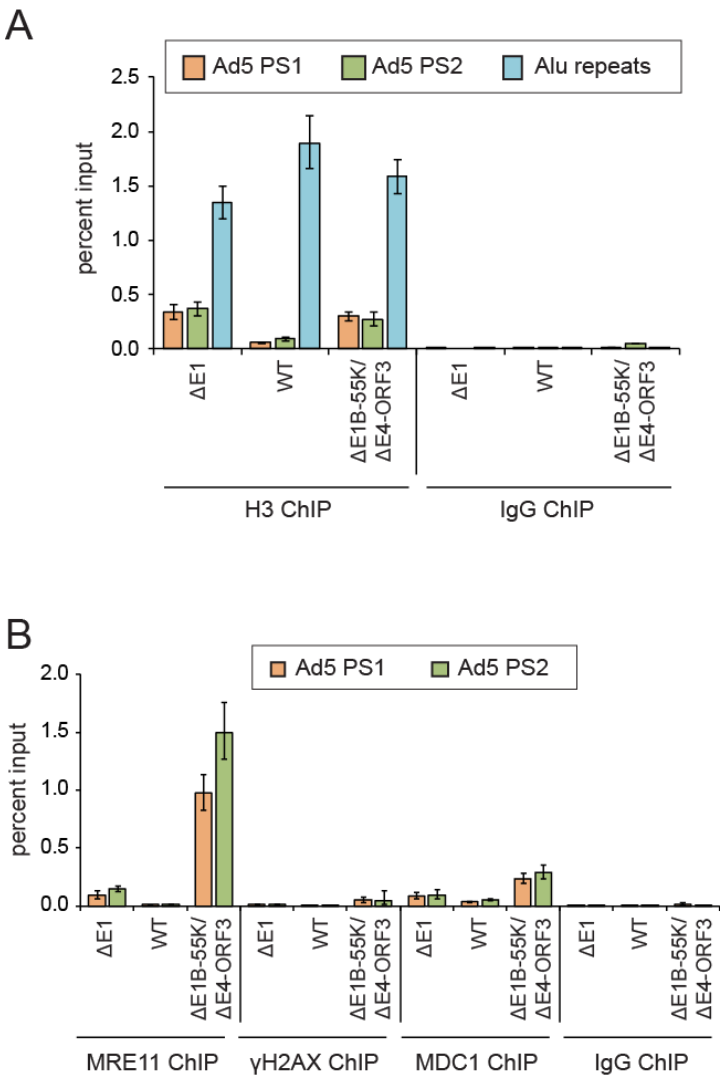

Figure 3.7. ΔE1B-55K/ΔE4-ORF3 virus genomes have less histone association and are not enriched for γH2AX and MDC1.

(A) A549 cells were infected with ΔE1, WT, or ΔE1B-55K/ΔE4-ORF3 viruses and harvested for ChIP analysis at 12 h.p.i. ChIP was performed using histone H3 antibodies or an IgG negative control. Virus genomes were quantified by Q-PCR using PS1 and PS2. Cellular Alu genome sequences were used to quantify cellular DNA and normalized to input. Data is expressed as percent input. Q-PCR was performed in quadruplicate, and error bars indicate the standard deviation.
(B) A549 cells were infected with ΔE1, WT or ΔE1B-55K/ΔE4-ORF3 viruses and harvested for ChIP analysis at 12 h.p.i. ChIP was performed using MRE11, γH2AX and MDC1 antibodies or an IgG control. Virus genomes were quantified by Q-PCR as in (A).

The localized MRN-ATM anti-viral DDR specifically prevents viral genome replication but not cellular replication and division

DDR foci are thought to play an important role in amplifying global DDR signaling (Polo and Jackson, 2011), such that even a single DSB is sufficient to elicit cell cycle arrest (Bennett et al., 1993; Huang et al., 1996; Moore and Haber, 1996). Moreover, the emulation a single DDR focus through the synthetic assembly of high concentration of DDR proteins at a single genomic locus is sufficient to induce cell cycle arrest (Soutoglou and Misteli, 2008). Here we show that MRN activates a localized DDR that prevents viral DNA replication (Figures 2.5, 2.7, 3.2 and 3.4) but does not trigger the assembly of DDR foci (Figure 3.6) and global signaling (Figures 2.2 and 2.4). We hypothesized that the activation of a localized MRN-ATM DDR at viral genomes that is not amplified by the assembly of DDR foci does not induce cell cycle arrest.

To determine if the MRN-ATM anti-viral DDR prevents viral but not cellular DNA replication, we analyzed S phase entry in quiescent SAECs that had been infected with ΔE1, WT, ΔE1B-55K, ΔE4-ORF3 and ΔE1B-55K/ΔE4-ORF3 viruses. Adenovirus E1A activates cellular and viral E2F target genes that drive S phase entry and viral genome replication (Ben-Israel and Kleinberger, 2002). We show that in contrast to ΔE1 virus infected cells, WT, ΔE1B-55K, ΔE4-ORF3, and ΔE1B-55K/ΔE4-ORF3 virus infections all induce S phase entry to equivalent levels (Figure 3.8A). Consistent with this, the E2F targets and S phase cyclins, CYCLIN A and CYCLIN B, are induced in WT, ΔE1B-55K, and ΔE1B-55K/ΔE4-ORF3 infected cells (Figure 3.8B). We conclude that the MRN-ATM anti-viral DDR specifically prevents viral genome but not cellular

genome replication.

We also examined if the MRN-ATM anti-viral DDR is uncoupled from mitotic arrest. To test this, we infected subconfluent A549 cells with ΔE1 or ΔE1B-55K/ΔE4-ORF3 viruses and analyzed them by immunofluorescence for Phospho-H3-Ser10, a marker of mitosis, as well as mitotic bodies. E2A was used as a marker to identify ΔE1B-55K/ΔE4-ORF3 infected cells and GFP to mark ΔE1 vector control infected cells. ΔE1 virus genomes are not sensed by MRN-ATM (Figures 3.2) and do not prevent cell division and mitosis (Figure 3.8C). Similarly, despite the activation of the MRN-ATM anti-viral DDR (Figures 2.5, 2.7, and 3.2) ΔE1B-55K/ΔE4-ORF3 infected cells induce Phospho-H3-Ser10 and form mitotic bodies (Figure 3.8C).

During mitosis, DDR signaling is attenuated (Orthwein et al., 2014; van Vugt et al., 2010), which permits mitotic exit but induces a subsequent G1 arrest (Giunta et al., 2010). Therefore, to determine if activation of the MRN-ATM anti-viral DDR induces a subsequent cell cycle arrest, we performed a population doubling analysis of infected cells over four days. WT virus inactivates MRN and undergoes productive lytic replication that kills infected cells after two days (Figure 3.8D). However, ΔE1B-55K/ΔE4-ORF3 infected cells double at similar rates to uninfected cells (Figure 3.8D). Thus, while the localized MRN-ATM anti-viral DDR stops ΔE1B-55K/ΔE4-ORF3 viral genome replication, it does not arrest cellular DNA replication or division. This provides an elegant mechanism by which an anti-viral MRN-ATM DDR, one that is distinct from the response to cellular DNA breaks, prevents viral replication without impacting cellular replication and viability (Figure 3.9). Furthermore, this localized MRN-ATM DDR is temporally and mechanistically distinct from global DDR signaling

triggered by viral genome replication upon WT infection, which is MRN independent (Figure 3.9).

Chapter acknowledgements

The contents of this chapter, in full, has been submitted for publication of the material as it may appear in Cell, 2015, Shah, G.S. and O'Shea, C.C. The dissertation author was the first author of this paper, and Clodagh C. O'Shea was the senior author, supervising this work.

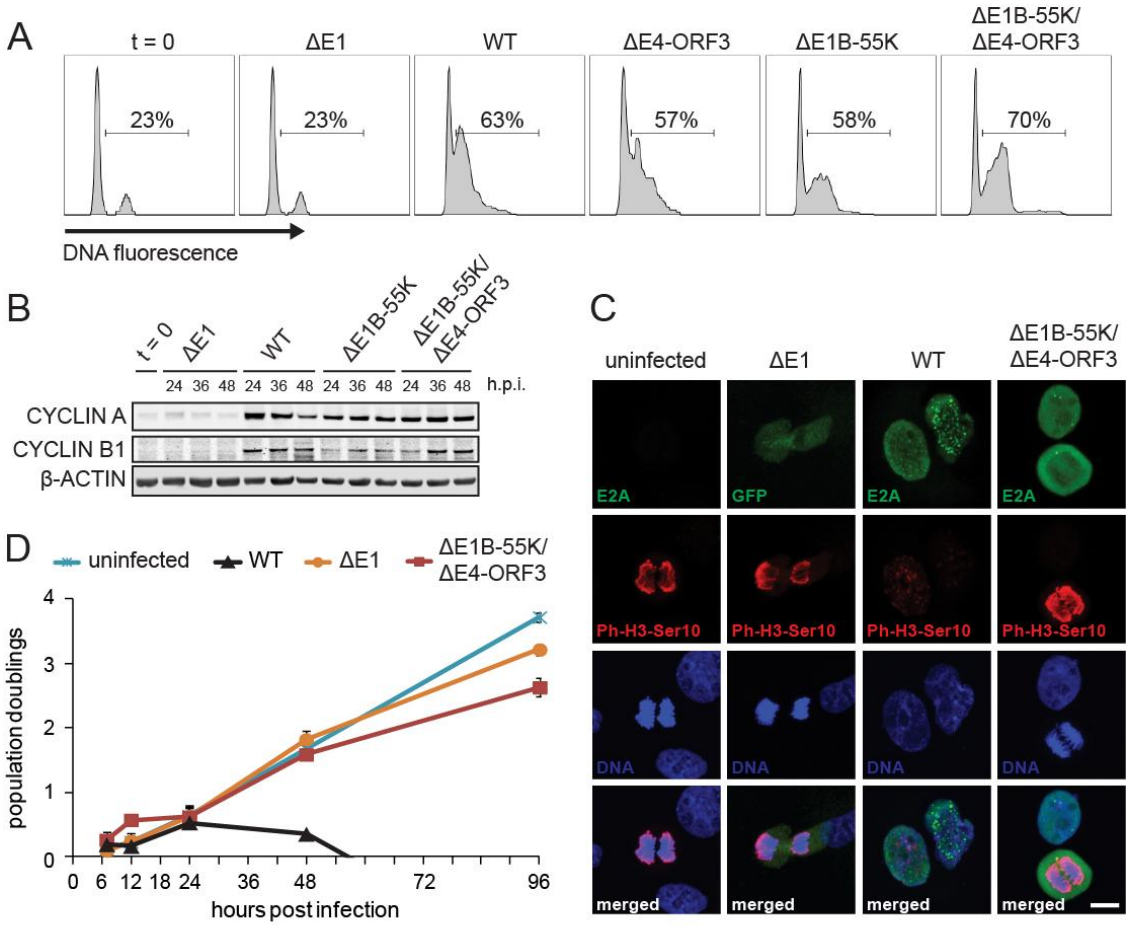

Figure 3.8. The localized MRN-ATM anti-viral DDR specifically prevents viral but not cellular replication.

(A) Quiescent SAECs were infected with ΔE1, WT, ΔE4-ORF3, ΔE1B-55K or ΔE1B-55K/ΔE4-ORF3 viruses. Cells were fixed at 48 h.p.i., stained with propidium iodide and analyzed by flow cytometry. The percentage of cells with DNA content greater than 2N is indicated above the marker.
(B) SAECs were infected with ΔE1, WT, ΔE1B-55K or ΔE1B-55K/ΔE4-ORF3 viruses and immunoblotted for CYCLIN A and CYCLIN B1. β-ACTIN is a loading control.
(C) A549 cells were untreated or infected with either ΔE1 or ΔE1B-55K/ΔE4-ORF3 viruses, fixed at 24 h.p.i. and stained for the mitotic marker, Phospho-H3-Ser10 (P-H3-Ser10) (red). Infected cells were identified by E2A or GFP staining (green). DNA was counterstained with Hoechst-33342 (blue). Scale bar: 10 μm.
(D) A549 cells were untreated or infected with either ΔE1 or ΔE1B-55K/ΔE4-ORF3 viruses. Triplicate wells were counted at 6, 12, 24, 48, and 96 h.p.i. Population doublings were calculated at each timepoint and plotted against hours post infection. Error bars indicate the standard deviation in population doublings across triplicates.

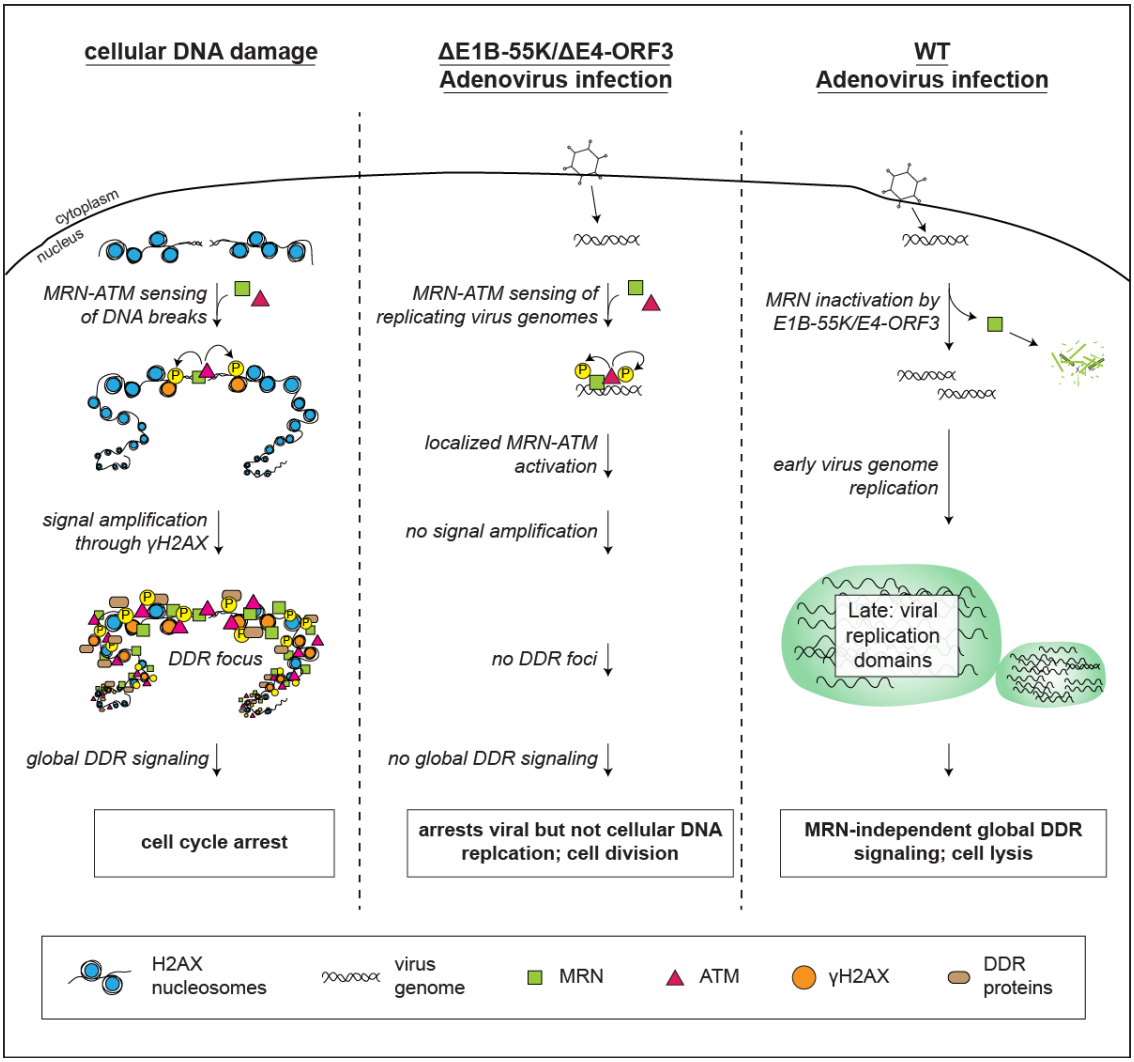

Figure 3.9. MRN and ATM activate temporal and mechanistically distinct DDRs to viral and cellular genomes.

MRN senses and binds to early replicating viral genomes where it recruits ATM and activates a localized DDR that prevents viral but not cellular genome replication. In contrast to cellular genome breaks, ATM activation is not amplified across megabases of chromatin at small viral genomes to trigger the assembly of DDR foci and global signaling. In WT virus infected cells, E1B-55K/E4-ORF3 prevent MRN binding and restriction of viral genome replication. The subsequent assembly of high concentrations of viral genomes in E2A domains triggers the activation of global DDR signaling through an MRN independent mechanism that does not impact viral genome replication.

Chapter 4. Cellular DNA damage sequesters MRN from blocking viral genome replication and render cells permissive to viral genome replication.

Cellular DNA damage prevents the recruitment of MRN to viral genomes and rescues viral genome replication.

Our data suggest that the assembly of γH2AX DDR foci provides the cell with a simple diagnostic device to distinguish the genomic context of MRN-ATM activation, 'self' or 'non-self', to determine if a local response will suffice or global signal amplification is more appropriate. We favor the model that the smaller size and low nucleosome content of viral genomes is below the threshold for the assembly of DDR foci and global signal amplification. However, an alternative explanation is that viral proteins or infection dominantly suppress critical cellular proteins or post-translational modifications that are required for the assembly of DDR foci. To distinguish between these possibilities, we determined if γH2AX DDR foci assemble at cellular DNA breaks in ΔE1B-55K/ΔE4-ORF3 infected cells. We treated ΔE1 and ΔE1B-55K/ΔE4-ORF3-infected A549 cells with etoposide and analyzed γH2AX and 53BP1 focus formation by immunofluorescence. In uninfected, ΔE1 and ΔE1B-55K/ΔE4-ORF3-infected cells, etoposide treatment induces the assembly of γH2AX and 53BP1 DDR foci (Figure 4.1). Thus, DDR foci assemble at cellular genome breaks but not viral genomes in ΔE1B-55K/ΔE4-ORF3 infected cells. These data strongly suggest that the assembly of DDR foci is determined by the genomic context. Thus, the formation of DDR foci, may provide the cell a mechanism to distinguish viral genome from cellular DNA breaks in order to enact an appropriate signaling response.

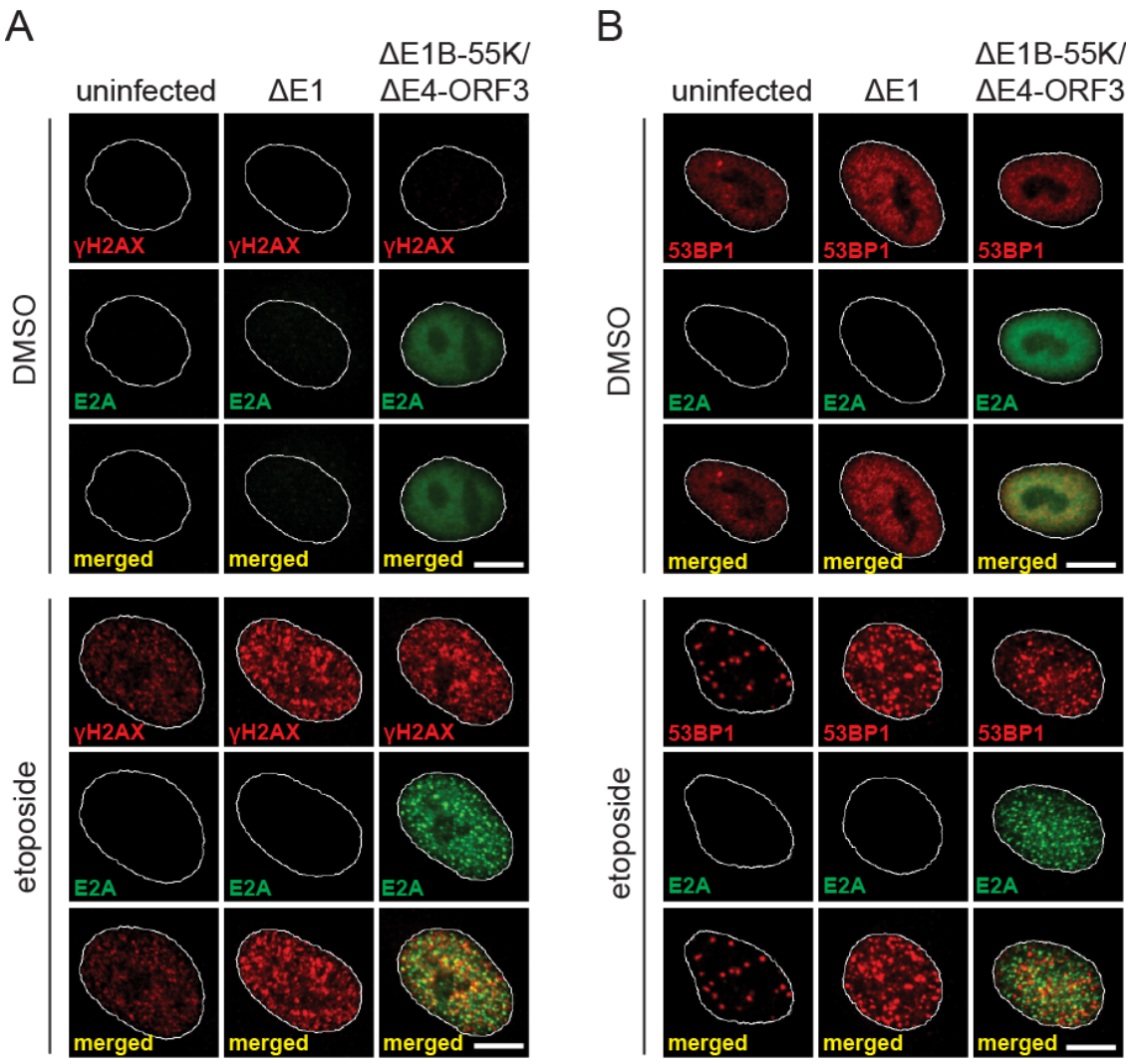

Figure 4.1. Cellular DNA damage triggers the formation of DDR foci and E2A viral replication domains in ΔE1B-55K/ΔE4-ORF3 infected cells.

A549 cells were untreated or infected with ΔE1 or ΔE1B-55K/ΔE4-ORF3 viruses. Cells were treated with DMSO or 10 μg/ml etoposide at 2 h.p.i. Cells were fixed at 12 h.p.i. and stained for E2A (green) and either γH2AX (red) (A) or 53BP1 (red) (B). Nuclei were counterstained with Hoechst-33342 and outlined in white. Representative images are shown. Scale bar: 10 μm.

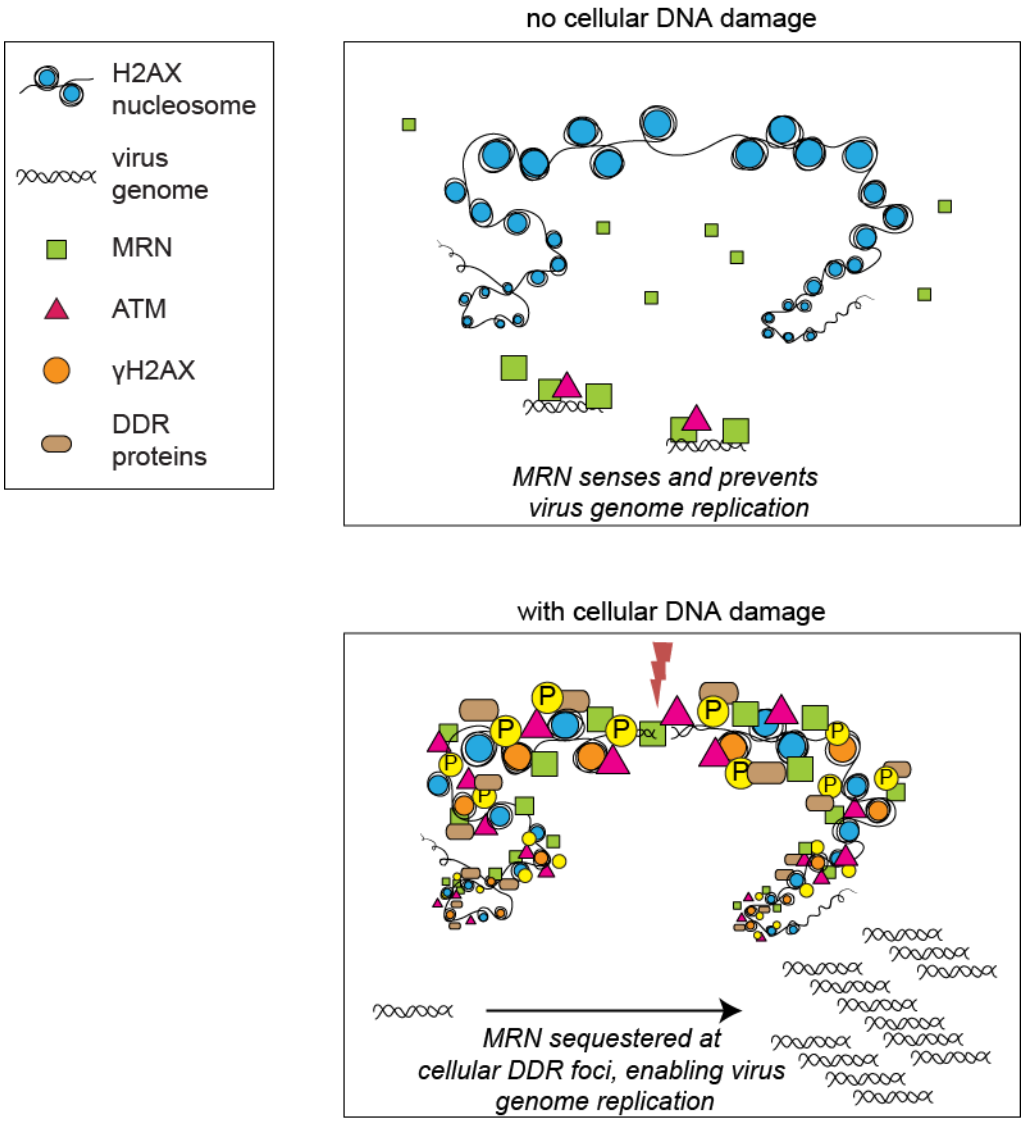

Figure 4.2. Model: Cellular DNA damage sequesters MRN and rescues ΔE1B-55K/ΔE4-ORF3 viral genome replication.

MRN is required for sensing both cellular DSBs and viral genomes. The induction of cellular DSBs recruits MRN to DDR foci and prevents MRN sensing and restriction of viral genome replication.

Strikingly, the induction of cellular genome breaks appears to rescue ΔE1B-55K/ΔE4-ORF3 viral genome replication, as evidenced by the assembly of E2A viral replication domains throughout the nucleus (Figure 4.1). We hypothesized that the recruitment of high concentrations of MRN into DDR foci at cellular genome breaks sequesters MRN and rescues viral genome replication (Figure 4.2). To test this, we treated ΔE1B-55K/ΔE4-ORF3-infected A549 cells with increasing etoposide concentrations. Etoposide activates global DDR phosphorylation to similar or higher levels than those seen upon WT infection, but rescues ΔE1B-55K/ΔE4-ORF3 viral genome replication in a dose dependent manner (Figures 4.3A and 4.3B). This result is also seen in ΔE1B-55K/ΔE4-ORF3 infected SAECs treated with etoposide or doxorubicin (Figure 4.3C and 4.3D). Of note, SAECs tolerate higher concentrations of etoposide and doxorubicin than A549 cells (Figures 4.3C, 4.3D, and data not shown). This demonstrates that treatment with genotoxic drugs can rescue ΔE1B-55K/ΔE4-ORF3 viral genome replication, irrespective of the induction of global DDR phosphorylation. Treatment with genotoxic drugs does not however affect WT virus genome replication in A549 cells and SAECs, consistent with their ability to rescue ΔE1B-55K/ΔE4-ORF3 virus genome replication (Figure 4.4A and data not shown). We conclude that global cellular DDR substrate phosphorylation does not prevent viral genome replication and is uncoupled from the localized MRN-ATM anti-viral DDR that restricts ΔE1B-55K/ΔE4-ORF3 viral genome replication. These results further support our conclusions from Chapters 2 and 3 that MRN restricts ΔE1B-55K/ΔE4-ORF3 viral genome replication without triggering the formation of DDR foci or global DDR phosphorylation, as these are also not sufficient to restrict viral genome replication.

Figure 4.3. Cellular DNA damage rescues ΔE1B-55K/ΔE4-ORF3 viral genome replication, irrespective of global DDR phosphorylation.

(A and B) A549 cells were infected with ΔE1, WT, or ΔE1B-55K/ΔE4-ORF3 viruses as in. At 6 h.p.i., etoposide was added at 0, 3.3, 10, or 30 μg/ml to ΔE1B-55K/ΔE4-ORF3 infected cells or at 0 or 30 μg/ml to WT infected cells. An equal volume of DMSO was added to all cells. (A) Protein lysates were collected at 24 h.p.i. and immunoblotted for ATM, Phospho-ATM-Ser1981, H2AX, γH2AX, TRIM28, Phospho-TRIM28-Ser824, RPA32, and Phospho-RPA32-Ser4/Ser8. β-ACTIN is a loading control. (B) Total DNA was harvested at 24 h.p.i., and virus genomes were quantified by Q-PCR. Virus genomes were normalized relative to cellular 18S rDNA. Q-PCR was performed in quadruplicate, and error bars indicate the standard deviation.
(C and D) SAECs were infected with ΔE1, WT or ΔE1B-55K/ΔE4-ORF3 viruses. At 4 h.p.i., etoposide at 0, 6, 30, or 150 μg/ml or doxorubicin at 0, 0.1, or 0.5 μg/ml was added to ΔE1B-55K/ΔE4-ORF3 infected cells. Uninfected cells were also treated with etoposide at 0, 6, or 30 μg/ml or doxorubicin at 0, 0.1, or 0.5 μg/ml for 12 hours. An equal volume of DMSO was added to all cells. (C) Protein lysates were collected at 36 h.p.i. and immunoblotted for H2AX, γH2AX, TRIM28, Phospho-TRIM28-Ser824, RPA32, and Phospho-RPA32-Ser4/Ser8. β-ACTIN is a loading control. (D) Total DNA was harvested at 36 h.p.i., and virus genomes were quantified by Q-PCR as in (B).

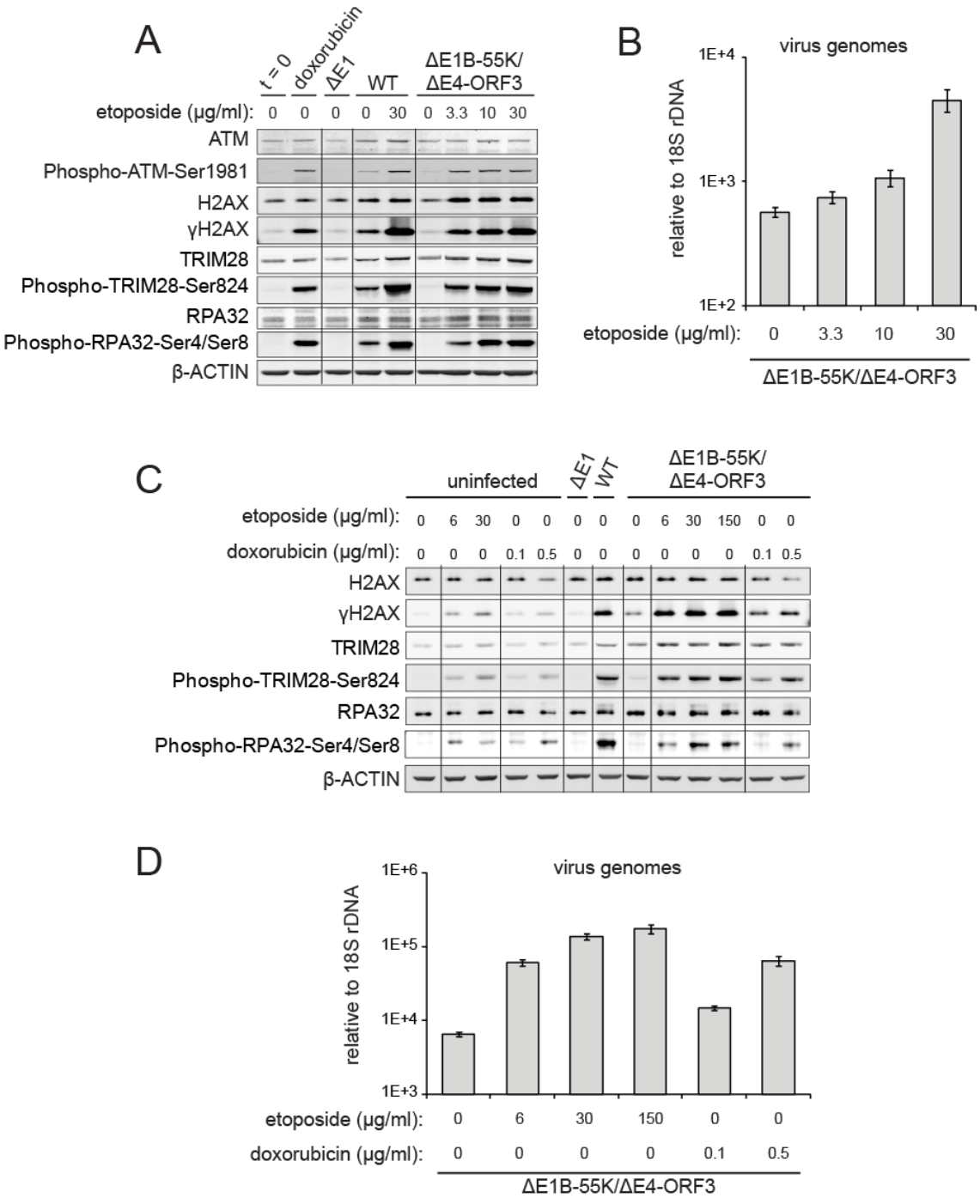
A
t = 0
doxorubicin
ΔE1
WT
ΔE1B-55K/
ΔE4-ORF3
etoposide (μg/ml): 0 0 0 0 30 0 3.3 10 30
ATM
Phospho-ATM-Ser1981
H2AX
γH2AX
TRIM28
Phospho-TRIM28-Ser824
RPA32
Phospho-RPA32-Ser4/Ser8
β-ACTIN
B
virus genomes
relative to 18S rDNA
1E+4
1E+3
1E+2
etoposide (μg/ml): 0 3.3 10 30
ΔE1B-55K/ΔE4-ORF3
C
uninfected
ΔE1
WT
ΔE1B-55K/
ΔE4-ORF3
etoposide (μg/ml): 0 6 30 0 0 0 0 0 6 30 150 0 0
doxorubicin (μg/ml): 0 0 0 0.1 0.5 0 0 0 0 0 0 0.1 0.5
H2AX
γH2AX
TRIM28
Phospho-TRIM28-Ser824
RPA32
Phospho-RPA32-Ser4/Ser8
β-ACTIN
D
virus genomes
relative to 18S rDNA
1E+6
1E+5
1E+4
1E+3
etoposide (μg/ml): 0 6 30 150 0 0
doxorubicin (μg/ml): 0 0 0 0 0.1 0.5
ΔE1B-55K/ΔE4-ORF3

MRN is required to sense and respond to both cellular DSBs and viral genome replication. As such, we reasoned that the recruitment of high concentrations of MRN to cellular DDR foci could saturate MRN binding and restriction of viral genome replication. To test this, we treated infected A549 cells with etoposide. In addition, we also used bleomycin, which induces cellular DNA damage through a distinct mechanism than etoposide (Povirk, 1996). Both etoposide and bleomycin activate high levels of cellular DDR kinase phosphorylated substrates (Figure 4.4B) but rescue ΔE1B-55K/ΔE4-ORF3 viral genome replication (Figure 4.4C). Similar results are seen upon aphidicolin and zeocin treatment (data not shown). These results rules out the possibility that the rescue of ΔE1B-55K/ΔE4-ORF3 viral genome replication is peculiar to etoposide and doxorubicin treatment. Furthermore, consistent with our hypothesis that cellular DNA breaks compete for MRN recruitment (Figure 4.2), etoposide and bleomycin treatment reduce MRE11 binding at ΔE1B-55K/ΔE4-ORF3 viral genomes to levels observed in ΔE1 samples (Figure 4.4D). Similar conclusions were obtained in an independent experiment using doxorubicin treatment (Figure 4.4E). We conclude that the recruitment and localization of MRE11 to viral genomes is critical to restrict Adenovirus genome replication and can be saturated by cellular DNA breaks.

Figure 4.4. Cellular DNA damage prevents the recruitment of MRN to viral genomes to rescue ΔE1B-55K/ΔE4-ORF3 viral genome replication.

(A-D) A549 cells were infected with ΔE1, WT or ΔE1B-55K/ΔE4-ORF3 viruses. At 6 h.p.i. WT and ΔE1B-55K/ΔE4-ORF3 infected cells were treated with 30 μg/ml etoposide or 10 μM bleomycin or 0.5 μg/ml doxorubicin as indicated. An equal volume of DMSO was added to all untreated cells. (A) Total DNA samples from ΔE1 and WT infected cells were collected at 24 h.p.i. Viral genomes were quantified by Q-PCR and normalized relative to cellular 18S rDNA. Q-PCR was performed in quadruplicate, and error bars indicate the standard deviation. (B) Protein lysates were collected at 24 h.p.i. and immunoblotted for Phospho-ATM-Ser1981, H2AX, γH2AX, TRIM28, Phospho-TRIM28-Ser824, RPA32, and Phospho-RPA32-Ser4/Ser8. β-ACTIN is a loading control. "t = 0" was harvested at time of infection. (C) Total DNA samples from ΔE1 and ΔE1B-55K/ΔE4-ORF3 infected cells were collected at 24 h.p.i. Virus genomes were quantified by Q-PCR as in (A). (D) ΔE1 and ΔE1B-55K/ΔE4-ORF3 infected cells were harvested for ChIP analysis at 12 h.p.i. ChIP was performed using MRE11 antibodies. An IgG ChIP control (not shown) yielded less than 0.05% input in all samples. Virus genomes were quantified by Q-PCR using two independent primer sets, Primer Set 1 (Ad5 PS1) and Primer Set 2 (Ad5 PS2). Data is expressed as percent input. Q-PCR was performed in quadruplicate, and error bars indicate the standard deviation.
(E) A549 cells were infected with either ΔE1 or ΔE1B-55K/ΔE4-ORF3 viruses. At 2 h.p.i., DMSO (-), 10 μg/ml etoposide, or 0.1 μg/ml doxorubicin were added to cells. Cells were harvested for ChIP analysis at 12 h.p.i. ChIP was performed using MRE11 antibodies. An IgG control (not shown) yielded less than 0.1% input in all samples. Virus genomes were quantified by Q-PCR using two independent primer sets, Primer Set 1 (Ad5 PS1) and Primer Set 2 (Ad5 PS2), and data is normalized relative to the ΔE1 sample. Q-PCR was performed in quadruplicate, and error bars indicate the standard deviation.

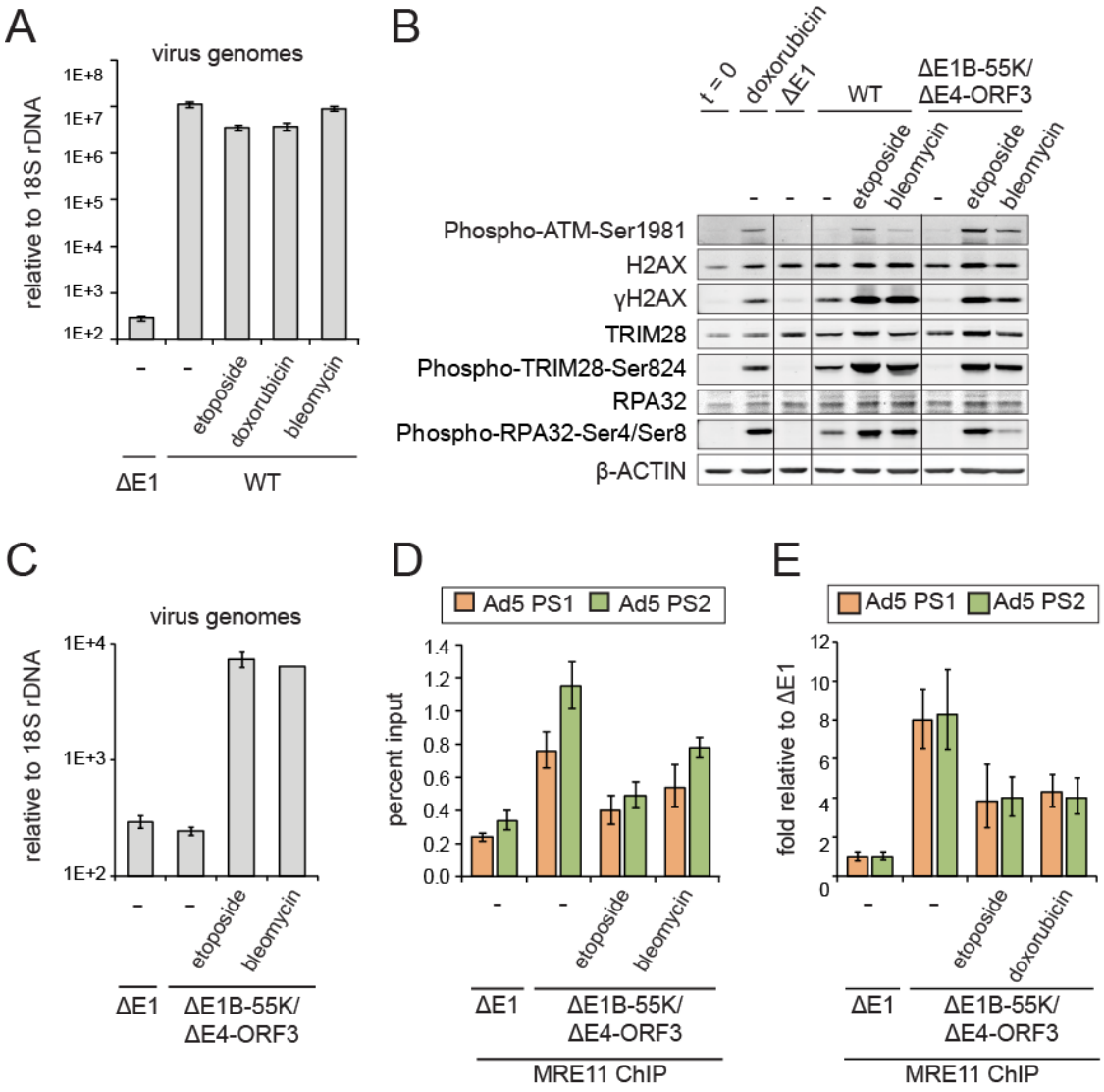
A
virus genomes
relative to 18S rDNA
1E+8
1E+7
1E+6
1E+5
1E+4
1E+3
1E+2
-
-
etoposide
doxorubicin
bleomycin
ΔE1
WT
B
t = 0
doxorubicin
ΔE1
WT
ΔE1B-55K/
ΔE4-ORF3
-
-
-
etoposide
bleomycin
-
etoposide
bleomycin
Phospho-ATM-Ser1981
H2AX
γH2AX
TRIM28
Phospho-TRIM28-Ser824
RPA32
Phospho-RPA32-Ser4/Ser8
β-ACTIN
C
virus genomes
relative to 18S rDNA
1E+4
1E+3
1E+2
-
-
etoposide
bleomycin
ΔE1
ΔE1B-55K/
ΔE4-ORF3
D
Ad5 PS1
Ad5 PS2
percent input
1.4
1.2
1.0
0.8
0.6
0.4
0.2
0.0
-
-
etoposide
bleomycin
ΔE1
ΔE1B-55K/
ΔE4-ORF3
MRE11 ChIP
E
Ad5 PS1
Ad5 PS2
fold relative to ΔE1
12
10
8
6
4
2
0
-
-
etoposide
doxorubicin
ΔE1
ΔE1B-55K/
ΔE4-ORF3
MRE11 ChIP

Superinfection or infection in permissive tumor cell lines permits viral genome replication in the absence of E1B-55K/E4-ORF3 expression.

Our results thus far demonstrate that MRN inactivation by E1B-55K and E4-ORF3 is vital to facilitate Ad5 genome replication in both primary lung epithelial cells and A549 cells. Interestingly, E1B-55K and E4-ORF3 proteins from other human Adenovirus serotypes do not target the MRN complex (Carson et al., 2009; Cheng et al., 2013; Forrester et al., 2011). Given the ubiquitous expression of the essential MRN complex proteins across tissues, the requirement for MRN inactivation to facilitate viral genome replication would be expected across Adenovirus serotypes. Further perplexing is that despite the requirement of E1B-55K and E4-ORF3 expression to facilitate viral genome replication in SAEC and A549 cells (Figures 2.2A and 2.4A), ΔE1B-55K/ΔE4-ORF3 has been reported to proceed to WT levels in HeLa cells (Shepard and Ornelles, 2004). Since these cell lines are frequently used to study DNA damage and are not deleted for MRN, we hypothesized that the anti-viral MRN properties are debilitated within tumor cell lines without direct mutations in MRN genes.

We considered the explanation that the competition and sequestration of MRN by genomic instability inherent to various tumor cell lines or high levels of incoming viral genomes can facilitate viral genome replication in the absence of E1B-55K and E4-ORF3. Consistent with this model, tumor cell lines widely display genomic instability and aneuploidy (Halazonetis et al., 2008; Hanahan and Weinberg, 2011), and *in vivo* Adenovirus infections may occur at both high and low MOI (Hendrickx et al., 2014).

To determine if high MOI can permit viral genome replication in the absence of

E1B-55K and E4-ORF3 expression, we infected A549 cells with ΔE1B-55K/ΔE4-ORF3 at an MOI of 10, 50 and 250 PFU/cell. Importantly, all experiments thus far have been conducted at MOI 10, which is the minimal MOI to reach complete infection in both SAECs and A549 cells. High MOIs of both 50 and 250 PFU/cell show significantly greater viral genomes at 24 h.p.i. (Figure 4.5A). This result demonstrates that high levels of viral genome replication can occur in the absence of E1B-55K and E4-ORF3 expression upon infection with high MOI. This result is best explained by the sequestration of limiting pools of MRN by high numbers of incoming viral genomes, bypassing the localized MRN anti-viral response that otherwise blocks viral genome replication. Furthermore, this result supports our earlier conclusion that MRN sensing of viral genomes is saturable, in this case, not by cellular DNA breaks, but by high numbers of viral genomes.

We next assessed ΔE1B-55K/ΔE4-ORF3 viral genome replication in H1299, HeLa, and U2OS cell lines. The defect in ΔE1B-55K/ΔE4-ORF3 genome replication relative to WT varies widely across all three cell lines (Figures 4.5B-D), all of which are more permissive for ΔE1B-55K/ΔE4-ORF3 genome replication than SAECs and A549 cells (Figures 2.2A and 2.4A). In U2OS and HeLa cell lines, which are widely used to study the anti-viral functions of the DDR pathway, ΔE1B-55K/ΔE4-ORF3 genome replication is defective by less than 10- and 40-fold, respectively (Figures 4.5C and 4.5D). This demonstrates that various tumor cell lines are differentially permissive for viral genome replication and can mask the defect in viral genome replication of ΔE1B-55K/ΔE4-ORF3 viruses. Together, these results may explain the contradictory results from previous studies regarding the functional requirement of E1B-55K/E4-

ORF3 for viral genome replication (Evans and Hearing, 2003, 2005; Gautam and Bridge, 2013; Lakdawala et al., 2008; Mathew and Bridge, 2007, 2008; Shepard and Ornelles, 2004).

Furthermore, given our result that cellular DNA damage can sequester MRN sensing of viral genomes, an important explanation for the elevated permissiveness of various tumor cell lines for viral genome replication is the sequestration of MRN by genomic instability inherent to various cell lines. This suggests that genomic instability may be a feature of cancer cells targetable for the selective replication of E1B-55K/E4-ORF3 mutant viruses.

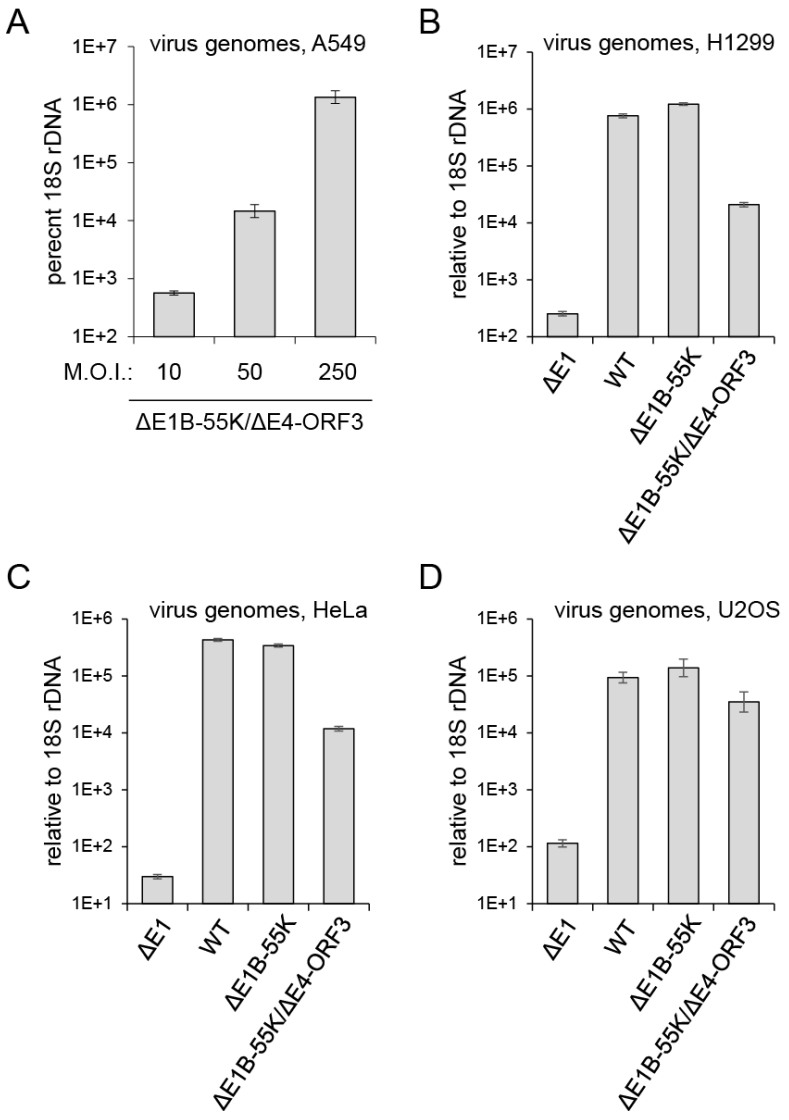

Figure 4.5. High MOI or infection in permissive cell lines rescues ΔE1B-55K/ΔE4-ORF3 viral genome replication.

(A) A549 cells were infected with the ΔE1B-55K/ΔE4-ORF3 virus at an MOI of 0, 50, or 250 PFU/cell. Total DNA samples were collected at 24 h.p.i. Viral genomes were quantified by Q-PCR and normalized relative to cellular 18S rDNA. Q-PCR was performed in quadruplicate, and error bars indicate the standard deviation.

(B-D) H1299 (B), HeLa (C), and U2OS (D) cells were infected ΔE1, WT, ΔE1B-55K and ΔE1B-55K/ΔE4-ORF3 viruses. Total DNA samples were collected at 36 h.p.i., and viral genomes were quantified as in (A).

Concatemer formation does not explain MRN restriction of viral genome replication.

Previous studies have demonstrated the formation of high molecular weight end-to-end concatemers of E4 mutant viral genomes (Boyer et al., 1999; Stracker et al., 2002; Weiden and Ginsberg, 1994). Viral concatemers are formed in a manner dependent on MRN proteins and MRE11 nuclease activity (Stracker et al., 2002). We have demonstrated that MRN localization to viral genomes is required for the restriction of viral genome replication, yet the precise mechanism by which MRN restricts viral genome replication remains unknown. An important explanation for our results is that nucleolytic processing of viral genomes restricts viral genome replication. This hypothesis would be consistent with the requirement of MRN localization to viral DNA to restrict viral genome replication demonstrated in our work (Figures 4.3-4.5).

To test whether MRE11 nuclease activity contributes to the restriction of ΔE1B-55K/ΔE4-ORF3 viral genome replication, ΔE1B-55K/ΔE4-ORF3 infected A549 cells were treated with Mirin, an inhibitor of MRE11 nuclease activity (Dupre et al., 2008). Treatment with 100 μM Mirin resulted in a less than 10-fold rescue of viral genome replication by 48 h.p.i. (Figure 2.6). This result demonstrates that MRE11 nuclease activity may contribute to the restriction of ΔE1B-55K/ΔE4-ORF3 viral genome replication. However, given that *MR* knockdown results in a far greater rescue of ΔE1B-55K/ΔE4-ORF3 viral genome replication, MRE11 nuclease activity likely plays only a minor role in restricting viral genome replication.

The formation of concatemers was also analyzed by Southern blot. Concatemeric products of ΔE1B-55K/ΔE4-ORF3 viral genomes are detectable upon

superinfection in A549 cells at 24 h.p.i. (data not shown), in which MRN restriction of viral genome replication is bypassed. However, ΔE1B-55K/ΔE4-ORF3 concatemeric DNA products were below the threshold of detection upon normal infection (data not shown). Furthermore, concatemeric DNA products were not detectable by high throughput sequencing of ΔE1B-55K/ΔE4-ORF3 viral DNA purified from A549 cells at 12 h.p.i., which was performed by Aaron Yun Chen in the O'Shea lab (data not shown). We conclude that the formation of viral concatemers does not coincide with MRN restriction of ΔE1B-55K/ΔE4-ORF3 viral genome replication. Together, with the minimal rescue of ΔE1B-55K/ΔE4-ORF3 viral genome replication by Mirin treatment, these data suggest that nucleolytic processing of viral genomes by MRE11 plays only a minor role in MRN restriction of viral genome replication.

Chapter acknowledgements

The contents of this chapter, in full, has been submitted for publication of the material as it may appear in Cell, 2015, Shah, G.S. and O'Shea, C.C. The dissertation author was the first author of this paper, and Clodagh C. O'Shea was the senior author, supervising this work.

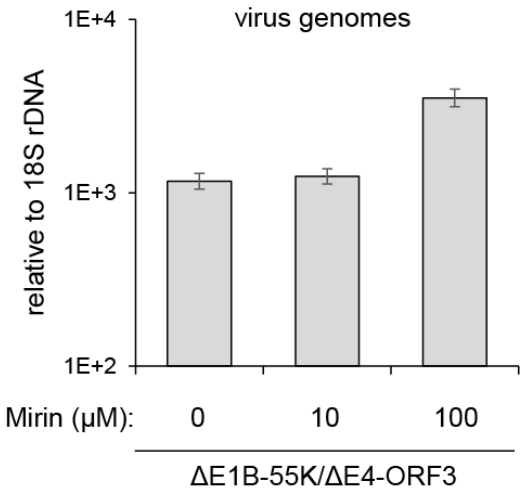

Figure 4.6. Treatment with Mirin, and MRE11 nuclease inhibitor only slightly rescues ΔE1B-55K/ΔE4-ORF3 viral genome replication.

A549 cells were infected with the ΔE1B-55K/ΔE4-ORF3 virus and treated with 0, 10, or 100 μM Mirin at 4 h.p.i. An equal volume of DMSO was added to all samples. Total DNA samples were collected at 48 h.p.i. Viral genomes were quantified by Q-PCR and normalized relative to cellular 18S rDNA. Q-PCR was performed in triplicate, and error bars indicate the standard deviation.

Chapter 5. Discussion

MRN-ATM activate distinct signaling responses to viral DNA versus cellular DNA damage.

Our studies demonstrate that MRN and ATM activate distinct signaling responses to protect the cell against DNA viruses and cellular DNA breaks. We identify a critical localized MRN-ATM response that is inactivated by viral oncoproteins and a subsequent MRN independent global ATM DDR that is a consequence of viral replication. This was completely unexpected and changes the longstanding model that MRN activates a global cellular DDR to Adenovirus genomes (Chaurushiya and Weitzman, 2009; Stracker et al., 2002; Turnell and Grand, 2012). In contrast to chromosomal DSBs, MRN-ATM activation at small viral genomes is not amplified through the recruitment of DDR proteins across megabases of chromatin. The localized MRN-ATM anti-viral response selectively prevents viral but not cellular replication. Thus, the assembly of DDR foci plays an important role in distinguishing MRN-ATM activation at ‘self’ and ‘non-self’ genomes to elicit differential signaling and replicative arrest responses. The localized MRN-ATM response provides an elegant mechanism to neutralize viral genomes without compromising cellular viability. This could be an important adaptive response for maintaining tissue homeostasis, especially in early development when we are more prone to infection.

Our data provide the following model (Figure 3.9). Incoming Adenovirus genomes are not detected by MRN. The expression of E1A activates E2F and the transcription of cellular and viral genes that drive S phase entry and viral genome

replication (Ben-Israel and Kleinberger, 2002). MRN senses and binds to replicating viral genomes where it recruits ATM and activates a local DDR that prevents viral genome replication. In WT virus infected cells, E1B-55K/E4-ORF3 prevent MRN binding and restriction of viral genome replication. The subsequent assembly of high concentrations of double and single-strand viral genomes in E2A domains triggers the MRN independent global activation of ATM and DDR kinase signaling but does not impact viral genome replication.

MRN plays a unique anti-viral role in cellular innate immunity by sensing replicating Adenovirus genomes.

The role of the MRN complex and ATM kinase in maintaining genomic stability and DNA repair is widely studied and largely conserved across eukaryotes (Harper and Elledge, 2007; Yoshiyama et al., 2013). However, the relevance of this pathway in response to nuclear viral genomes remains unclear. Using E1B-55K/E4-ORF3 double deletion Adenoviruses, we have uncovered the anti-viral role of MRN. This study helps place the role of MRN DNA-sensing within cellular innate immunity and reveals an important role of MRN that is uncoupled from the response to cellular DNA breaks.

The prevailing model has been that the linear ends of Adenovirus genomes resemble cellular DNA breaks and are the targets for MRN binding (Stracker et al., 2002; Weitzman et al., 2010). If this is true, then MRN should also bind to the ends of replication incompetent ΔE1 viruses that neither replicate nor express viral genes. However, we show that MRN associates to ΔE1B-55K/ΔE4-ORF3 but not ΔE1 viral DNA and that viral DNA replication inhibitors prevent MRN binding to ΔE1B-

55K/ΔE4-ORF3 genomes (Figure 3.2 and 3.3). These data demonstrate that MRN specifically senses replicating viral genomes, consistent with the requirement of MRN during replication (Adelman et al., 2009).

Of note, Adenovirus genome replication results in various replication intermediates and products including branched DNA structures, linear single strand DNA, single strand DNA stem-loops (also known as pan-handle structures), and strand-invasion cross-over structures (Ahern et al., 1991; Hu et al., 1992; Lechner and Kelly, 1977). Both linear double strand DNA and pan-handle structures can be used as templates for Adenovirus DNA synthesis (de Jong et al., 2003; Knipe and Howley, 2013). Our study suggests that MRN senses one or more of these structures in order to restrict Adenovirus genome replication. Consistent with this model, *in vitro* binding studies have demonstrated that in addition to linear double strand DNA substrates, the human MRN complex also has affinity for circular double strand DNA and single strand DNA (Lee et al., 2003). Furthermore, structural studies of the *Pyrococcus furiosus* MRE11/RAD50 (MR) complex demonstrate that the MR complex can bind both linear DNA ends and branched DNA structures resembling either blunt DNA breaks or replication forks, respectively (Williams et al., 2008). Thus, our results are consistent with the model that MRN senses replicating Adenovirus genomes through one or more of the known MRN DNA-sensing properties. Our studies, however, do not rule out the possibility that other DDR proteins such as KU70/80, DNA-PK, or PARP-1 function upstream of MRN binding to Adenovirus genomes in the manner that they may in response to cellular double strand DNA breaks (Ciccia and Elledge, 2010).

Furthermore, our results suggest an important role for the Adenovirus genome

capping protein, TP/pTP. All incoming and newly synthesized Adenovirus genomes are covalently attached to TP or pTP, respectively, at terminal 5' Cytosine residues (Rekosh et al., 1977). Therefore, our finding that the MRN complex does not bind non-replicating Adenovirus genomes suggests that the covalent attachment of TP at 5' ends physically occludes or actively represses the recruitment of MRN to non-replicating viral genomes and incoming replication-competent viral genomes. This may enable Adenovirus genomes to remain undetected upon infection to initiate the transcription of early viral proteins that drive the viral lifecycle.

Irrespective of the viral substrates detected by MRN, our study contributes to the understanding of how DDR proteins function in cellular innate immunity. Viral nucleic acids are important molecules for pathogen recognition. Toll-like receptors can detect viral nucleic acids; however, they are membrane bound proteins localized to the cell membrane and endosomes (Wu and Chen, 2014). Outside of the endocytic compartment, cytosolic sensors such as cGAS and members of the RIGI-like family can detect viral nucleic acids (Wu and Chen, 2014). Viral envelopes and capsids may shield viral nucleic acids from such sentinels upon infection, overcoming these defenses. Here we show that MRN, which is ubiquitously expressed throughout tissues, is a specific sensor of replicating Adenovirus DNA that blocks further viral DNA replication (Figures 2.5, 2.7, and 3.2). Since Adenovirus DNA replication can only occur in the nucleus, where viral and cellular replication factors are present, MRN therefore fulfils a unique anti-viral role in the nucleus that cannot be fulfilled by membrane bound or cytosolic sensors of viral nucleic acids.

MRN restricts viral genome replication through a localized DDR that is uncoupled from the MRN response to cellular DNA breaks.

A critical downstream effector of MRN in response to DNA damage is ATM which mediates responses through activation of various downstream substrates (Shiloh and Ziv, 2013). However, global phosphorylation of ATM and DDR kinase substrates, such as NBS1, H2AX, TRIM28, RPA32, ATM, CHK1 and CHK2, is absent in total cell lysates from ΔE1B-55K/ΔE4-ORF3 infected cells (Figures 2.2 and 2.4), in which MRN restricts viral genome replication (Figures 2.5 and 2.7). Thus, MRN functional activation in the context of ΔE1B-55K/ΔE4-ORF3 viral infection has a distinct consequence from its activation in response to cellular DSBs. However, similar to its recruitment to cellular DSBs (Figure 3.1) (Berkovich et al., 2007), we show that ATM is recruited to ΔE1B-55K/ΔE4-ORF3 viral genomes (Figures 3.2D and 3.3). ATM, ATR and DNA-PK phosphorylate SQ/TQ peptide motifs (Kim et al., 1999; O'Neill et al., 2000). Consistent with MRN induced ATM activation at viral genomes, we show that DDR kinase phosphorylated epitopes are enriched at viral genomes in ΔE1B-55K/ΔE4-ORF3 but not WT virus infected cells (Figures 3.2D and 3.3). Furthermore, we show that an ATM kinase inhibitor rescues ΔE1B-55K/ΔE4-ORF3 viral genome replication (Figure 3.4), albeit less than MRN knockdown (Figures 2.5 and 2.7). This is consistent with a previous study (Gautam and Bridge, 2013). Together, these data suggest that MRN-mediated ATM activation at viral genomes is restricted to sites of viral DNA and has an important but subsidiary role to MRN sensing and restricting viral genome replication.

One mechanism by which MRN-ATM activation and localization to viral

genomes may restrict viral genome replication is through nucleolytic processing. MRN is known to exhibit unwinding and nuclease activity and to mediate 5' to 3' resection at double strand breaks for which localization of MRN to breaks is necessary (Paull and Deshpande, 2014; Stracker and Petrini, 2011). At early times post infection, at which there are very few viral genomes within the nucleus, the nucleolytic processing of Adenovirus DNA would render viral genome replication defective. An additional mediator of DNA end processing in response to cellular DNA damage is CtIP (You and Bailis, 2010). CtIP can bind to MRN and DNA breaks and contribute to resection at DNA ends (Sartori et al., 2007; You et al., 2009; Yuan and Chen, 2009). Importantly, the resection of DNA ends can trigger the activation of ATR downstream of MRN sensing of DNA breaks by exposing single strand DNA (Paull and Deshpande, 2014; Stracker and Petrini, 2011). As a result, the resection of Adenovirus DNA has been considered an important mechanism by which MRN restricts Adenovirus replication based on high levels of ATR activation upon infection with E4 deleted viruses (Carson et al., 2009; Carson et al., 2003).

In previous studies (Carson et al., 2009; Carson et al., 2003), the activation of ATR signaling upon infection with E4 deleted viruses is not consistent with our studies using ΔE1B-55K/ΔE4-ORF3 viruses. The differences are best explained by high levels of viral genome replication seen in permissive cancer cell lines as discussed previously. Therefore, the activation of ATR signaling in previous studies does not correspond to the early MRN restriction of viral genome replication and may not be indicative the prominence of CtIP mediated resection in the restriction of Adenovirus genome replication. This does not exclude the possibility that MRN nuclease activity or CtIP

contribute to the restriction of viral genome replication irrespective of high levels of DDR kinase signaling. However, given the minimal rescue of ΔE1B-55K/ΔE4-ORF3 DNA replication upon treatment with Mirin, the MRE11 nuclease inhibitor (Figure 4.6), our data suggest that MRE11 nuclease activity does not play an important role in MRN restriction of viral genome replication. The role of CtIP remains unexplored in our studies.

MRN-ATM localization to viral DNA may also restrict viral genome replication through the phosphorylation of one or more novel anti-viral targets of ATM kinase. Given the auxiliary role of ATM in restricting viral genome replication, we do not prefer this mechanism. Alternatively, ATM may modulate MRN activity and binding at viral genomes to prevent access to factors required for viral genome replication. These include the viral replication proteins, E2B Polymerase, E2A, and E2B pTP or cellular proteins, OCT-1, NFI family proteins, And class I topoisomerases (de Jong et al., 2003). Consistent with the latter, there is an inverse correlation between MRE11 and E2A binding at ΔE1B-55K/ΔE4-ORF3 viral genomes (data not shown), which is required for unwinding viral genomes, strand displacement and replication (de Jong et al., 2003). Furthermore, there are thousands of potential cellular DDR phosphorylated substrates (Matsuoka et al., 2007), and it is possible that the anti-viral DDR induces the phosphorylation and activation of a discrete subset. However, the activation of global DDR phosphorylation by doxorubicin, etoposide and bleomycin, which may activate such substrates, does not prevent viral genome replication in ΔE1B-55K/ΔE4-ORF3 infected cells (Figures 4.3 and 4.4). Irrespective of its precise mechanism, we conclude that the MRN-ATM anti-viral DDR acts locally to restrict viral genome replication and

is uncoupled from the activation of global cellular DDR phosphorylated substrates.

The assembly of DDR foci distinguish cellular DNA damage from viral genomes.

An important distinction between the cellular and anti-viral MRN-ATM DDR is the absence of DDR foci in response to viral genomes (Figure 3.6). Our studies suggest an intriguing role for DDR foci and the logic of modifying vast tracts of chromatin flanking a cellular DSB (Polo and Jackson, 2011). We propose that the assembly of γH2AX DDR foci provides an elegant diagnostic device for the cell to distinguish the MRN-ATM signaling response to cellular DSBs and viral genomes.

Adenovirus genomes are vastly smaller than cellular chromosomes and exhibit a unique chromatin composition from cellular DNA (Figure 3.7). The assembly of DDR foci depends on the spreading of ATM activation through phosphorylation of H2AX across large tracts of chromatin (Fernandez-Capetillo et al., 2004). The entire Adenovirus genome is only 36 kb, which by definition precludes the recruitment of DDR proteins across megabases of nucleosome bound DNA. H2AX comprises approximately 10% of the cellular H2A pool and is broadly distributed throughout chromatin (Bewersdorf et al., 2006; Fernandez-Capetillo et al., 2004; Seo et al., 2012; Yukawa et al., 2014). In contrast to other DDR proteins, H2AX is prepositioned rather than recruited. Adenovirus genomes are compacted by the late viral protein VII and are not associated with nucleosomes in incoming capsids (Chatterjee et al., 1986; Everitt et al., 1973; Knipe and Howley, 2013), suggesting that viral genomes are not fitted with the H2AX response mechanism. In consistence, we show that there is less H3 at viral versus cellular genome sequences (Figure 3.7A). Furthermore, in contrast to MRE11

and ATM, γH2AX association to ΔE1B-55K/ΔE4-ORF3 viral genomes is below the limits of detection (Figures 3.7B). Cellular chromosomes occupy distinct territories within the nucleus and their associated DSBs exhibit limited mobility (Cremer and Cremer, 2010; Soutoglou et al., 2007). However, Adenovirus genomes diffuse throughout the nucleus (Pombo et al., 1994), which may also impair the assembly of stable DDR domains. Thus, in contrast to chromosomal breaks, viral genomes may not meet the threshold criteria for the assembly of DDR foci. An alternative explanation is that viral infection or proteins inactivate critical cellular targets required for the assembly of DDR foci and global signal amplification. However, we show that DDR foci assemble at cellular genome breaks but not viral genomes in ΔE1B-55K/ΔE4-ORF3-infected cell (Figure 4.1). These data strongly suggest that the assembly of DDR foci is precluded in the context of viral genomes.

The differential assembly of DDR foci provides an elegant mechanism to elicit a distinct MRN-ATM signaling and replicative arrest response to viral and cellular genomes. The assembly of DDR foci amplifies global DNA damage signaling such that even a single cellular DSB is sufficient to induce cell cycle arrest and repair (Bennett et al., 1993; Huang et al., 1996; Moore and Haber, 1996). Furthermore, the synthetic assembly of high concentration of DDR proteins, which mimics the assembly of DDR foci, is sufficient to induce cell cycle arrest even in the absence of DNA breaks (Soutoglou and Misteli, 2008). There are at least ten replication competent ΔE1B-55K/ΔE4-ORF3 virus genomes per nucleus in our experiments (Figure 3.2B). However, the localized anti-viral DDR selectively prevents viral genome replication but not cellular genome replication and division (Figures 2.5, 2.7, and 3.8). Adenovirus

genomes do not integrate into cellular DNA and are dependent on nuclear-localized viral and cellular proteins for gene expression and genome replication. Thus, the selective restriction of viral genome replication and propagation of ΔE1B-55K/ΔE4-ORF3 infected cells through mitosis and cell division may serve an anti-viral purpose by purging viral genomes from the nucleus. This is consistent with the evolution of mechanisms that block mitosis encoded by DNA viruses that replicate within the nucleus, including HCMV and HPV (Fehr and Yu, 2013). Together, these results suggest that the uncoupling of the anti-viral DDR from the formation of DDR foci and cell cycle arrest serves to enact a proportional response to viral genomes.

In apparent contradiction to our studies, global ATM activation is achieved in *Xenopus* egg extracts upon addition of DNA fragments ranging from 200-2000 bp at a concentration of 18-64 DNA ends per nucleoplasmic volume (You et al., 2007). These conditions are similar to our experiments that result in ~10 viral genome copies per A549 cell nucleus (Figure 3.2B). An important distinction of the *Xenopus* egg extract system is the formation of large macromolecular complexes that resemble DDR foci and contain large quantities of MRN, ATM, and DNA fragments (Costanzo et al., 2004). Additionally, DNA fragments in *Xenopus* egg extracts assemble nucleosomal structure (You et al., 2007), whereas viral genomes in our experiments have fewer histones than cellular DNA. Therefore, an important explanation for these apparently contradictory results is that DNA fragments *Xenopus* egg extracts may facilitate the amplification of ATM kinase signaling by accumulating into large structures and by exhibiting nucleosomal properties like cellular chromosomes.

The sequestration of MRN under conditions of high genotoxic stress such as cancer may attenuate MRN anti-viral functions.

The reliance of both the anti-viral and cellular DDR on MRN sensing has profound consequences and renders it susceptible to saturation. We show that the induction of cellular DNA damage by genotoxic drugs rescues ΔE1B-55K/ΔE4-ORF3 viral genome replication in a dose-dependent manner, despite the activation of global DDR signaling (Figure 4.3). Cellular DNA breaks appear to compete with viral genomes for MRN binding and saturate MRN's capacity to simultaneously sense and restrict viral genome replication (Figure 4.4). In this respect, the recruitment of high concentrations of MRN to DDR foci at cellular genome breaks phenocopies E4-ORF3 in sequestering MRN from viral genomes (Figures 2.1C, 2.1D, 4.1 and 4.2). Furthermore, superinfection with high MOI can bypass the requirement for MRN inactivation to facilitate viral genome replication (Figure 4.5A).

This result may explain the prevalence of Adenovirus infection across the human population and has important implications for the use of Adenovirus vectors for oncolytic therapy. Almost 80% of the human population has been exposed to Ad5 infection at some point in life as evidenced by the seroprevalance of Ad5 neutralizing antibodies (Yu et al., 2012). Ad5 is the vector of choice for transient gene expression studies both in basic research and gene therapy protocols. However, even in laboratory preparations, many progeny virions are infectious but carry partial viral genomes.

We show that the induction of cellular DNA breaks recruits MRN away from viral genomes and rescues ΔE1B-55K/ΔE4-ORF3 genome replication, thus bypassing the MRN anti-viral checkpoint (Figures 4.1-4.4). These results lead to a number of

important conclusions. First, the ability of cellular breaks to trigger the assembly of MRN foci and mediate widespread ATM signaling is perfectly intact in ΔE1B-55K/ΔE4-ORF3 infected cells. This excludes the possibility that virus infection suppresses the assembly of DNA damage induced foci in general, which would be expected to have trans-dominant effects. This also demonstrates that the formation of DNA damage induced foci and very high levels of ATM signaling are not sufficient to restrict ΔE1B-55K/ΔE4-ORF3 genomes replication. Second, it demonstrates that the local binding of MRN and ATM to viral genomes, in the absence of DDR foci or global DDR kinase signaling, is sufficient to restrict viral replication. Third, it shows that the induction of cellular DDR foci and global DDR kinase signaling have no effect in limiting viral genome replication. Instead, the recruitment of MRN to cellular breaks prevents the sensing and restriction of viral genome replication, thereby rescuing ΔE1B-55K/ΔE4-ORF3 viral genome replication. These data indicate that the anti-viral DDR acts locally and neither triggers nor requires the global activation of DNA damage proteins and substrates that typify the response to cellular DNA breaks. Moreover these studies demonstrate that high levels of genotoxic stress mute the ability of the cell to sense and defend itself against viral genome replication.

This model suggests a synergistic relationship between natural sources of genotoxic stress and viral infection. These may include environmental agents such as cigarette smoke or biological sources such as infection with bacteria that can trigger DNA damage and DNA damage signaling in host cells (Cuevas-Ramos et al., 2010; Elsen et al., 2013; Toller et al., 2011). Importantly, the prevalence of virus infections, including Adenovirus, is a serious and often fatal complication in cancer patients treated

with chemotherapy (Hough et al., 2005; Lee et al., 2014; Steiner et al., 2008). Based on our model, genotoxic chemotherapies may exacerbate or facilitate Adenovirus infection by compromising MRN sensing of viral genomes.

Moreover, the sequestration of MRN by DNA damage has important implications for the design of oncolytic virus vectors and our understanding of pathological conditions in which genotoxic stress is common. For example, telomere shortening, laminopathies, and replicative senescence, hallmarks of aging, can trigger DDR signaling that could sequester MRN, rendering 'old' cells more permissive for viral replication (Pospelova et al., 2009; Scaffidi and Misteli, 2008; Suram and Herbig, 2014). Also, perpetual genomic instability, an emerging hallmark of cancer cells (Hanahan and Weinberg, 2011), may contribute to elevated permissiveness in viral genome replication by sequestering MRN. DDR signaling can, in fact, be used to distinguish precancerous lesions from normal cells (Bartkova et al., 2005; Gorgoulis et al., 2005). Consistent with this hypothesis, we demonstrate that tumor cell lines are differentially permissive for viral genome replication (Figures 4.5B-D). Of note, the most permissive of the tested cell lines, U2OS, undergoes telomere lengthening through the ALT pathway, which is characterized by the requirement for and accumulation of MRN at very long telomeres (Cesare and Reddel, 2010). The sequestration of MRN in U2OS cells by ALT-associated mechanisms is consistent with our model that MRN sensing of viral genomes is saturable. Thus, our studies provide key mechanistic insights that could enable the development of E1B-55K/E4-ORF3 mutant viruses as novel cancer therapies (O'Shea, 2005) that selectively replicate in precancerous lesions and tumor cells that have high levels of DNA damage. These viral agents could also be

exciting and rational combination therapies with drugs that selectively agonize or antagonize DDR pathways dysregulated in cancer (Curtin, 2012).

Sequestration of MRN may also explain the mechanism by which viruses incapable of targeting MRN can still replicate. For example, there are over 60 human Adenoviruses, all of which express E1B-55K and E4-ORF3. However, the ability of E4-ORF3 to bind and mislocalize MRN may be peculiar to Ad5/2 (Carson et al., 2009), and various Adenovirus serotypes do not target the MRN complex for degradation (Cheng et al., 2013; Forrester et al., 2011). As MRN sensing of viral genomes is a critical checkpoint of the virus lifecycle, viruses that do not encode proteins that inactivate MRN would not replicate at low MOIs. Such viruses may rely on high MOI infection to bypass the MRN checkpoint using high numbers of incoming genomes. This would also explain the biological relevance of producing large quantities of defective particles per infectious cycle, as partial genomes may serve as competitive substrates of MRN upon infection.

WT Adenovirus infection triggers MRN-independent global DDR kinase signaling.

The activation of global DDR signaling in WT virus infected cells is MRN independent and does not impact viral genome replication (Figures 2.2, 2.4, 2.5, 2.7, 2.9, and 2.10). MRN is generally thought to play a critical role in activating ATM (Costanzo et al., 2004; Falck et al., 2005; Lee and Paull, 2004, 2005; Uziel et al., 2003). However, WT virus infection activates global ATM and DDR kinase phosphorylation despite MRN inactivation by E1B-55K, E4-ORF3 and RNAi (Figures 2.2, 2.4, 2.5, 2.7, 2.9, and 2.10). Perhaps most compelling, *MR* knockdown activates global DDR kinase

signaling in ΔE1B-55K/ΔE4ORF3 infected cells, most likely as a downstream consequence of rescuing viral genome replication (Figures 2.5 and 2.7). Consistent with the latter, the inhibition of viral genome replication by HU prevents the activation of global DDR signaling in WT virus infected cells where MRN is inactivated by E1B-55K/E4-ORF3 (Figure 2.9). Together, these data demonstrate that global ATM and DDR kinase signaling is activated through a novel MRN independent mechanism as a downstream consequence of virus genome replication (Figure 2.8B).

Adenovirus genome replication is also required for the transcription of late viral capsid mRNAs (Thomas and Mathews, 1980). Therefore, it is possible that the expression of late viral structural proteins activate DDR kinases. However, the high concentrations of double and single strand viral DNA genomes in E2A domains within the nucleus (Figure 2.8A) seem a more likely candidate (Pombo et al., 1994). ATM kinase inhibitors reduce but do not ablate DDR phosphorylated substrates, indicating that additional DDR kinases may also be activated (Figure 2.10A). ATR (Carson et al., 2003) and ATR activators, including RAD9, RAD17, E1B-AP5, ATRIP, RPA32 (Blackford et al., 2008) and TOPBP1 localize to viral replication centers in WT virus infected cells (Blackford et al., 2010; Carson et al., 2009). Therefore, ATM may be activated downstream of ATR in response to high levels of single strand genomes (Zou, 2007). However, treatment with an ATR kinase inhibitor, AZ-20 (Foote et al., 2013), does not affect induction of DDR kinase phosphorylated substrates in WT infected A549 cells by 24 h.p.i. (data not shown). This result, and the minimal phosphorylation of canonical ATR substrates during WT infection (data not shown), suggests that ATM and other DDR kinases are activated independently of ATR during WT infection.

Previous studies have revealed that ATM can be activated independently of MRN by reactive oxygen species that crosslink ATM monomers at Cysteine 2991, explaining the initial burst of ATM activation upon γ-irradiation (Guo et al., 2010). However, in peroxide treated cells, although ATM crosslinking can be detected, ATM induced phosphorylation of chromatin associated substrates, such as TRIM28-Ser824 and H2AX-Ser139, are not induced (Guo et al., 2010). Interestingly, recent studies have demonstrated that Adenovirus induces changes in cellular oxidative metabolism analogous to the Warburg effect (Thai et al., 2014). This is consistent with WT infection triggering ATM activation directly through the production of reactive oxygen rather than the production of DNA or protein intermediates. However, in our results, TRIM28-Ser824 and H2AX-Ser139 are highly phosphorylated in WT virus infected cells (Figures 2.2, 2.4, 2.9, and 2.10), suggesting that the MRN independent activation of ATM is distinct from the initial burst of ATM activation by γ-irradiation induced reactive oxygen species.

The corruption of chromatin and nuclear structure can also trigger ATM activation in the apparent absence of DNA breaks (Bakkenist and Kastan, 2003; Pospelova et al., 2009; Scaffidi and Misteli, 2008). Also, upon sensing Trimethyl-H3-Lys9 within corrupted chromatin, the TIP60 acetyltransferase can mediate the acetylation and activation of ATM (Kaidi and Jackson, 2013; Sun et al., 2009; Sun et al., 2007). Finally, the localized concentration of ATM and other DDR proteins within the nucleus can mediate the activation of ATM irrespective of DNA damage (Soutoglou and Misteli, 2008). Thus, ATM can be activated through cellular mechanisms that detect changes within chromatin.

Our lab has previous shown that during WT infection, cellular chromatin compacts tremendously and is marked by regions of concentrated Trimethyl-H3-Lys9 that surround late viral replication centers which contain high local concentration of viral DNA (Soria et al., 2010). Furthermore, an important feature of viral replication centers is the high concentration of single strand viral DNA (Pombo et al., 1994). Here we show that Adenovirus DNA replication, which occurs simultaneously with the formation of late viral replication domains and the compaction of cellular chromatin, triggers high levels of MRN independent ATM activation (Figures 2.8-2.10). Therefore, an important explanation is that the assembly of viral genomes into late replication centers triggers the recruitment, activation, and amplification of ATM signaling through a sensor of chromatin corruption such as TIP60, the concentration of DDR proteins around viral replication domains, or a novel mechanism that detects single strand DNA in late viral replication centers directly.

As the ATM is a central regulator of checkpoint activation and apoptosis in response to genotoxic chemotherapy, the discovery of an MRN independent and DNA damage independent mechanism to activate ATM signaling may lead to an important advancement in cancer therapies that rely on ATM activation. Furthermore, although global DDR signaling does not impact viral genome replication (Figure 2.10B), it may still play an important role *in vivo* in modulating the host immune response and inflammation (Brzostek-Racine et al., 2011; Figueiredo et al., 2013; Gasser and Raulet, 2006).

Distinct DDR signaling mechanisms may explain discrepancies between this and previous studies.

The existence of two mechanistically distinct DDRs to early and late Adenovirus genome replication is an exciting but unanticipated complexity that helps to reconcile the confounding observations of numerous studies. The majority of previous studies have used various E4 deleted viruses that still express E1B-55K to study the anti-viral DDR (Carson et al., 2009; Carson et al., 2003; Gautam and Bridge, 2013; Mathew and Bridge, 2007, 2008; Stracker et al., 2002). In contrast to ΔE1B-55K/ΔE4-ORF3 viruses (Figure 2.8A), E4 deleted viruses appear to bypass the early MRN dependent checkpoint as evidenced by the assembly of late E2A viral genome replication domains (Carson et al., 2003; Gautam and Bridge, 2013; Mathew and Bridge, 2007, 2008; Stracker et al., 2002). E1B-55K binds to MRE11 in the absence of E4-ORF6 (Carson et al., 2003; Schwartz et al., 2008), which may be sufficient to disrupt MRN functions and facilitate early viral genome replication in E4 deletion virus infected cells. E1B-55K also localizes to E2A domains (O'Shea et al., 2004) that may nucleate MRE11 and generate artifactual viral genome concatemers and DDR signaling in E4 deletion virus infected cells (Boyer et al., 1999; Stracker et al., 2002; Weiden and Ginsberg, 1994). However, the nucleation of MRN components or the formation of E2A domains are not observed in primary cells infected with viruses that have minimal and targeted mutations in E1B-55K and E4-ORF3 (Figures 2.1). Thus, the colocalization between MRN components and viral replication domains is likely indicative of conditions in which the early MRN restriction of viral genome replication has been bypassed. In addition to our model that MRN sensing of viral genomes is

saturable and our demonstration that various cell lines are differentially permissive to viral genome replication, these results may explain discrepancies between this study and previous studies.

Chapter acknowledgements

The contents of this chapter, in full, has been submitted for publication of the material as it may appear in Cell, 2015, Shah, G.S. and O'Shea, C.C. The dissertation author was the first author of this paper, and Clodagh C. O'Shea was the senior author, supervising this work.

Chapter 6. Future Studies

Investigating the precise mechanism by which MRN restricts viral genome replication

Our results demonstrate that MRN serves as a critical checkpoint to viral genome replication, yet the contribution of other components of the DDR network remains unclear. While MRE11 or RAD50 knockdown rescues viral genome replication to nearly WT levels (Figures 2.5 and 2.7), treatment with an ATM kinase inhibitor only partially rescues viral genome replication (Figure 2.10). This suggests that it is MRN itself, rather than other downstream components of the DDR pathway, that serves as the major anti-viral function upon Adenovirus infection. This is further supported by the evolution of two independent mechanisms that target MRN, rather than ATM or other DDR proteins.

An epistasis map of DDR pathway components that restrict ΔE1B-55K/ΔE4-ORF3 viral genome replication via RNAi screening would help determine whether MRN stand alone in restricting viral genome replication or relies on downstream pathway components. Important candidates would include H2AX and MDC1, which should have little to no contribution to restricting viral genome replication given their apparent lack of phosphorylation upon ΔE1B-55K/ΔE4-ORF3 infection. Other important candidates include KU70, KU80, and PARP-1, which may act upstream of MRN sensing of viral genomes, as in the response to cellular DNA damage. However, the near-complete rescue of ΔE1B-55K/ΔE4-ORF3 genome replication by MRN

knockdown, implies that upstream activators of MRN such as KU70, KU80, and PARP-1, are not sufficient to restrict viral genome replication without MRN.

Alternatively, the identification of proteins associated with viral genomes in MRN-viral genome complexes by mass spectrometry would help identify anti-viral DDR candidates. One approach to purify such complexes would be to epitope tag viral early proteins involved genome replication such as E2A, E2B-Polymerase, and E2B-pTP and to immunoprecipitate complexes from infected cell lysates. Multiple epitope tagged proteins and immunoprecipitation steps would be helpful to exclude free viral proteins from those in viral genome complexes. Another approach would be to prepare infectious virions with labeled nucleotides or epitope tagged TP and then purify viral genome complexes assembled on incoming genomes directly. Finally, given the distinct size of viral genomes relative to host chromosomes, sucrose gradient centrifugation of lysates from infected cells may be used to purify viral genome complexes based on their presumably unique densities. An important challenge is the low yields likely to be obtained from all approaches given that our infection conditions lead to roughly 10 genome copies per infected cell (Figure 3.4B).

As discussed in Chapter 5, viral genome replication results in various intermediates and products, and the precise structure of viral genomes sensed by MRN remains unknown. Therefore, an important advantage to optimizing the purification of viral genome complexes from infected cells is the ability to identify viral genome substrates for MRN binding through EM imaging of DNA. Tagging systems such the tetracysteine tag, miniSOG, and APX may be used to address the challenge of visualizing MRN protein associated to viral genomes in EM (Gaietta et al., 2002;

Martell et al., 2012; Shu et al., 2011). An additional advantage to optimizing the purification of viral genome complexes is the ability to quantify the amount of MRN associated to ΔE1B-55K/ΔE4-ORF3 viral genomes. While ChIP analysis demonstrates the enrichment of MRN at viral genome ends, it cannot be used to quantify MRN binding to viral genomes versus cellular DNA breaks. The quantification of MRN at viral genomes may indicate the mechanism by which MRN restricts viral genome replication and why cellular DNA breaks result in a differential response.

Given the likelihood of MRN restricting viral genome replication without additional cellular factors, the most likely explanation for its anti-viral role given the current results is the occlusion of viral genomes to cellular and viral factors required for genome replication. Importantly, the replication of Adenovirus genomes and the binding of MRN to DNA breaks have been emulated *in vitro* (Challberg and Kelly, 1979; Lee et al., 2003; Paull and Gellert, 1999). The combination of these technologies may serve as a powerful tool to reveal whether the MRN binding of viral genomes is sufficient to block further viral genome replication. Moreover, an *in vitro* system can be used to interrogate the role of MRE11 nuclease activity and nucleotide depending binding modes of the MRN complex (Paull and Deshpande, 2014). An *in vitro* system may also be used to generate high concentrations of viral genome-MRN complexes for either EM or AFM imaging as well as for the quantitation of MRN associated to viral genomes. Such studies would contribute to understanding the mechanism by which MRN restricts viral genome replication.

Finally, an investigation of MRE11 complexes in other organism may reveal the conservation of its anti-viral role. For example the genes encoding MRN components

and ATM are conserved in *Arabidopsis thaliana*, in which their deletion is not lethal (Yoshiyama et al., 2013). Thus, plants offer a unique genetic tool, as MRN- and ATM-defective plants can be challenged by plant DNA viruses to determine the contribution MRN and ATM in viral immunity. Furthermore, MRE11 and RAD50 are conserved across all domains of life, including bacteria and archaea (Shin et al., 2014), and animal and bacterial viruses can share common ancestors (Hendrix, 1999). Hence, both the expression of the MRE11 complex and the threat of DNA virus infection is common to all organisms. Therefore, it is possible that the mechanism by which the human MRE11 complex restricts Adenovirus genome replication is conserved even across domains, yet the anti-viral role of MRE11 in prokaryotes is not well-studied.

Investigating the restriction of MRN-ATM signaling at viral genomes

We show that despite the recruitment of MRN-ATM and the presence of phosphorylated SQ/TQ proteins at sites of viral genomes, global ATM phosphorylation is restricted. The lack of H2AX may explain this, which can be determined by ChIP analysis of Adenovirus genomes specifically for H2AX. The corollary experiment would be to tag an early and abundant viral protein that bind viral DNA such as E2A with the H2AX tail peptide. This would allow for the phosphorylation of the H2AX tail by ATM and the potential amplification of global ATM activation. This experiment may distinguish whether the lack of H2AX or the absolute genome size is what restricts global ATM activation upon ΔE1B-55K/ΔE4-ORF3 infection. Also, knockdown of WIP1, a phosphatase that targets ATM (Shreeram et al., 2006), may demonstrate if

WIP1 protein phosphatase activity restricts ATM activation in extrachromosomal contexts.

Determining the fate of viral genomes upon MRN sensing

The ability of ΔE1B-55K/ΔE4-ORF3 infected cells to divide suggests that the activation of mitosis and nuclear membrane breakdown may purge viral genomes from the nucleus. ΔE1 genomes are rapidly eliminated from the nucleus upon infection. Therefore, this model may explain the uncoupling the cellular and anti-viral DDRs, allowing viral DNA to be eliminated upon ΔE1 infection. If this model is correct, inhibitors of mitosis that block nuclear membrane breakdown should block the depletion of ΔE1 genomes. Also, ΔE1B-55K/ΔE4-ORF3 infected cells that have undergone cell division, which can be traced and sorted using dyes such as CFSE, should have a lower amount of viral early proteins and fewer genome copies. Finally, live imaging of viral genomes and MRE11 throughout mitosis may demonstrate the localization of viral genome upon MRN sensing. This may be achieved by with fluorescently labeling incoming viral DNA or by inserting a genetic element into the viral genome that can be used to localize fluorescent proteins, such as an array of tetracycline response elements or lac operator sequences.

Determining whether natural sources of DNA damage facilitate viral replication.

Our data present a model in which cellular genomic DNA damage mutes the ability of MRN to restrict viral genome replication by competing with viral genomes. Sidestream smoke has been used to study Adenovirus biology in airway epithelial cells

(Sharma et al., 2012) and emulates a relevant source genotoxic stress in modern times. Sidestream smoke may likely rescue ΔE1B-55K/ΔE4-ORF3 viral genome replication and contribute to the relevance of our model. An important caveat to this experiment is that sidestream smoke results in high levels of oxidative DNA damage (Sarker et al., 2014) and may not induce the type or abundance of breaks required to result in the rescue of viral genome replication. In addition to sidestream smoke, UV exposure and other relevant sources of damage should be tested. Also, strains of bacterial pathogens such as *E. coli*, *H. pylori*, and *P. aeruginosa* may induce DNA damage and/or DDR signaling within human cells (Cuevas-Ramos et al., 2010; Elsen et al., 2013; Toller et al., 2011). Adenovirus and such bacteria can be found in similar tissues, and there is a synergistic relationship between various bacteria and viruses (Bosch et al., 2013). Co-infection with DNA damage inducing bacteria may rescue ΔE1B-55K/ΔE4-ORF3 viral genome replication, and expand upon the known mechanisms by which bacteria and viruses interact as human pathogens. Furthermore, if DNA damage inducing bacteria can help viruses bypass MRN restriction of viral genome replication, this may explain the prevalence of Adenoviruses that do not encode mechanisms to inactivate MRN through co-evolution and commensal relationships with such bacteria.

Generating a virus that selectively replicates in cancer cells based on elevated genomic instability in cancer cells

Our data demonstrate that various tumor cell lines are differentially permissive for viral genome replication, and this is best explained by the saturation of MRN by genomic instability in cancer cells. This implies that genomic instability in cancer cells

can be targeted for the development of novel oncolytic vectors bearing E1B-55K/E4-ORF3 mutations. The panel of cell lines in which the permissiveness for ΔE1B-55K/ΔE4-ORF3 viral genome replication was tested should be greatly expanded. To verify that the differential permissiveness of such cells is dependent on MRN status, cancer cell lines that express very low levels of MRN complex proteins, such as HCT-116 (Garner and Eastman, 2011), should be included. Other cancer cell lines that elongate telomeres through the ALT pathway should also be included to determine if very high permissiveness for viral genome replication is peculiar to ALT cells. A variety of cell lines including SAOS-2, GM847, and KMST-6 exhibit ALT (Henson et al., 2002).

Subsequently, upon identification of permissive cell lines, features of the DDR in highly permissive cells should be analyzed to verify if selective viral genome replication correlates with markers of genomic instability. Assays should include immunofluorescence analysis for the frequency and abundance of γH2AX and other DDR foci, as well as biophysical assays for DNA damage such as pulsed field gel electrophoreses or single cell gel electrophoresis (COMET). Of note, MRN knockdown and etoposide treatment only very minimally rescue late viral protein production in ΔE1B-55K/ΔE4-ORF3 infected cells (data not shown), which is likely due to various other functions of E1B-55K/E4-ORF3 in the virus lifecycle. Point mutants of E1B-55K and E4-ORF3 that abrogate their MRN inactivating properties have been previously described (Carson et al., 2003; Ou et al., 2012). Oncolytic viruses should therefore incorporate such point mutations to minimize functional defects of E1B-55K/E4-ORF3 in other viral processes and maximize oncolytic potential prior to proceeding.

The precise mechanism by which viral genome replication trigger MRN independent ATM and DDR kinase activation

ATM mediated phosphorylation contributes to checkpoint activation and apoptosis in response to DNA breaks (Shiloh and Ziv, 2013). The very high levels of ATM and DDR kinase signaling in the absence of the MRN complex during WT Adenovirus infection suggests the existence of a mechanism that can trigger robust ATM activation without DNA breaks. Understanding this mechanism can inform cancer therapies that activate ATM to achieve cell cycle arrest or apoptosis without damaging DNA with genotoxic drugs, which can result in secondary malignancies.

We demonstrate that upon WT Adenovirus infection viral genome replication, which is coincident with the formation of E2A viral genome replication domains, triggers high levels of global ATM and DDR kinase signaling (Figures 2.7-2.10). One explanation is that a sensor of viral genomes triggers DDR kinase activation through a related kinase. Preliminary results using an ATR inhibitor (not shown) suggest that ATM activation in response to WT infection is not dependent on ATR kinase and that the DDR kinases are activated independently during WT virus infection. To support this conclusion components of the ATR signaling machinery such as ATR itself and ATRIP should be knocked down by RNAi to assess their contribution to the global DDR phosphorylation phenotype. Another related DNA damage sensor and kinase is KU70/KU80 and DNA-PKcs. KU70 does not colocalize with E2A viral replication centers (data not shown), which is inconsistent with this hypothesis. Nevertheless, to support this argument, KU70/KU80 and DNA-PK should be knocked down by RNAi to assess their contribution to the global DDR phosphorylation phenotype. Of note, despite

high levels of phosphorylated SQ/TQ containing proteins upon WT infection, phosphorylated SQ/TQ epitopes are not enriched on WT Adenovirus genomes (Figures 3.2D and 3.3), which is inconsistent with the activation of DDR kinases by a sensor of viral DNA.

An informative experiment going forward would be to measure the relative contribution of ATM kinase activity to the global DDR phosphorylation phenotype by performing a dot blot for phosphorylated SQ/TQ motifs with lysates from cells treated with and without an ATM inhibitor. However, based on immunoblot analysis of selected DDR substrates, much of the DDR phosphorylation observed upon WT infection is dependent on ATM (Figure 2.10). Thus, the most likely explanation for DDR kinase phosphorylation is that ATM is activated in a manner independent of MRN and DNA breaks. As discussed in Chapter 5, the sensing of chromatin corruption during WT infection may trigger MRN independent ATM activation. TIP60 acetyltransferase activity and CK2 kinase activity have been implicated in activating these responses (Sun et al., 2005; Sun et al., 2009). Therefore, TIP60 knockdown and CK2 drug inhibition would determine if ATM activation upon WT infection occurs through this well-studied mechanism. The corruption of the nuclear lamina through the expression of defective Lamin A has also been shown to activate DDR signaling (Scaffidi and Misteli, 2008). Examining the nuclear lamina upon WT infection through immunofluorescence analysis may demonstrate similarities between these phenomena and inform further investigation.

Cells, culturing conditions and viral infections. Primary human small airway epithelial cells (SAECs) were obtained from Lonza, cultured in Small Airway Growth Medium (SAGM) without gentamycin at 3% O_2 as described (Ou et al., 2012; Soria et al., 2010). Primary SAECs were cultured no more than 4 passages. hTERT-SAECs were generated by transducing primary SAECs with a lentivirus expressing hTERT and were cultured to no more than 10 passages. SAECs were cultured to confluence and then maintained for 10 days to promote quiescence prior to infection. A549, H1299, HeLa, and U2OS cell lines were cultured in DMEM supplemented with 10% heat-inactivated FBS without antibiotics. For infection, cells were seeded at 90% confluency and infected in 2% FBS DMEM. Infections were carried out at a multiplicity of infection (MOI) of 10 plaque forming units (PFU) per cell for SAEC, A549, H1299, and HeLa cells and an MOI of 30 PFU/cell U2OS. Media containing virus was removed between 2 to 4 h.p.i. and replaced with complete growth media in all experiments.

Drugs. DNA damage was induced by treating cells with 0.5 μg/ml doxorubicin (Sigma) or 30 μg/ml etoposide (Sigma) for 12 hours, unless otherwise indicated. Hydroxyurea (Sigma) was used at 2 mM, aphidicolin (Sigma) at 1 μM, KU-55933 (Calbiochem) at 10 μM, bleomycin at 10 μM, Roscovitine (Cell Signaling) at 20 μM, 5-fluorouracil at 50 μg/ml, camptothecin at 10 μM, and nutlin-3b (Sigma) at 10 μM.

Viruses. Viruses were titered on 293/E4/pIX cells, as described previously (O'Shea et al., 2004). Mock infection was performed with a ΔE1 virus (designated AdSyn-CO117), an E1 and E4-ORF3 deleted non-replicating Adenovirus expressing GFP under the control of the CMV promoter. The additional deletion of E4-ORF3 prevents any E1A independent expression of E4-ORF3 that could inactivate MRN. Wild-type virus is Ad5. The ΔE1B-55K virus (AdSyn-CO124) was created by mutating the start codon of E1B-55K (ATG to GTG) and I90 of E1B-55K to a stop codon (ATT to TAG). The ΔE4-ORF3 virus (AdSyn-CO118) was created by deleting the coding region of E4-ORF3. The ΔE1B-55K/ΔE4-ORF3 virus (AdSyn-CO140) is the same as ΔE1B-55K except the E4-ORF3 coding region is deleted.

In experiments using the previous generation of Ad5/Ad2 hybrid viruses, mock infection was performed with the E1 deleted non-replicating Adenovirus *dl*312 (Jones and Shenk, 1979). Wild-type virus is WtD (Barker and Berk, 1987), ΔE1B-55K is *dl*1520/ONYX-015 (Barker and Berk, 1987; Bischoff et al., 1996). The ΔE1B-55K/ΔE4-ORF3 virus, *dl*3112, has an identical genome backbone to *dl*1520/ONYX-015 but has a single base pair deletion (nucleotide 7143r) that ablates E4-ORF3 expression (Shepard and Ornelles, 2003).

Immunofluorescence. Cells were fixed in 4% paraformaldehyde/$PBS^{-/-}$ for 30 minutes at room temperature, permeabilized in 0.5% TritonX-100/$PBS^{-/-}$, and stained as described previously (O'Shea et al., 2004; O'Shea et al., 2005). For MRE11 and NBS1 staining in SAECs, cells were pre-permeabilized (20 mM HEPES-KOH pH 7.9, 50 mM NaCl, 3 mM $MgCl_2$, 300 mM sucrose, 0.5% TritonX-100) for 5 minutes at room

temperature prior to fixing. For NBS1 and MDC1 staining in A549 cells, cells were fixed directly in ice-cold methanol for 15 minutes. Primary antibodies are described in Table S1. Alexa 488- and 555-conjugated secondary antibodies (Molecular Probes) were used for detection of primary antibodies. Hoechst-33342 was used to counter-stain DNA, and nucleus borders were outlined using Adobe Photoshop. Images were acquired with a Zeiss LSM780 imaging system with a 63× objective. For analyzing E2A viral replication centers in SAECs and mitotic bodies in A549 cells, a maximum intensity projection of 40 optical z-stacks across 16 μm was generated. All other images are single z-planes.

Immunoblot. Cells were directly harvested in SDS-PAGE loading buffer and sonicated using a Misonix S-4000 cup horn bath sonicator. Cells were counted from an identical well at the time of harvest. Lysate from an equal number of cells was loaded from each sample for SDS-PAGE and immunoblot analysis. Primary antibodies used are described in Table S1. Anti-mouse, anti-rat, and anti-rabbit secondary antibodies conjugated to either IRDye800 (Rockland) or Alexa Fluor 680 (Molecular Probes) fluorophores were used to detect primary antibody staining on a LI-COR-Odyssey scanner. Quantification was performed using the LI-COR Odyssey 3.0 software, using the user defined background normalization method. Antibody signals were analyzed as integrated intensities of regions defined around the bands of interest. For assessing phosphorylation, Phospho-protein levels were divided by total-protein levels and normalized to the "t = 0" sample. For MRE11 and RAD50 knockdown, MRE11 and

RAD50 protein levels were divided by β-ACTIN levels and normalized to the control siRNA treated sample.

Q-PCR analysis of viral genomes. Total DNA was extracted using the QiaAMP DNA Micro kit (Qiagen) following the manufacturer's protocol. Taqman probes for quantifying Adenovirus DNA were as described previously (Johnson et al., 2002). Q-PCR was performed with 2.5 ng of total DNA in 5 µl reactions using the Applied Biosystems 7900HT device (Life Technologies), as described previously (O'Shea et al., 2004). Reactions were performed in triplicate or quadruplicate. Viral DNA was quantified relative to 18S rDNA to obtain a ΔC_t for each sample (Livak and Schmittgen, 2001). The standard deviation for target N, is calculated by: $2^{-\Delta Ct}$ with ΔC_t+s and ΔC_t-s, where s is the standard deviation of the ΔC_t value. For absolute quantitation, cells were trypsinized and submitted to nuclear fractionation prior to DNA purification. Q-PCR was performed using a standard curve of Ad5 DNA to determine absolute virus genome copy numbers using the SDS 2.3 software (Life Technologies).

Chromatin immunoprecipitation. A549 cells were infected as described above and harvested at 12 h.p.i. Plates were incubated with 20 mM HEPES-KOH pH 7.9, 50 mM NaCl, 3 mM $MgCl_2$, 300 mM sucrose, 0.5% TritonX-100 for 5 minutes at room temperature prior to fixing. Samples were processed as described previously for ChIP (Soria et al., 2010). Briefly, cells were fixed with 1% formaldehyde for 10 minutes and stopped with 0.125 M glycine, lysed in 50 mM Tris pH 8.0, 10 mM EDTA pH 8.0, 1% SDS and sonicated to shear genomic DNA. Lysates from 1×10^6 cells were diluted 1:10

in 20 mM Tris pH 8.0, 2 mM EDTA pH 8.0, 150 mM NaCl, 1% Triton X-100 and immunoprecipitated with 5 μl of anti-MRE11, anti-γH2AX, or anti-Phospho-SQ/TQ motif antibodies (Cell Signaling) or 5 μg of an anti-H3 (Abcam), anti-ATM (Novus), or anti-MDC1 (Genetex) antibodies. 5 μg of an anti-GST antibody (Santa Cruz) was used as a control for specificity. Immuno-complexes were isolated using Protein G Dynabeads (Life Technologies). Crosslinking was reversed by incubation at 65^{o}C overnight. DNA was purified using the QiaAMP DNA Micro kit (Qiagen). For Real-time Quantitative PCR, ChIP DNA samples were analyzed in quadruplicate using the Power SYBR green master mix (Life Technologies) using the Applied Biosystems 7900HT device. Primers for Q-PCR were designed against the Ad5 genome, Ad5 Primer Set 1 (5'-GTTACTCATAGCGCGTAATATTTGTCTAG-3' and 5'-CCCGGAACGCGGAAA-3'), which amplifies base pairs 323-424 and Ad5 Primer Set 2, (5'-CGGAAGTGACGATTTGAGGAA-3' and 5'-AAACCGCACGCGAACCTA-3'), which amplifies base pairs 35,689-35,759. Q-PCR Primers for cellular Alu genome sequences (5'-ACGAGGTCAGGAGATCGAGA-3' and 5'-CTCAGCCTCCCAAGTAG CTG-3') were as described (Zheng et al., 2014). A 10-fold dilution series of input DNA was used to determine the efficiency of the PCR for each primer set. Each primer set demonstrated linear amplification with an R^2 value of at least 0.9 across 15 C_t values. ChIP DNA samples were normalized relative to their respective input DNAs using the ΔC_t method to obtain percent input values or normalized relative to the ΔE1 sample using the $\Delta\Delta C_t$ method (Livak and Schmittgen, 2001) to obtain values 'relative to ΔE1'. Standard deviations from ΔC_t or $\Delta\Delta C_t$ values were incorporated into the statistical range as described above and referred to as 'standard deviation' in the legends.

Cell cycle analysis. For DNA content analysis, quiescent SAECs were infected with the indicated viruses and fixed in 70% EtOH/1.5 mM glycine, pH 2.8. Cells were treated with RNaseA overnight and stained with 0.5 μg/ml propidium iodide immediately before flow cytometry using an LSR II flow cytometer (BD Biosciences). Data were analyzed using FlowJo. For analyzing the effects of HU and aphidicolin on cellular DNA replication, cells were fixed, stained with Hoechst-33342, and DNA content quantified using the ImageXpress Micro high content screening device (Molecular Devices). Data were analyzed by ImageJ (NIH) to generate integrated density values from at least 30,000 nuclei. Cell cycle phase distribution was analyzed in Microsoft Excel.

RNAi. Stealth siRNAs were purchased from Life Technologies: *RAD50* (5'-GGAAGCCCAGUUAACAUCUUCAAAG-3' and 5'-GGACCAUUCAGUGAAAGA CAGAUUA-3') and *MRE11* (5'-ACAUGUUGGUUUGCUGCGUAUUAAA-3' and 5'-UCAUGGAGGAUAUUGUUCUAGCUAA -3') in addition to corresponding non-silencing control siRNAs (Cat# 12935-200). siRNAs were transfected using PepMute Plus (Signagen) at a concentration of 20 nM, unless otherwise indicated. p53 knockdown was performed using a lentivirus vector shp53 pLKO.1 puro (Godar et al., 2008) or a pLKO.1 puro scramble control shRNA (Sarbassov et al., 2005). Stable A549 cell pools were selected using puromycin.

Population doubling analysis. A549 cells were infected and seeded in triplicate at subconfluent densities in 24-well plates. At 6 hours, 12 hours, 1 day, 2 days, and 4 days

post infection, cells were trypsinized and counted. Population doublings were calculated according to the following formula $\log_2$ (number of cells at time of harvest/number of cells at time of seeding). Error bars indicate standard deviations from cell counts across three wells.

Antibodies. See Table 1.

Table 1. Primary antibodies used for ChIP, immunoblot (IB), and immunofluorescence (IF).

Antibody	**Company**	**Catalog Number**	**Lot**	**Application**
β-ACTIN (Clone AC-15)	Sigma	A5441	10TK480	IB
MRE11 (Clone 12D7)	Genetex	GTX70212	26626	IB
MRE11 (Clone 31H4)	Cell Signaling	4847	1, 2	ChIP
RAD50 (Clone 13B3/2C6)	Genetex	GTX71228	9111	IB
NBS1 (Clone 1D7)	Genetex	GTX70224	26330	IB
NBS1 (polyclonal)	Novus	NB100-143	L-2, L-3	IF
NBS1 phospho-Ser343 (Clone EP178)	Novus	NBP1-44411	YG080801	IB
ATM/ATR phospho-S/TQ substrate motif antibody (polyclonal)	Cell Signaling	2851	3	ChIP
ATM (Clone MAT3-4G10/8)	Sigma	A1106-24ul	010M4826	IB
ATM (polyclonal)	Novus	NB100-104	P-1	ChIP
ATM phospho-Ser1981 (Clone EP1890Y)	Epitomics	2152-1	YH101212D	IB
DNA-PKcs (Clone Ab-2)	Calbiochem	NA57	D00114972	IB
DNA-PKcs phospho-Ser2056 (polyclonal)	Abcam	ab18192-100	696143	IB
CHK2 (Clone 7)	Upstate/Millipore	05-649	28044	IB
CHK2 phospho-Thr68 (polyclonal)	Cell Signaling	2661	7	IB
CHK1 (Clone 2611D5)	Upstate/Millipore	05-965	DAM1447556	IB
CHK1 phospho-Ser345 (Clone 133D3)	Cell Signaling	2348	8	IB
H2AX (Clone 322105)	RnD Systems	MAB2406	YBU0110121	IB

Table 1 (continued). Primary antibodies used for ChIP, immunoblot (IB), and immunofluorescence (IF).

Antibody	**Company**	**Catalog Number**	**Lot**	**Application**
H2AX phospho-Ser139 (Clone 20E3)	Cell Signaling	9718	8	IB, IF, ChIP
TRIM28 (Clone 4E1)	Cell Signaling	5868	1	IB
TRIM28 phospho-Ser824 (polyclonal)	Cell Signaling	4127	1	IB
RPA32 (Clone 4E4)	Cell Signaling	2208	1	IB
RPA32 phospho-S4/S8 (polyclonal)	Bethyl	A300-245A	A300-245A-2	IB
53BP1 (polyclonal)	Novus	NB 100-304	A4	IF
MDC1 (polyclonal)	Genetex	GTX11170	28485	IF, ChIP
CYCLIN B1 (Clone Ab-3 GNS1)	NeoMarkers	MS-868-P	868P911E	IB
CYCLIN A (Clone Ab-6 6E6)	NeoMarkers	MS-1061-S	1061S10040	IB
Histone H3 phospho-Ser10 (polyclonal)	Upstate/Millipore	06-570	0703053576	IF
Histone H3	Abcam	ab1791	GR66870-1	ChIP
p53 (Clone DO-1)	Santa Cruz	sc-126	G1112	IB
MDM2 (Clone 2A10)	Calbiochem	OP115	D00124127	IB
p21 (Clone CP36, CP74)	Upstate/Millipore	05-345	DAM1787838	IB
GST (Clone B-14)	Santa Cruz	sc-138	L3005, I1009	ChIP
E1B-55K (Clone 2A6)				IB
E2A (Clone B-6)	received from Dr. Arnold Levine's laboratory			IF
E4-ORF3 (Clone 6A11)	Ascention			IB, IF
E1A (Clone m73)	Dr. Edward Harlow			IB

Chapter 8. References

Adelman, C.A., De, S., and Petrini, J.H. (2009). Rad50 is dispensable for the maintenance and viability of postmitotic tissues. Molecular and cellular biology *29*, 483-492.

Ahern, K.G., Wang, K., Xu, F.Y., Mathews, C.Z., and Pearson, G.D. (1991). Strands hybridize in postreplicative adenovirus overlap recombination. Proceedings of the National Academy of Sciences of the United States of America *88*, 105-109.

Bakkenist, C.J., and Kastan, M.B. (2003). DNA damage activates ATM through intermolecular autophosphorylation and dimer dissociation. Nature *421*, 499-506.

Barker, D.D., and Berk, A.J. (1987). Adenovirus proteins from both E1B reading frames are required for transformation of rodent cells by viral infection and DNA transfection. Virology *156*, 107-121.

Bartkova, J., Horejsi, Z., Koed, K., Kramer, A., Tort, F., Zieger, K., Guldberg, P., Sehested, M., Nesland, J.M., Lukas, C., Orntoft, T., Lukas, J., and Bartek, J. (2005). DNA damage response as a candidate anti-cancer barrier in early human tumorigenesis. Nature *434*, 864-870.

Bassing, C.H., Chua, K.F., Sekiguchi, J., Suh, H., Whitlow, S.R., Fleming, J.C., Monroe, B.C., Ciccone, D.N., Yan, C., Vlasakova, K., Livingston, D.M., Ferguson, D.O., Scully, R., and Alt, F.W. (2002). Increased ionizing radiation sensitivity and genomic instability in the absence of histone H2AX. Proceedings of the National Academy of Sciences of the United States of America *99*, 8173-8178.

Ben-Israel, H., and Kleinberger, T. (2002). Adenovirus and cell cycle control. Frontiers in bioscience : a journal and virtual library *7*, d1369-1395.

Bennett, C.B., Lewis, A.L., Baldwin, K.K., and Resnick, M.A. (1993). Lethality induced by a single site-specific double-strand break in a dispensable yeast plasmid. Proceedings of the National Academy of Sciences of the United States of America *90*, 5613-5617.

Berkovich, E., Monnat, R.J., Jr., and Kastan, M.B. (2007). Roles of ATM and NBS1 in chromatin structure modulation and DNA double-strand break repair. Nature cell biology *9*, 683-690.

Bewersdorf, J., Bennett, B.T., and Knight, K.L. (2006). H2AX chromatin structures and their response to DNA damage revealed by 4Pi microscopy. Proceedings of the National Academy of Sciences of the United States of America *103*, 18137-18142.

Bischoff, J.R., Kirn, D.H., Williams, A., Heise, C., Horn, S., Muna, M., Ng, L., Nye, J.A., Sampson-Johannes, A., Fattaey, A., and McCormick, F. (1996). An adenovirus mutant that replicates selectively in p53-deficient human tumor cells. Science *274*, 373-376.

Blackford, A.N., Bruton, R.K., Dirlik, O., Stewart, G.S., Taylor, A.M., Dobner, T., Grand, R.J., and Turnell, A.S. (2008). A role for E1B-AP5 in ATR signaling pathways during adenovirus infection. Journal of virology *82*, 7640-7652.

Blackford, A.N., Patel, R.N., Forrester, N.A., Theil, K., Groitl, P., Stewart, G.S., Taylor, A.M., Morgan, I.M., Dobner, T., Grand, R.J., and Turnell, A.S. (2010). Adenovirus 12 E4orf6 inhibits ATR activation by promoting TOPBP1 degradation. Proceedings of the National Academy of Sciences of the United States of America *107*, 12251-12256.

Bosch, A.A., Biesbroek, G., Trzcinski, K., Sanders, E.A., and Bogaert, D. (2013). Viral and bacterial interactions in the upper respiratory tract. PLoS pathogens *9*, e1003057.

Boyer, J., Rohleder, K., and Ketner, G. (1999). Adenovirus E4 34k and E4 11k inhibit double strand break repair and are physically associated with the cellular DNA-dependent protein kinase. Virology *263*, 307-312.

Brzostek-Racine, S., Gordon, C., Van Scoy, S., and Reich, N.C. (2011). The DNA damage response induces IFN. Journal of immunology *187*, 5336-5345.

Burma, S., Chen, B.P., Murphy, M., Kurimasa, A., and Chen, D.J. (2001). ATM phosphorylates histone H2AX in response to DNA double-strand breaks. The Journal of biological chemistry *276*, 42462-42467.

Carson, C.T., Orazio, N.I., Lee, D.V., Suh, J., Bekker-Jensen, S., Araujo, F.D., Lakdawala, S.S., Lilley, C.E., Bartek, J., Lukas, J., and Weitzman, M.D. (2009). Mislocalization of the MRN complex prevents ATR signaling during adenovirus infection. The EMBO journal *28*, 652-662.

Carson, C.T., Schwartz, R.A., Stracker, T.H., Lilley, C.E., Lee, D.V., and Weitzman, M.D. (2003). The Mre11 complex is required for ATM activation and the G2/M checkpoint. The EMBO journal *22*, 6610-6620.

Celeste, A., Petersen, S., Romanienko, P.J., Fernandez-Capetillo, O., Chen, H.T., Sedelnikova, O.A., Reina-San-Martin, B., Coppola, V., Meffre, E., Difilippantonio, M.J., Redon, C., Pilch, D.R., Olaru, A., Eckhaus, M., Camerini-Otero, R.D., Tessarollo, L., Livak, F., Manova, K., Bonner, W.M., Nussenzweig, M.C., and Nussenzweig, A. (2002). Genomic instability in mice lacking histone H2AX. Science *296*, 922-927.

Cesare, A.J., and Reddel, R.R. (2010). Alternative lengthening of telomeres: models, mechanisms and implications. Nature reviews Genetics *11*, 319-330.

Challberg, M.D., and Kelly, T.J., Jr. (1979). Adenovirus DNA replication in vitro. Proceedings of the National Academy of Sciences of the United States of America *76*, 655-659.

Chatterjee, P.K., Vayda, M.E., and Flint, S.J. (1986). Adenoviral protein VII packages intracellular viral DNA throughout the early phase of infection. The EMBO journal *5*, 1633-1644.

Chaurushiya, M.S., and Weitzman, M.D. (2009). Viral manipulation of DNA repair and cell cycle checkpoints. DNA repair *8*, 1166-1176.

Cheng, C.Y., Gilson, T., Wimmer, P., Schreiner, S., Ketner, G., Dobner, T., Branton, P.E., and Blanchette, P. (2013). Role of E1B55K in E4orf6/E1B55K E3 ligase complexes formed by different human adenovirus serotypes. Journal of virology *87*, 6232-6245.

Ciccia, A., and Elledge, S.J. (2010). The DNA damage response: making it safe to play with knives. Molecular cell *40*, 179-204.

Cleaver, J.E. (2011). gammaH2Ax: biomarker of damage or functional participant in DNA repair "all that glitters is not gold!". Photochemistry and photobiology *87*, 1230-1239.

Costanzo, V., Paull, T., Gottesman, M., and Gautier, J. (2004). Mre11 assembles linear DNA fragments into DNA damage signaling complexes. PLoS biology *2*, E110.

Cremer, T., and Cremer, M. (2010). Chromosome territories. Cold Spring Harbor perspectives in biology *2*, a003889.

Cuevas-Ramos, G., Petit, C.R., Marcq, I., Boury, M., Oswald, E., and Nougayrede, J.P. (2010). Escherichia coli induces DNA damage in vivo and triggers genomic instability in mammalian cells. Proceedings of the National Academy of Sciences of the United States of America *107*, 11537-11542.

Curtin, N.J. (2012). DNA repair dysregulation from cancer driver to therapeutic target. Nature reviews Cancer *12*, 801-817.

de Jong, R.N., van der Vliet, P.C., and Brenkman, A.B. (2003). Adenovirus DNA replication: protein priming, jumping back and the role of the DNA binding protein DBP. Current topics in microbiology and immunology *272*, 187-211.

Dupre, A., Boyer-Chatenet, L., Sattler, R.M., Modi, A.P., Lee, J.H., Nicolette, M.L., Kopelovich, L., Jasin, M., Baer, R., Paull, T.T., and Gautier, J. (2008). A forward chemical genetic screen reveals an inhibitor of the Mre11-Rad50-Nbs1 complex. Nature chemical biology *4*, 119-125.

Elsen, S., Collin-Faure, V., Gidrol, X., and Lemercier, C. (2013). The opportunistic pathogen Pseudomonas aeruginosa activates the DNA double-strand break signaling and repair pathway in infected cells. Cellular and molecular life sciences : CMLS *70*, 4385-4397.

Evans, J.D., and Hearing, P. (2003). Distinct roles of the Adenovirus E4 ORF3 protein in viral DNA replication and inhibition of genome concatenation. Journal of virology *77*, 5295-5304.

Evans, J.D., and Hearing, P. (2005). Relocalization of the Mre11-Rad50-Nbs1 complex by the adenovirus E4 ORF3 protein is required for viral replication. Journal of virology *79*, 6207-6215.

Everitt, E., Sundquist, B., Pettersson, U., and Philipson, L. (1973). Structural proteins of adenoviruses. X. Isolation and topography of low molecular weight antigens from the virion of adenovirus type 2. Virology *52*, 130-147.

Falck, J., Coates, J., and Jackson, S.P. (2005). Conserved modes of recruitment of ATM, ATR and DNA-PKcs to sites of DNA damage. Nature *434*, 605-611.

Fax, P., Lipinski, K.S., Esche, H., and Brockmann, D. (2000). cAMP-independent activation of the adenovirus type 12 E2 promoter correlates with the recruitment of CREB-1/ATF-1, E1A(12S), and CBP to the E2-CRE. The Journal of biological chemistry *275*, 8911-8920.

Fehr, A.R., and Yu, D. (2013). Control the host cell cycle: viral regulation of the anaphase-promoting complex. Journal of virology *87*, 8818-8825.

Fernandez-Capetillo, O., Celeste, A., and Nussenzweig, A. (2003). Focusing on foci: H2AX and the recruitment of DNA-damage response factors. Cell cycle *2*, 426-427.

Fernandez-Capetillo, O., Chen, H.T., Celeste, A., Ward, I., Romanienko, P.J., Morales, J.C., Naka, K., Xia, Z., Camerini-Otero, R.D., Motoyama, N., Carpenter, P.B., Bonner, W.M., Chen, J., and Nussenzweig, A. (2002). DNA damage-induced G2-M checkpoint activation by histone H2AX and 53BP1. Nature cell biology *4*, 993-997.

Fernandez-Capetillo, O., Lee, A., Nussenzweig, M., and Nussenzweig, A. (2004). H2AX: the histone guardian of the genome. DNA repair *3*, 959-967.

Figueiredo, N., Chora, A., Raquel, H., Pejanovic, N., Pereira, P., Hartleben, B., Neves-Costa, A., Moita, C., Pedroso, D., Pinto, A., Marques, S., Faridi, H., Costa, P., Gozzelino, R., Zhao, J.L., Soares, M.P., Gama-Carvalho, M., Martinez, J., Zhang, Q., Doring, G., Grompe, M., Simas, J.P., Huber, T.B., Baltimore, D., Gupta, V., Green, D.R., Ferreira, J.A., and Moita, L.F. (2013). Anthracyclines induce DNA damage response-mediated protection against severe sepsis. Immunity *39*, 874-884.

Foote, K.M., Blades, K., Cronin, A., Fillery, S., Guichard, S.S., Hassall, L., Hickson, I., Jacq, X., Jewsbury, P.J., McGuire, T.M., Nissink, J.W., Odedra, R., Page, K., Perkins, P., Suleman, A., Tam, K., Thommes, P., Broadhurst, R., and Wood, C. (2013). Discovery of 4-{4-[(3R)-3-Methylmorpholin-4-yl]-6-[1-(methylsulfonyl)cyclopropyl]pyrimidin-2-y l}-1H-indole (AZ20): a potent and selective inhibitor of ATR protein kinase with monotherapy in vivo antitumor activity. Journal of medicinal chemistry *56*, 2125-2138.

Forrester, N.A., Sedgwick, G.G., Thomas, A., Blackford, A.N., Speiseder, T., Dobner, T., Byrd, P.J., Stewart, G.S., Turnell, A.S., and Grand, R.J. (2011). Serotype-specific inactivation of the cellular DNA damage response during adenovirus infection. Journal of virology *85*, 2201-2211.

Foster, D.A., Hantzopoulos, P., and Zubay, G. (1982). Resistance of adenoviral DNA replication to aphidicolin is dependent on the 72-kilodalton DNA-binding protein. Journal of virology *43*, 679-686.

Gaietta, G., Deerinck, T.J., Adams, S.R., Bouwer, J., Tour, O., Laird, D.W., Sosinsky, G.E., Tsien, R.Y., and Ellisman, M.H. (2002). Multicolor and electron microscopic imaging of connexin trafficking. Science *296*, 503-507.

Garner, K.M., and Eastman, A. (2011). Variations in Mre11/Rad50/Nbs1 status and DNA damage-induced S-phase arrest in the cell lines of the NCI60 panel. BMC cancer *11*, 206:201-213.

Gasser, S., and Raulet, D.H. (2006). The DNA damage response arouses the immune system. Cancer research *66*, 3959-3962.

Gautam, D., and Bridge, E. (2013). The kinase activity of ataxia-telangiectasia mutated interferes with adenovirus E4 mutant DNA replication. Journal of virology *87*, 8687-8696.

Giunta, S., Belotserkovskaya, R., and Jackson, S.P. (2010). DNA damage signaling in response to double-strand breaks during mitosis. The Journal of cell biology *190*, 197-207.

Godar, S., Ince, T.A., Bell, G.W., Feldser, D., Donaher, J.L., Bergh, J., Liu, A., Miu, K., Watnick, R.S., Reinhardt, F., McAllister, S.S., Jacks, T., and Weinberg, R.A. (2008). Growth-inhibitory and tumor- suppressive functions of p53 depend on its repression of CD44 expression. Cell *134*, 62-73.

Goldberg, M., Stucki, M., Falck, J., D'Amours, D., Rahman, D., Pappin, D., Bartek, J., and Jackson, S.P. (2003). MDC1 is required for the intra-S-phase DNA damage checkpoint. Nature *421*, 952-956.

Gorgoulis, V.G., Vassiliou, L.V., Karakaidos, P., Zacharatos, P., Kotsinas, A., Liloglou, T., Venere, M., Ditullio, R.A., Jr., Kastrinakis, N.G., Levy, B., Kletsas, D., Yoneta, A., Herlyn, M., Kittas, C., and Halazonetis, T.D. (2005). Activation of the DNA damage checkpoint and genomic instability in human precancerous lesions. Nature *434*, 907-913.

Greber, U.F., Willetts, M., Webster, P., and Helenius, A. (1993). Stepwise dismantling of adenovirus 2 during entry into cells. Cell *75*, 477-486.

Guo, Z., Kozlov, S., Lavin, M.F., Person, M.D., and Paull, T.T. (2010). ATM activation by oxidative stress. Science *330*, 517-521.

Haaf, T., Golub, E.I., Reddy, G., Radding, C.M., and Ward, D.C. (1995). Nuclear foci of mammalian Rad51 recombination protein in somatic cells after DNA damage and its localization in synaptonemal complexes. Proceedings of the National Academy of Sciences of the United States of America *92*, 2298-2302.

Haince, J.F., McDonald, D., Rodrigue, A., Dery, U., Masson, J.Y., Hendzel, M.J., and Poirier, G.G. (2008). PARP1-dependent kinetics of recruitment of MRE11 and NBS1 proteins to multiple DNA damage sites. The Journal of biological chemistry *283*, 1197-1208.

Halazonetis, T.D., Gorgoulis, V.G., and Bartek, J. (2008). An oncogene-induced DNA damage model for cancer development. Science *319*, 1352-1355.

Hanahan, D., and Weinberg, R.A. (2011). Hallmarks of cancer: the next generation. Cell *144*, 646-674.

Harper, J.W., and Elledge, S.J. (2007). The DNA damage response: ten years after. Molecular cell *28*, 739-745.

Hendrickx, R., Stichling, N., Koelen, J., Kuryk, L., Lipiec, A., and Greber, U.F. (2014). Innate immunity to adenovirus. Human gene therapy *25*, 265-284.

Hendrix, R.W. (1999). Evolution: the long evolutionary reach of viruses. Current biology : CB *9*, R914-917.

Henson, J.D., Neumann, A.A., Yeager, T.R., and Reddel, R.R. (2002). Alternative lengthening of telomeres in mammalian cells. Oncogene *21*, 598-610.

Hickson, I., Zhao, Y., Richardson, C.J., Green, S.J., Martin, N.M., Orr, A.I., Reaper, P.M., Jackson, S.P., Curtin, N.J., and Smith, G.C. (2004). Identification and characterization of a novel and specific inhibitor of the ataxia-telangiectasia mutated kinase ATM. Cancer research *64*, 9152-9159.

Hough, R., Chetwood, A., Sinfield, R., Welch, J., and Vora, A. (2005). Fatal adenovirus hepatitis during standard chemotherapy for childhood acute lymphoblastic leukemia. Journal of pediatric hematology/oncology *27*, 67-72.

Hu, C.H., Xu, F.Y., Wang, K., Pearson, A.N., and Pearson, G.D. (1992). Symmetrical adenovirus minichromosomes have hairpin replication intermediates. Gene *110*, 145-150.

Huang, L.C., Clarkin, K.C., and Wahl, G.M. (1996). Sensitivity and selectivity of the DNA damage sensor responsible for activating p53-dependent G1 arrest. Proceedings of the National Academy of Sciences of the United States of America *93*, 4827-4832.

Iacovoni, J.S., Caron, P., Lassadi, I., Nicolas, E., Massip, L., Trouche, D., and Legube, G. (2010). High-resolution profiling of gammaH2AX around DNA double strand breaks in the mammalian genome. The EMBO journal *29*, 1446-1457.

Johnson, L., Shen, A., Boyle, L., Kunich, J., Pandey, K., Lemmon, M., Hermiston, T., Giedlin, M., McCormick, F., and Fattaey, A. (2002). Selectively replicating adenoviruses targeting deregulated E2F activity are potent, systemic antitumor agents. Cancer cell *1*, 325-337.

Jones, N., and Shenk, T. (1979). Isolation of adenovirus type 5 host range deletion mutants defective for transformation of rat embryo cells. Cell *17*, 683-689.

Kaidi, A., and Jackson, S.P. (2013). KAT5 tyrosine phosphorylation couples chromatin sensing to ATM signalling. Nature *498*, 70-74.

Kastan, M.B., and Bartek, J. (2004). Cell-cycle checkpoints and cancer. Nature *432*, 316-323.

Kim, S.T., Lim, D.S., Canman, C.E., and Kastan, M.B. (1999). Substrate specificities and identification of putative substrates of ATM kinase family members. The Journal of biological chemistry *274*, 37538-37543.

Knipe, D.M., and Howley, P.M. (2013). Fields virology, 6th edn (Philadelphia, PA: Wolters Kluwer/Lippincott Williams & Wilkins Health).

Kwant, M.M., and van der Vliet, P.C. (1980). Differential effect of aphidicolin on adenovirus DNA synthesis and cellular DNA synthesis. Nucleic acids research *8*, 3993-4007.

Lakdawala, S.S., Schwartz, R.A., Ferenchak, K., Carson, C.T., McSharry, B.P., Wilkinson, G.W., and Weitzman, M.D. (2008). Differential requirements of the C terminus of Nbs1 in suppressing adenovirus DNA replication and promoting concatemer formation. Journal of virology *82*, 8362-8372.

Lechner, R.L., and Kelly, T.J., Jr. (1977). The structure of replicating adenovirus 2 DNA molecules. Cell *12*, 1007-1020.

Lee, J.H., Ghirlando, R., Bhaskara, V., Hoffmeyer, M.R., Gu, J., and Paull, T.T. (2003). Regulation of Mre11/Rad50 by Nbs1: effects on nucleotide-dependent DNA binding and association with ataxia-telangiectasia-like disorder mutant complexes. The Journal of biological chemistry *278*, 45171-45181.

Lee, J.H., and Paull, T.T. (2004). Direct activation of the ATM protein kinase by the Mre11/Rad50/Nbs1 complex. Science *304*, 93-96.

Lee, J.H., and Paull, T.T. (2005). ATM activation by DNA double-strand breaks through the Mre11-Rad50-Nbs1 complex. Science *308*, 551-554.

Lee, Y.J., Palomino-Guilen, P., Babady, N.E., Lamson, D.M., St George, K., Tang, Y.W., and Papanicolaou, G.A. (2014). Disseminated adenovirus infection in cancer patients presenting with focal pulmonary consolidation. Journal of clinical microbiology *52*, 350-353.

Lisby, M., Barlow, J.H., Burgess, R.C., and Rothstein, R. (2004). Choreography of the DNA damage response: spatiotemporal relationships among checkpoint and repair proteins. Cell *118*, 699-713.

Livak, K.J., and Schmittgen, T.D. (2001). Analysis of relative gene expression data using real-time quantitative PCR and the 2(-Delta Delta C(T)) Method. Methods *25*, 402-408.

Lou, Z., Minter-Dykhouse, K., Franco, S., Gostissa, M., Rivera, M.A., Celeste, A., Manis, J.P., van Deursen, J., Nussenzweig, A., Paull, T.T., Alt, F.W., and Chen, J. (2006). MDC1 maintains genomic stability by participating in the amplification of ATM-dependent DNA damage signals. Molecular cell *21*, 187-200.

Lukas, C., Melander, F., Stucki, M., Falck, J., Bekker-Jensen, S., Goldberg, M., Lerenthal, Y., Jackson, S.P., Bartek, J., and Lukas, J. (2004). Mdc1 couples DNA double-strand break recognition by Nbs1 with its H2AX-dependent chromatin retention. The EMBO journal *23*, 2674-2683.

Luo, G., Yao, M.S., Bender, C.F., Mills, M., Bladl, A.R., Bradley, A., and Petrini, J.H. (1999). Disruption of mRad50 causes embryonic stem cell lethality, abnormal embryonic development, and sensitivity to ionizing radiation. Proceedings of the National Academy of Sciences of the United States of America *96*, 7376-7381.

Mah, L.J., El-Osta, A., and Karagiannis, T.C. (2010). gammaH2AX: a sensitive molecular marker of DNA damage and repair. Leukemia *24*, 679-686.

Martell, J.D., Deerinck, T.J., Sancak, Y., Poulos, T.L., Mootha, V.K., Sosinsky, G.E., Ellisman, M.H., and Ting, A.Y. (2012). Engineered ascorbate peroxidase as a

genetically encoded reporter for electron microscopy. Nature biotechnology *30*, 1143-1148.

Maser, R.S., Monsen, K.J., Nelms, B.E., and Petrini, J.H. (1997). hMre11 and hRad50 nuclear foci are induced during the normal cellular response to DNA double-strand breaks. Molecular and cellular biology *17*, 6087-6096.

Mathew, S.S., and Bridge, E. (2007). The cellular Mre11 protein interferes with adenovirus E4 mutant DNA replication. Virology *365*, 346-355.

Mathew, S.S., and Bridge, E. (2008). Nbs1-dependent binding of Mre11 to adenovirus E4 mutant viral DNA is important for inhibiting DNA replication. Virology *374*, 11-22.

Matsuoka, S., Ballif, B.A., Smogorzewska, A., McDonald, E.R., 3rd, Hurov, K.E., Luo, J., Bakalarski, C.E., Zhao, Z., Solimini, N., Lerenthal, Y., Shiloh, Y., Gygi, S.P., and Elledge, S.J. (2007). ATM and ATR substrate analysis reveals extensive protein networks responsive to DNA damage. Science *316*, 1160-1166.

Moore, J.K., and Haber, J.E. (1996). Cell cycle and genetic requirements of two pathways of nonhomologous end-joining repair of double-strand breaks in Saccharomyces cerevisiae. Molecular and cellular biology *16*, 2164-2173.

Nagata, K., Guggenheimer, R.A., and Hurwitz, J. (1983). Adenovirus DNA replication in vitro: synthesis of full-length DNA with purified proteins. Proceedings of the National Academy of Sciences of the United States of America *80*, 4266-4270.

Nelms, B.E., Maser, R.S., MacKay, J.F., Lagally, M.G., and Petrini, J.H. (1998). In situ visualization of DNA double-strand break repair in human fibroblasts. Science *280*, 590-592.

Nichols, G.J., Schaack, J., and Ornelles, D.A. (2009). Widespread phosphorylation of histone H2AX by species C adenovirus infection requires viral DNA replication. Journal of virology *83*, 5987-5998.

O'Neill, T., Dwyer, A.J., Ziv, Y., Chan, D.W., Lees-Miller, S.P., Abraham, R.H., Lai, J.H., Hill, D., Shiloh, Y., Cantley, L.C., and Rathbun, G.A. (2000). Utilization of oriented peptide libraries to identify substrate motifs selected by ATM. The Journal of biological chemistry *275*, 22719-22727.

O'Shea, C.C. (2005). Viruses - seeking and destroying the tumor program. Oncogene *24*, 7640-7655.

O'Shea, C.C., Johnson, L., Bagus, B., Choi, S., Nicholas, C., Shen, A., Boyle, L., Pandey, K., Soria, C., Kunich, J., Shen, Y., Habets, G., Ginzinger, D., and McCormick, F. (2004). Late viral RNA export, rather than p53 inactivation, determines ONYX-015 tumor selectivity. Cancer cell *6*, 611-623.

O'Shea, C.C., Soria, C., Bagus, B., and McCormick, F. (2005). Heat shock phenocopies E1B-55K late functions and selectively sensitizes refractory tumor cells to ONYX-015 oncolytic viral therapy. Cancer cell *8*, 61-74.

Orthwein, A., Fradet-Turcotte, A., Noordermeer, S.M., Canny, M.D., Brun, C.M., Strecker, J., Escribano-Diaz, C., and Durocher, D. (2014). Mitosis inhibits DNA double-strand break repair to guard against telomere fusions. Science *344*, 189-193.

Ou, H.D., Kwiatkowski, W., Deerinck, T.J., Noske, A., Blain, K.Y., Land, H.S., Soria, C., Powers, C.J., May, A.P., Shu, X., Tsien, R.Y., Fitzpatrick, J.A., Long, J.A., Ellisman, M.H., Choe, S., and O'Shea, C.C. (2012). A structural basis for the assembly and functions of a viral polymer that inactivates multiple tumor suppressors. Cell *151*, 304-319.

Paull, T.T., and Deshpande, R.A. (2014). The Mre11/Rad50/Nbs1 complex: Recent insights into catalytic activities and ATP-driven conformational changes. Experimental cell research.

Paull, T.T., and Gellert, M. (1999). Nbs1 potentiates ATP-driven DNA unwinding and endonuclease cleavage by the Mre11/Rad50 complex. Genes & development *13*, 1276-1288.

Paull, T.T., Rogakou, E.P., Yamazaki, V., Kirchgessner, C.U., Gellert, M., and Bonner, W.M. (2000). A critical role for histone H2AX in recruitment of repair factors to nuclear foci after DNA damage. Current biology : CB *10*, 886-895.

Polo, S.E., and Jackson, S.P. (2011). Dynamics of DNA damage response proteins at DNA breaks: a focus on protein modifications. Genes & development *25*, 409-433.

Pombo, A., Ferreira, J., Bridge, E., and Carmo-Fonseca, M. (1994). Adenovirus replication and transcription sites are spatially separated in the nucleus of infected cells. The EMBO journal *13*, 5075-5085.

Pospelova, T.V., Demidenko, Z.N., Bukreeva, E.I., Pospelov, V.A., Gudkov, A.V., and Blagosklonny, M.V. (2009). Pseudo-DNA damage response in senescent cells. Cell cycle *8*, 4112-4118.

Povirk, L.F. (1996). DNA damage and mutagenesis by radiomimetic DNA-cleaving agents: bleomycin, neocarzinostatin and other enediynes. Mutation research *355*, 71-89.

Prakash, A., Jayaram, S., and Bridge, E. (2012). Differential activation of cellular DNA damage responses by replication-defective and replication-competent adenovirus mutants. Journal of virology *86*, 13324-13333.

Querido, E., Blanchette, P., Yan, Q., Kamura, T., Morrison, M., Boivin, D., Kaelin, W.G., Conaway, R.C., Conaway, J.W., and Branton, P.E. (2001). Degradation of p53

by adenovirus E4orf6 and E1B55K proteins occurs via a novel mechanism involving a Cullin-containing complex. Genes & development *15*, 3104-3117.

Rekosh, D.M., Russell, W.C., Bellet, A.J., and Robinson, A.J. (1977). Identification of a protein linked to the ends of adenovirus DNA. Cell *11*, 283-295.

Rogakou, E.P., Boon, C., Redon, C., and Bonner, W.M. (1999). Megabase chromatin domains involved in DNA double-strand breaks in vivo. The Journal of cell biology *146*, 905-916.

Rogakou, E.P., Pilch, D.R., Orr, A.H., Ivanova, V.S., and Bonner, W.M. (1998). DNA double-stranded breaks induce histone H2AX phosphorylation on serine 139. The Journal of biological chemistry *273*, 5858-5868.

Sarbassov, D.D., Guertin, D.A., Ali, S.M., and Sabatini, D.M. (2005). Phosphorylation and regulation of Akt/PKB by the rictor-mTOR complex. Science *307*, 1098-1101.

Sarker, A.H., Chatterjee, A., Williams, M., Lin, S., Havel, C., Jacob, P., 3rd, Boldogh, I., Hazra, T.K., Talbot, P., and Hang, B. (2014). NEIL2 protects against oxidative DNA damage induced by sidestream smoke in human cells. PloS one *9*, e90261.

Sartori, A.A., Lukas, C., Coates, J., Mistrik, M., Fu, S., Bartek, J., Baer, R., Lukas, J., and Jackson, S.P. (2007). Human CtIP promotes DNA end resection. Nature *450*, 509-514.

Savitsky, K., Bar-Shira, A., Gilad, S., Rotman, G., Ziv, Y., Vanagaite, L., Tagle, D.A., Smith, S., Uziel, T., Sfez, S., Ashkenazi, M., Pecker, I., Frydman, M., Harnik, R., Patanjali, S.R., Simmons, A., Clines, G.A., Sartiel, A., Gatti, R.A., Chessa, L., Sanal, O., Lavin, M.F., Jaspers, N.G., Taylor, A.M., Arlett, C.F., Miki, T., Weissman, S.M., Lovett, M., Collins, F.S., and Shiloh, Y. (1995). A single ataxia telangiectasia gene with a product similar to PI-3 kinase. Science *268*, 1749-1753.

Scaffidi, P., and Misteli, T. (2008). Lamin A-dependent misregulation of adult stem cells associated with accelerated ageing. Nature cell biology *10*, 452-459.

Schultz, L.B., Chehab, N.H., Malikzay, A., and Halazonetis, T.D. (2000). p53 binding protein 1 (53BP1) is an early participant in the cellular response to DNA double-strand breaks. The Journal of cell biology *151*, 1381-1390.

Schwartz, R.A., Lakdawala, S.S., Eshleman, H.D., Russell, M.R., Carson, C.T., and Weitzman, M.D. (2008). Distinct requirements of adenovirus E1b55K protein for degradation of cellular substrates. Journal of virology *82*, 9043-9055.

Seo, J., Kim, S.C., Lee, H.S., Kim, J.K., Shon, H.J., Salleh, N.L., Desai, K.V., Lee, J.H., Kang, E.S., Kim, J.S., and Choi, J.K. (2012). Genome-wide profiles of H2AX and gamma-H2AX differentiate endogenous and exogenous DNA damage hotspots in human cells. Nucleic acids research *40*, 5965-5974.

Sharma, P., Kolawole, A.O., Core, S.B., Kajon, A.E., and Excoffon, K.J. (2012). Sidestream smoke exposure increases the susceptibility of airway epithelia to adenoviral infection. PloS one *7*, e49930.

Shepard, R.N., and Ornelles, D.A. (2003). E4orf3 is necessary for enhanced S-phase replication of cell cycle-restricted subgroup C adenoviruses. Journal of virology *77*, 8593-8595.

Shepard, R.N., and Ornelles, D.A. (2004). Diverse roles for E4orf3 at late times of infection revealed in an E1B 55-kilodalton protein mutant background. Journal of virology *78*, 9924-9935.

Shiloh, Y., and Ziv, Y. (2013). The ATM protein kinase: regulating the cellular response to genotoxic stress, and more. Nature reviews Molecular cell biology *14*, 197-210.

Shin, D.S., Pratt, A.J., and Tainer, J.A. (2014). Archaeal genome guardians give insights into eukaryotic DNA replication and damage response proteins. Archaea *2014*, 206735.

Shreeram, S., Demidov, O.N., Hee, W.K., Yamaguchi, H., Onishi, N., Kek, C., Timofeev, O.N., Dudgeon, C., Fornace, A.J., Anderson, C.W., Minami, Y., Appella, E., and Bulavin, D.V. (2006). Wip1 phosphatase modulates ATM-dependent signaling pathways. Molecular cell *23*, 757-764.

Shu, X., Lev-Ram, V., Deerinck, T.J., Qi, Y., Ramko, E.B., Davidson, M.W., Jin, Y., Ellisman, M.H., and Tsien, R.Y. (2011). A genetically encoded tag for correlated light and electron microscopy of intact cells, tissues, and organisms. PLoS biology *9*, e1001041.

Soria, C., Estermann, F.E., Espantman, K.C., and O'Shea, C.C. (2010). Heterochromatin silencing of p53 target genes by a small viral protein. Nature *466*, 1076-1081.

Soutoglou, E., Dorn, J.F., Sengupta, K., Jasin, M., Nussenzweig, A., Ried, T., Danuser, G., and Misteli, T. (2007). Positional stability of single double-strand breaks in mammalian cells. Nature cell biology *9*, 675-682.

Soutoglou, E., and Misteli, T. (2008). Activation of the cellular DNA damage response in the absence of DNA lesions. Science *320*, 1507-1510.

Steiner, I., Aebi, C., Ridolfi Luthy, A., Wagner, B., and Leibundgut, K. (2008). Fatal adenovirus hepatitis during maintenance therapy for childhood acute lymphoblastic leukemia. Pediatric blood & cancer *50*, 647-649.

Stewart, G.S., Wang, B., Bignell, C.R., Taylor, A.M., and Elledge, S.J. (2003). MDC1 is a mediator of the mammalian DNA damage checkpoint. Nature *421*, 961-966.

Stracker, T.H., Carson, C.T., and Weitzman, M.D. (2002). Adenovirus oncoproteins inactivate the Mre11-Rad50-NBS1 DNA repair complex. Nature *418*, 348-352.

Stracker, T.H., and Petrini, J.H. (2011). The MRE11 complex: starting from the ends. Nature reviews Molecular cell biology *12*, 90-103.

Stucki, M., Clapperton, J.A., Mohammad, D., Yaffe, M.B., Smerdon, S.J., and Jackson, S.P. (2005). MDC1 directly binds phosphorylated histone H2AX to regulate cellular responses to DNA double-strand breaks. Cell *123*, 1213-1226.

Sun, Y., Jiang, X., Chen, S., Fernandes, N., and Price, B.D. (2005). A role for the Tip60 histone acetyltransferase in the acetylation and activation of ATM. Proceedings of the National Academy of Sciences of the United States of America *102*, 13182-13187.

Sun, Y., Jiang, X., Xu, Y., Ayrapetov, M.K., Moreau, L.A., Whetstine, J.R., and Price, B.D. (2009). Histone H3 methylation links DNA damage detection to activation of the tumour suppressor Tip60. Nature cell biology *11*, 1376-1382.

Sun, Y., Xu, Y., Roy, K., and Price, B.D. (2007). DNA damage-induced acetylation of lysine 3016 of ATM activates ATM kinase activity. Molecular and cellular biology *27*, 8502-8509.

Suram, A., and Herbig, U. (2014). The replicometer is broken: telomeres activate cellular senescence in response to genotoxic stresses. Aging cell *13*, 780-786.

Thai, M., Graham, N.A., Braas, D., Nehil, M., Komisopoulou, E., Kurdistani, S.K., McCormick, F., Graeber, T.G., and Christofk, H.R. (2014). Adenovirus E4ORF1-induced MYC activation promotes host cell anabolic glucose metabolism and virus replication. Cell metabolism *19*, 694-701.

Thomas, G.P., and Mathews, M.B. (1980). DNA replication and the early to late transition in adenovirus infection. Cell *22*, 523-533.

Toller, I.M., Neelsen, K.J., Steger, M., Hartung, M.L., Hottiger, M.O., Stucki, M., Kalali, B., Gerhard, M., Sartori, A.A., Lopes, M., and Muller, A. (2011). Carcinogenic bacterial pathogen Helicobacter pylori triggers DNA double-strand breaks and a DNA damage response in its host cells. Proceedings of the National Academy of Sciences of the United States of America *108*, 14944-14949.

Turnell, A.S., and Grand, R.J. (2012). DNA viruses and the cellular DNA-damage response. The Journal of general virology *93*, 2076-2097.

Uziel, T., Lerenthal, Y., Moyal, L., Andegeko, Y., Mittelman, L., and Shiloh, Y. (2003). Requirement of the MRN complex for ATM activation by DNA damage. The EMBO journal *22*, 5612-5621.

van Vugt, M.A., Gardino, A.K., Linding, R., Ostheimer, G.J., Reinhardt, H.C., Ong, S.E., Tan, C.S., Miao, H., Keezer, S.M., Li, J., Pawson, T., Lewis, T.A., Carr, S.A., Smerdon, S.J., Brummelkamp, T.R., and Yaffe, M.B. (2010). A mitotic phosphorylation feedback network connects Cdk1, Plk1, 53BP1, and Chk2 to inactivate the G(2)/M DNA damage checkpoint. PLoS biology *8*, e1000287.

Weiden, M.D., and Ginsberg, H.S. (1994). Deletion of the E4 region of the genome produces adenovirus DNA concatemers. Proceedings of the National Academy of Sciences of the United States of America *91*, 153-157.

Weitzman, M.D., Lilley, C.E., and Chaurushiya, M.S. (2010). Genomes in conflict: maintaining genome integrity during virus infection. Annual review of microbiology *64*, 61-81.

Williams, R.S., Moncalian, G., Williams, J.S., Yamada, Y., Limbo, O., Shin, D.S., Groocock, L.M., Cahill, D., Hitomi, C., Guenther, G., Moiani, D., Carney, J.P., Russell, P., and Tainer, J.A. (2008). Mre11 dimers coordinate DNA end bridging and nuclease processing in double-strand-break repair. Cell *135*, 97-109.

Wu, J., and Chen, Z.J. (2014). Innate immune sensing and signaling of cytosolic nucleic acids. Annual review of immunology *32*, 461-488.

Wu, X., Avni, D., Chiba, T., Yan, F., Zhao, Q., Lin, Y., Heng, H., and Livingston, D. (2004). SV40 T antigen interacts with Nbs1 to disrupt DNA replication control. Genes & development *18*, 1305-1316.

Xiao, Y., and Weaver, D.T. (1997). Conditional gene targeted deletion by Cre recombinase demonstrates the requirement for the double-strand break repair Mre11 protein in murine embryonic stem cells. Nucleic acids research *25*, 2985-2991.

Xu, X., and Stern, D.F. (2003). NFBD1/MDC1 regulates ionizing radiation-induced focus formation by DNA checkpoint signaling and repair factors. FASEB journal : official publication of the Federation of American Societies for Experimental Biology *17*, 1842-1848.

Yoshiyama, K.O., Sakaguchi, K., and Kimura, S. (2013). DNA damage response in plants: conserved and variable response compared to animals. Biology *2*, 1338-1356.

You, Z., and Bailis, J.M. (2010). DNA damage and decisions: CtIP coordinates DNA repair and cell cycle checkpoints. Trends in cell biology *20*, 402-409.

You, Z., Bailis, J.M., Johnson, S.A., Dilworth, S.M., and Hunter, T. (2007). Rapid activation of ATM on DNA flanking double-strand breaks. Nature cell biology *9*, 1311-1318.

You, Z., Chahwan, C., Bailis, J., Hunter, T., and Russell, P. (2005). ATM activation and its recruitment to damaged DNA require binding to the C terminus of Nbs1. Molecular and cellular biology *25*, 5363-5379.

You, Z., Shi, L.Z., Zhu, Q., Wu, P., Zhang, Y.W., Basilio, A., Tonnu, N., Verma, I.M., Berns, M.W., and Hunter, T. (2009). CtIP links DNA double-strand break sensing to resection. Molecular cell *36*, 954-969.

Yu, B., Zhou, Y., Wu, H., Wang, Z., Zhan, Y., Feng, X., Geng, R., Wu, Y., Kong, W., and Yu, X. (2012). Seroprevalence of neutralizing antibodies to human adenovirus type 5 in healthy adults in China. Journal of medical virology *84*, 1408-1414.

Yuan, J., and Chen, J. (2009). N terminus of CtIP is critical for homologous recombination-mediated double-strand break repair. The Journal of biological chemistry *284*, 31746-31752.

Yukawa, M., Akiyama, T., Franke, V., Mise, N., Isagawa, T., Suzuki, Y., Suzuki, M.G., Vlahovicek, K., Abe, K., Aburatani, H., and Aoki, F. (2014). Genome-wide analysis of the chromatin composition of histone H2A and H3 variants in mouse embryonic stem cells. PloS one *9*, e92689.

Zheng, H., Chen, L., Pledger, W.J., Fang, J., and Chen, J. (2014). p53 promotes repair of heterochromatin DNA by regulating JMJD2b and SUV39H1 expression. Oncogene *33*, 734-744.

Zhu, J., Petersen, S., Tessarollo, L., and Nussenzweig, A. (2001). Targeted disruption of the Nijmegen breakage syndrome gene NBS1 leads to early embryonic lethality in mice. Current biology : CB *11*, 105-109.

Zou, L. (2007). Single- and double-stranded DNA: building a trigger of ATR-mediated DNA damage response. Genes & development *21*, 879-885.